Strain-Promoted Alkyne-Nitrone Cycloadditions:

Developing Bioorthogonal Labelling Strategies

Thesis submitted to the

Faculty of Graduate and Postdoctoral Studies

In partial fulfilment of the requirements of the

M.Sc. degree in chemistry

uOttawa

In the Ottawa-Carleton Chemistry Institute

Department of chemistry, University of Ottawa

Candidate

Douglas Allan MacKenzie

Supervisor

Dr. John Paul Pezacki

Acknowledgements

First and foremost, I would like to thank Dr. John Pezacki for allowing me the opportunity to pursue an advanced degree in chemistry under his leadership. He has shown patience in giving me the freedom to make mistakes, wisdom in teaching me how to correct them, and generosity in giving me every opportunity I needed to succeed and to share my research with the scientific community. Dr. Pezacki has been a great mentor to me and I will always be grateful for his belief in me and his willingness to support me in pursuing my goals.

I would also like to thank my colleagues, who I could not have done this without. Particularly, I would like to thank Mariya Chigrinova, for her expertise in instrumental analysis and her willingness to share her experience and her knowledge with me. I would like to thank Dr. Allison Sherratt for her insight and persistence in helping to make the biological goals of this project a reality. Her advice in experimental troubleshooting and planning has been greatly appreciated, and I am thankful to have had the opportunity to learn from her and to work together in developing new bioanalytical tools. I would also like to thank Dr. Craig McKay and Dr. Louis-Philippe Bonhomme-Beaulieau for their demonstration of practical hands-on laboratory skills. More generally, I would like to thank the colleagues I have had the pleasure of getting to know over the course of my graduate studies, all of whom have become wonderful friends.

Finally, I would like to thank my parents, family, and close friends for their continued support in pursuing and achieving my dreams. I have never had to worry about where to turn for help, and that has made a major impact in ensuring no obstacle or challenge was impossible to overcome, and that no goal was out of reach. For this, I sincerely thank you.

Abstract

Chemical transformations that join two molecular components together rapidly while remaining highly efficient and selective are valued for their elegant simplicity and effectiveness in a myriad of applications. By applying the principles of 'click' chemistry to biology, information about molecular interactions *in vivo* can therefore be gained from minimally perturbing bioorthogonal coupling reactions. Developing bioorthogonal 'click' reactions – reactions that do not cross-react with biological components – provides new ways to accurately study biological systems at the molecular level. This thesis describes the development of such tools.

Strain-promoted alkyne-nitrone cycloadditions (SPANC) represent rapid, efficient, selective, and tunable conjugation strategies that are applicable to biomolecular labelling experiments. Herein, SPANC reactions with bicyclo[6.1.0]nonyne are examined using physical organic methods to determine the stereoelectronic factors governing SPANC reactivity. Second-order rate constants (k_2) of up to 1.49 $M^{-1}s^{-1}$ were measured and the resulting cycloadditions are applied to the design and synthesis of nitrone-based molecular probes. The first example of SPANC-mediated metabolic labelling in live-cell bacteria is reported, establishing SPANC as an efficient and bioorthogonal metabolic labelling strategy for cellular labelling.

Table of Contents

List of Abbreviations

ABP – Activity-based probe

ABPP – Activity-based protein profiling

Ala - Alanine

BCN – Bicyclo[6.1.0]nonyne

Boc – *tert*-Butoxycarbonyl

$CDCl_3$ – Deuterated chloroform

CuAAC – Copper (I) catalyzed Azide-Alkyne Cycloaddition

DA – Diels-Alder

DBCO - Dibenzylcyclooctyne

DCM – Dichloromethane

DIBO – 4-Dibenzocyclooctynol

DIC - Diisopropylcarbodiimide

DMF – Dimethylformamide

Et_2O – Diethyl ether

Et_3N - Triethylamine

EtOH - Ethanol

EtOAc – Ethyl Acetate

FMO – Frontier Molecular Orbital Theory

Fmoc – Fluorenylmethyloxycarbonyl

FP – Fluorescent Protein

HEK – Human Embryonic Kidney

HOMO – Highest Occupied Molecular Orbital

IED – Inverse Electron Demand

LCMS – Liquid Chromatography Mass Spectrometry

LFER – Linear Free-Energy Relationship

LUMO – Lowest Unoccupied Molecular Orbital

Lys – Lysine

m-CPBA – *meta*-Chloroperoxybenzoic acid

MeOD – Deuterated Methanol

OCT – Cyclooct-1-yne

PG – Peptidoglycan

R.T. – Room temperature

SAR – Structure-activity relationship

SPAAC – Strain-Promoted Azide-Alkyne Cycloaddition

SPANC – Strain-Promoted Alkyne-Nitrone Cycloaddition

TFA – Trifluoroacetic acid

UV - Ultraviolet

List of Figures

List of Schemes

List of Equations

List of Tables

1. Bioorthogonal Chemistry

Introduction – The Chemistry of Conjugation

Efficiency and selectivity in organic transformations have always been important considerations in establishing new routes to synthetic targets. The classic dogma where increased reactivity leads to decreased selectivity plagues the design of ideal chemistries that allow waste-free access to highly specific targets. The influential work performed by Kolb, Finn, and Sharpless, on 'click' chemistry, however, has highlighted a strategy that mimics the concepts used by nature to develop highly complex molecules from a simple set of starting materials by capitalizing on reactions that are rapid only where specific functional groups are present.[1] The modular approach devised by Sharpless *et al* employs a series of 'near-perfect' coupling reactions with high regio- and stereochemical control in the synthesis of complex organic molecules. The intention of these efforts was to modify the strategies taken by synthetic organic chemists in their pursuit of lead pharmaceutical compounds. Given the enormous estimate of number of potential drug candidates (approximately 10^{62}-10^{63} molecules),[2] it seems reasonable to pursue those that involve practical and easy to carry out transformations before expending a great deal of time, effort, and resources attempting to generate difficult C-C bonds only observed in nature after centuries of evolution.

The majority of these thermodynamically favourable transformations stem from simple alkenes or involve activated or catalyzed cycloadditions, and produce compounds that evolve in complexity through iterations of heterocycle-forming oxidations and nucleophilic ring-opening reactions. The colloquial example of 'click' chemistry, which is based on Rolf Huisgen's work on 1,3-dipolar cycloadditions, is the copper (I) catalyzed cycloaddition of organic azides and

terminal alkynes (CuAAC, equation 1.1).[3] Although CuAAC is often the first 'click' reaction to come to mind, many others have been developed based on the criteria set forth by Sharpless *et al*[1] that have the potential to be used in concert in an orthogonal fashion to access a rich diversity of scaffolds with very little wasted materials.[4,5] The impact of 'click' chemistry has reached not only the pharmaceutical industry, but also materials science,[6,7] nanoparticle functionalization,[8] and chemical biology with great success.[9-11] As the evolution of 'click' chemistry continues, the depth of scope, applications, and benefits of this influential concept continue to grow.

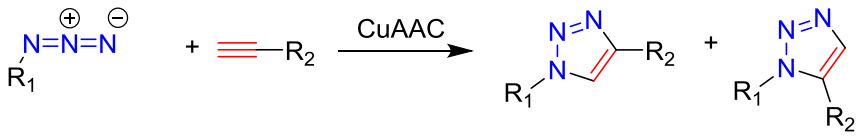

Equation 1.1 - Copper (I) catalyzed variant of Huisgen 1,3-dipolar cycloaddition. Copper catalysis allows the formation of a stable triazole from a terminal alkyne and an azide to proceed efficiently at room temperature.

Bioorthogonal Chemistry

'Click' chemistry has become widely known as a powerful tool for studying the dynamics of biomolecules by tracking them through time and space in their native settings.[12-14] By modifying the target biomolecule to bear a chemical reporter, such as an azide or alkyne, it is possible to perform a 'click' reaction *in vivo* in order to couple the biomolecule target to a chemical label. These labels are often fluorescent molecules used for live-cell imaging, allowing for the visualization of compartmentalization or for the visual comparison of particular biomolecules in diseased versus healthy cells. Biotin is also commonly used for labelling because of its high affinity for streptavidin, allowing for visualization with fluorescein isothiocyanate (FITC) or for

sequestering tethered biomolecules that can then be identified by mass spectrometry or other analytical techniques.[15] Bertozzi *et al*, and subsequently an entire community of chemical biologists have shown that employing 'click' reactions to observe and monitor biological processes in living systems is a valuable approach to answering questions pertaining to how life works on the molecular level, and that the reactions used are subject to additional constraints.[13] Reactions employed for this purpose must meet all of the criteria of 'click' chemistry – high yielding, minimal formation of byproducts, modular, wide in scope and be highly thermodynamically favourable, all while remaining inert to the biological surroundings.[13] In order to be inert to its biological surroundings, the reaction must display rapid kinetics in aqueous media at physiological pH and temperature while resulting in products that are stable under the same conditions, produce benign products or byproducts, and not interfere or be interfered with by any of the biological processes that are simultaneously occurring. Though these criteria are quite stringent, a number of 'near-perfect' and bioorthogonal chemical transformations have been developed to study the dynamics of biomolecules in their native environments.[9,16-18]

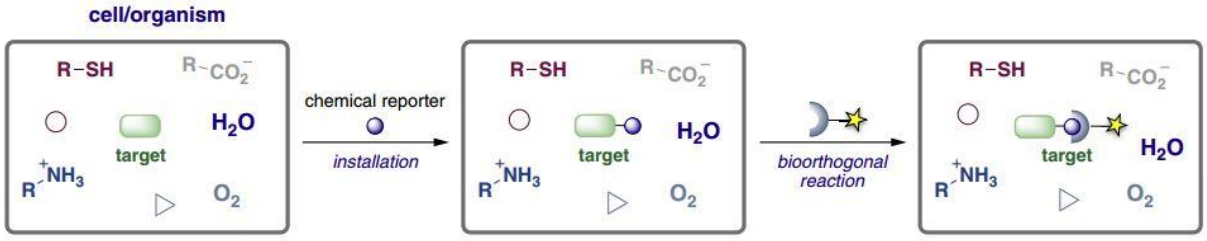

Equation 1.2 - Two-stage bioorthogonal chemical labelling strategy. Highly selective coupling chemistries provide a means of joining biological targets to chemical reporters for isolation or fluorescent imaging without interfering with the surrounding chemical environment. Adapted from reference 13.

Classical fluorescent protein (FP) molecular labelling methods remain powerful strategies in protein-based studies, however, two-stage small molecule-based molecular probes offer alternative methods to study biological molecules and may prove more effective for certain metabolic labelling applications. The diversity of information gained from a widened array of labelling strategies exemplifies the importance of developing additional tools for biological studies.[19] Fluorescent proteins (FP) have been used in a host of fluorescent microscopy experiments since the discovery of green fluorescent protein (GFP) in 1962 and their initial uses as molecular markers in the early 1990's and continue to serve as protein markers and genetic reporters.[20-22] The use of FPs requires genetic manipulation to tag proteins of interest and due to their large size have the potential to interfere with the function of the target protein. Zornetta *et al* report the study of the translocation of Anthrax toxins lethal factor (LF) and oedema factor (EF) across cell membranes, finding that the incorporation of FP mCherry at the C-terminus prevents cellular entry of either protein by disrupting the necessary folding and unfolding events.[23] Zheng *et al* undertook a similar study in 2014 making use of several two-stage bioorthogonal labelling strategies to observe in a time-delay fashion the translocation of LF variants across the endosomal membrane in mouse J774A.1 cells.[24] The smaller size of the fluorescent molecule used allowed for the proper folding and unfolding events to occur and made the study of the unhindered protein translocation possible. These experiments show by example the utility in developing bioorthogonal labelling methods and outline some potential applications of rapidly evolving biomolecular labelling techniques.

In spite of the numerous obstacles impeding the development of bioorthogonal click reactions, several strategies have been successful. One of the first examples was the use of Staudinger

ligation that was applied to the labelling of cell-surface glycans by the Bertozzi group, paving the way for the incorporation of azide-functionalized biomolecules into living cells.[25]

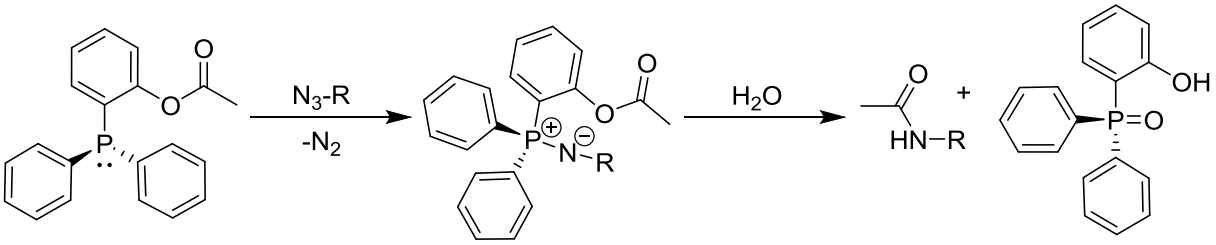

Equation 1.3 - Traceless Staudinger Ligation.[26,27] A modified triarylphosphine bearing an intramolecular electrophilic trap enables the formation of an amide bond omitting the triarylphosphine from the coupled product.

Organic azides, which are effectively absent from natural systems, are inert under physiological conditions and because of their small size, cause minimal disruption of enzyme substrates. Minimizing the disruption of natural substrates and interactions with non-target biomolecules assures that the information gained from imaging experiments reflects the true conditions that occur naturally and limits the amount of non-specific labelling observed. It is therefore important to apply coupling strategies that capitalize on exogenous chemical reactivity. Carbon-carbon triple bonds are also nearly excluded from living systems but are easily prepared from vicinal dihalides through elimination. Huisgen 1,3-dipolar cycloaddition couples organic azides to terminal alkynes in high yield with no byproduct formation and therefore is capable of taking advantage of exogenous chemical reactivity, but requires a metal catalyst in order to proceed at temperatures relevant to biological study. CuAAC occurs at ~10^7 times faster than the non-catalyzed reaction at room temperature which increases the utility of the reaction; however, the copper catalysts used typically show ligand-dependent metabolic effects and toxicity which excludes CuAAC from being widely bioorthogonal.[28,29] The undesired consequences of copper

catalysts in living systems has prompted the need for bioorthogonal coupling strategies with less interfering reaction profiles.

The rate constants of chemical transformations can be increased by reducing the energetic barrier required for reactants to reach the overall highest-energy transition state complex. In CuAAC, this reduced energy barrier is obtained by altering the reaction pathway to proceed through several lower-energy transitions that are stabilized by association with the copper catalyst rather than proceeding through one high-energy transition state complex.[30]

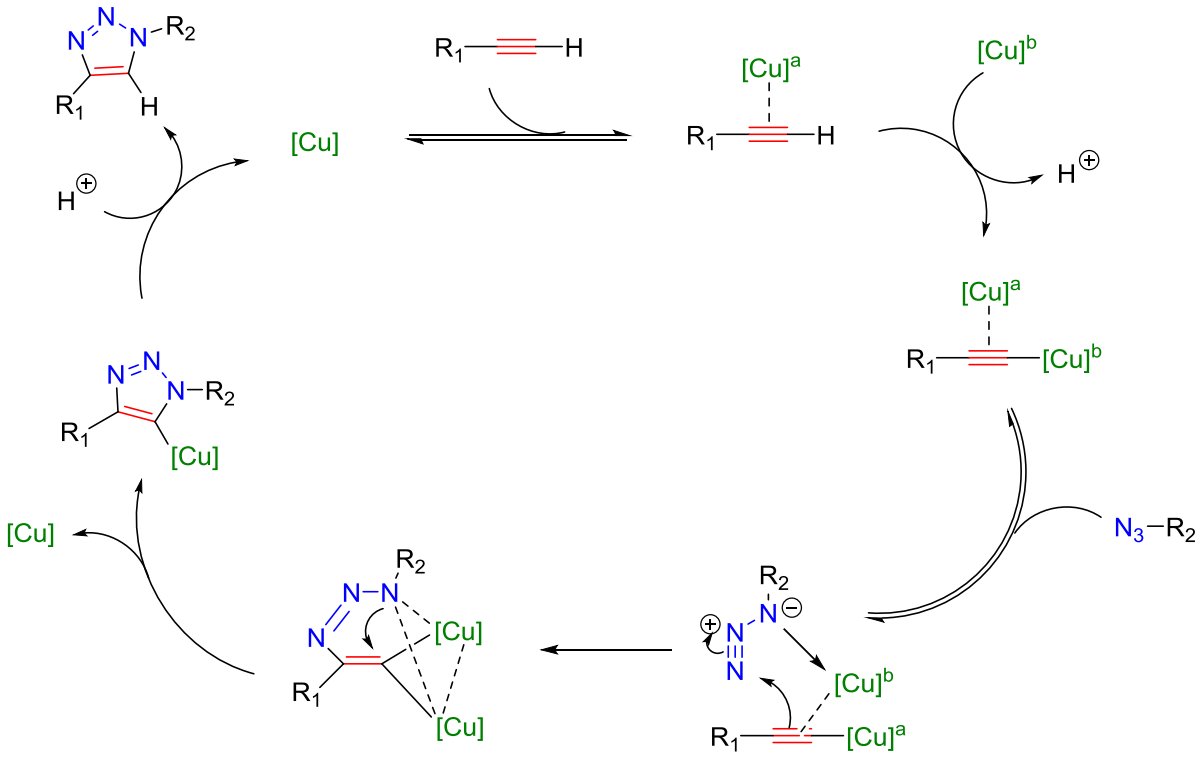

Figure 1.1 – Multistep catalytic cycle of CuAAC, proposed by Worrell *et al*, adapted from reference 30. Recent mechanistic studies suggest that two copper atoms are required to facilitate the transformation of an azide and a terminal alkyne to the respective traizole product under copper (I) catalytic conditions.

An alternative method in reducing the overall energy barrier is to destabilize the ground-state energy of one or more reactants. Classically, this is done by increasing the density of repulsive forces within a molecule that can be relieved upon formation of a product molecule. For example, H-X addition across an olefin in the Z-configuration often displays reduced activation energy when compared to the analogous reaction employing an olefin in the E-configuration because the energy of the activated complex is similar in each situation, while the ground state energy of the Z-olefin is higher than that of the E-olefin. The reduced activation energy is described graphically in Scheme 1.1.

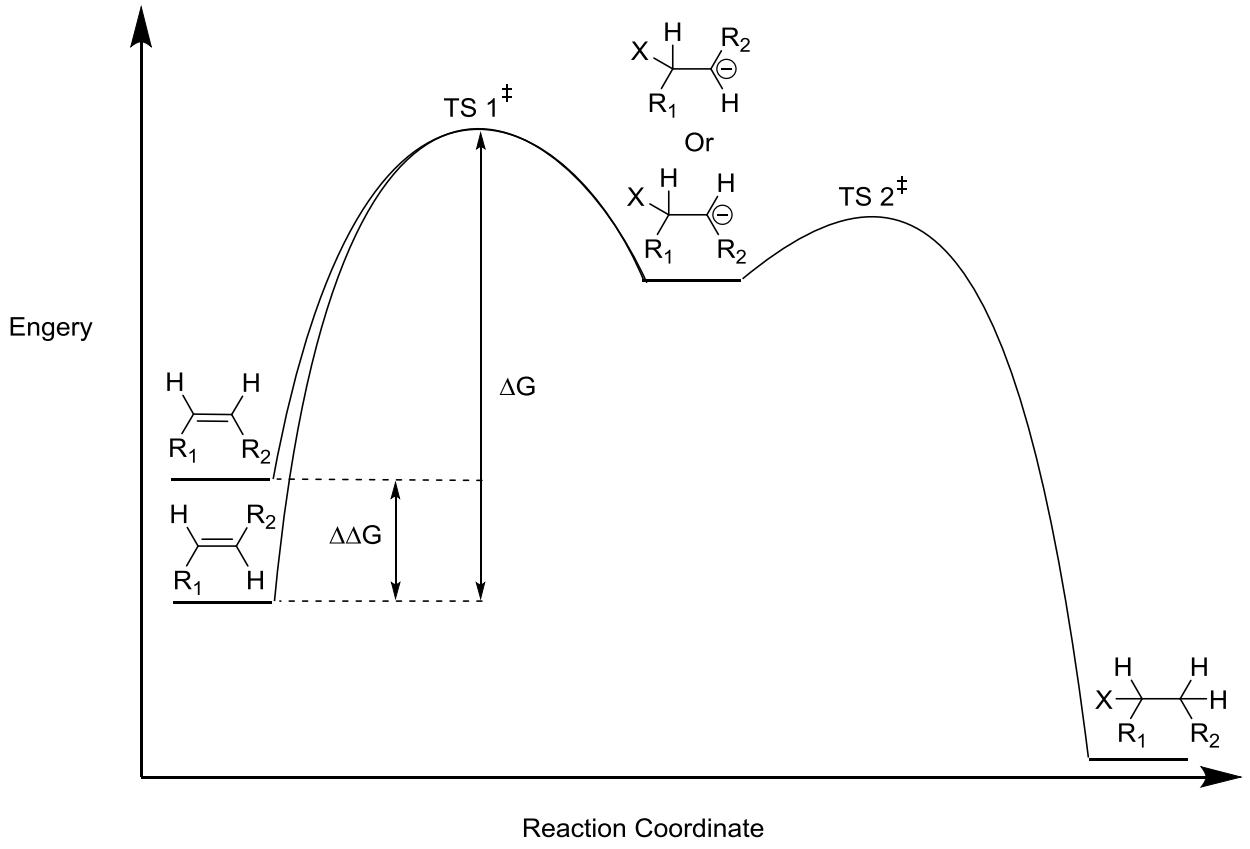

Scheme 1.1– Reducing energy barriers through ground-state destabilization of starting materials. The activation energy of a reaction is based on the largest global energy difference for a transformation, which determines the rate-limiting step. This energy difference can be minimized through lowering the energy of the high-energy activated complex by stabilization, or by raising the ground-state energy of the reactants.

Taking this principle into account, Bertozzi *et al* eliminated the need for high temperatures by modifying the Huisgen 1,3-dipolar cycloaddition to employ alkynes locked in 8-membered rings to destabilize the ground-state energy of the reactants and drive the reaction to completion through the release of the strain energy upon cycloaddition. Strain-Promoted Alkyne-Azide Cycloaddition (SPAAC) was therefore developed by the Bertozzi group in 2004 as an alternative to CuAAC, and since its introduction numerous efforts to produce novel bioorthogonal conjugation strategies have been undertaken.[31]

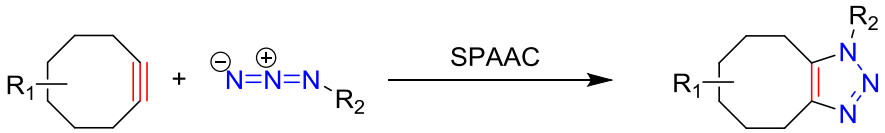

Equation 1.4– Strain-Promoted Alkyne-Azide Cycloaddition (SPAAC). Inclusion of an alkyne into an eight-membered ring lowers the activation energy of the azide-alkyne cycloaddition by raising the ground-state energy of the alkyne reagent through the introduction of ring strain. This ring strain is partially relieved upon cycloaddition and allows for triazole formation at ambient temperatures without copper (I) catalysis, leading to an increase in bioorthogonality.

Modification of strained alkynes, typically by increasing the molecular rigidity through benzanulation or reducing the number of saturated carbon-carbon bonds in the cyclooctyne core, or by introducing electron-withdrawing groups, has been central to the evolution of SPAAC.[13] Increasing the rigidity of the molecule increases the amount of ring strain exerted on the alkyne moiety, which in turn increases the overall reactivity of the alkyne. Introducing electron withdrawing groups at the propargyl position also leads to increased reactivity in SPAAC reactions by lowering the alkyne LUMO energy level to achieve better energetic matching with the azide HOMO. This trend has been observed with few exceptions by the van Delft group who compared the DFT calculated LUMO energy levels of a series of strained alkynes to their reactivity with benzyl azide.[32] Highly reactive strained alkynes have also been shown to be

susceptible to nucleophilic addition and thermal rearrangements. In particular, biarylazacyclooctanone (BARAC), the most reactive strained alkyne to date and displaying the largest second-order rate constant in reactions with benzyl azide, has been shown to undergo an acid-promoted migration of the *N*-alkyl group as well as addition of acetonitrile across the alkyne, both of which reduce the ability of BARAC to form the desired adducts.[33] The progression of SPAAC reactions in terms of reactivity and reaction rate is largely limited to the potential modifications of the alkyne, since azides are terminal functional groups which possess only one site for covalent modification. Azides are therefore quite inflexible toward modulation of their reactivity, particularly in labelling experiments that require the azide to be directly bound to a specific molecular probe.

The concept of imparting ring strain to increase one reagent's reactivity in cycloadditions has been taken to extremes by Fox *et al* in their synthesis of the potent dieneophile *trans*-cyclooctene.[16] A cyclic *cis* alkene, strained by a fused cyclopropane group, was photochemically isomerized resulting in a highly strained and electron-rich *trans* alkene that was found to react rapidly and selectively in [4+2] cycloadditions with tetrazines, releasing benign nitrogen gas as the only byproduct.

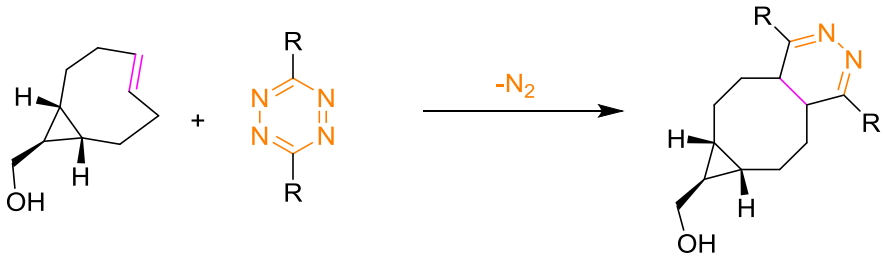

Equation 1.5 – *trans*-Cyclooctene/Tetrazine ligation. The strained internal olefin in the *Z*-configuration is highly reactive toward [4+2] inverse electron demand Diels-Alder cycloaddition in the presence of electron-deficient tetrazines.

The electron-rich nature of the dieneophile causes *trans*-Cyclooctene/Tetrazine ligation to proceed through an inverse electron demand Diels-Alder (IEDDA) reaction where the HOMO of the dieneophile is high enough in energy to preferentially react with the diene LUMO of the tetrazine. Lowering the LUMO energy level of the diene by incorporating electron-withdrawing R groups has been shown to increase the second-order rate constant of these cycloadditions, while increasing the distortion energy of the cyclooctene has increased the rate constant from ~2000$M^{-1}s^{-1}$ to ~22 000$M^{-1}s^{-1}$ through cyclopropanation.[34] Both reaction partners can be tuned electronically to achieve the optimal balance between reactivity and selectivity, and second-order rate constants of up to $k_2 = 10^6$ $M^{-1}s^{-1}$ have been reported for these tuned reactions.[35] The rapid reaction kinetics allow biomolecule labelling to occur efficiently with lower reagent concentrations, resulting in minimal perturbation of the native environment and minimal background labelling.

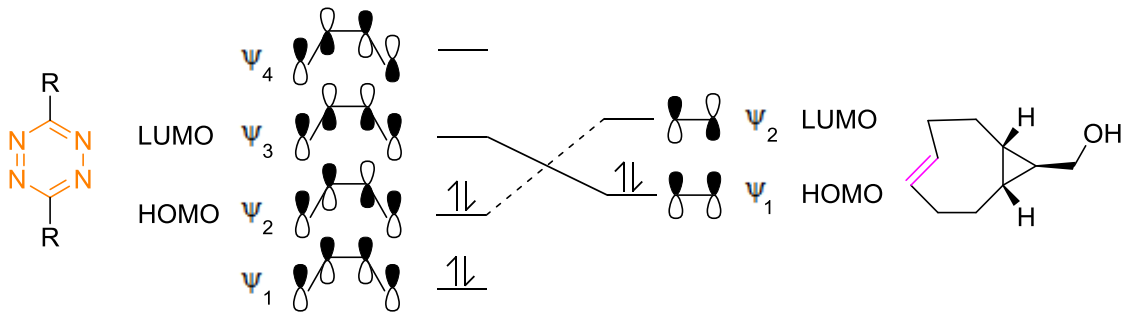

Figure 1.2 – Frontier molecular analysis of *trans*-Cyclooctene/Tetrazine ligation. Dashed line indicates the symmetry-allowed interaction of the tetrazine HOMO (Ψ_2) and alkene LUMO (Ψ_2) orbitals in a forward electron demand fashion while the solid line indicates the interaction of the tetrazine LUMO (Ψ_3) with the alkene HOMO (Ψ_1) in the inverse electron demand fashion observed in this Diels-Alder cycloaddition.

Alternatively, nitrones have emerged as highly reactive 1,3-dipoles in strain-promoted alkyne-nitrone cycloadditions (SPANC), showing a greater sensitivity to stereoelectronic modifications

when compared to organic azides. The high degree of tunability stems from the basic structure of nitrones, offering three potential sites for direct modification.

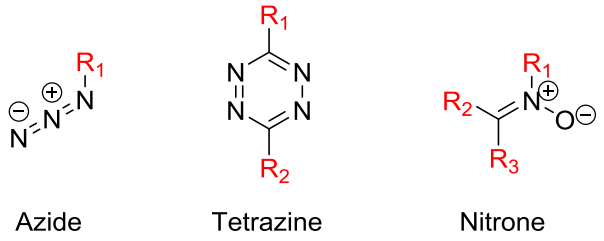

Figure 1.3 – Potential attachment sites for common dipoles/dienes used in strain-promoted cycloadditions. As the number of attachment sites increases, the potential to modify the stereoelectronic properties of the dipole/diene also increases. Stereoelectronic modification of nitrones by inclusion in ring structures and functional group substitution has been shown to impact the observed second-order rate constant (k_2).[17,36-39]

Each modification site allows for the attachment of biomolecules, reporter molecules, electronic-modulating functional groups, as well as the introduction of ring strain to the dipole – a feature not present in azides or tetrazines. Previously in our lab, we have shown that the resulting endocyclic nitrones display generally greater reaction kinetics and hydrolytic stability when compared to their acyclic counterparts, and that nitrones can be used for cell-surface labelling of mammalian cells.[17] Although acyclic nitrones have been shown to hydrolyze in acidic and basic aqueous solutions, hydrolysis has not been observed under similar conditions with endocyclic nitrones. Equally important to the stability of the starting materials in bioorthogonal 'click' reactions is the stability of the resulting product (equation 1.6).

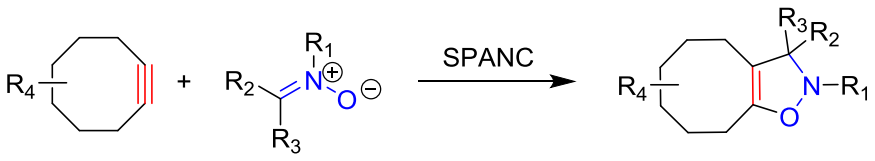

Equation 1.6 – Isoxazoline synthesis via SPANC. Selection of $R_{(1-3)}$ groups at the three attachment sites on the nitrone allow for diverse bioorthogonal probe development while allowing modulation of SPANC reactivity and product stability.

The isoxazoline product formed by SPANC reactions involving activated acyclic nitrones has been shown to be thermally unstable, resulting in a rearranged azomethine ylide followed by hydrolysis. While this may hinder the application of certain acyclic nitrones in metabolic labelling experiments, covalent connectivity remains intact and with proper design of the nitrone reporter, metabolic labelling is still viable. Thermal degradation of this type has not been observed for isoxazolines derived from endocyclic nitrones, which taken together with the generally superior reaction rates and hydrolytic stability observed, makes endocyclic nitrones more attractive for biological applications.

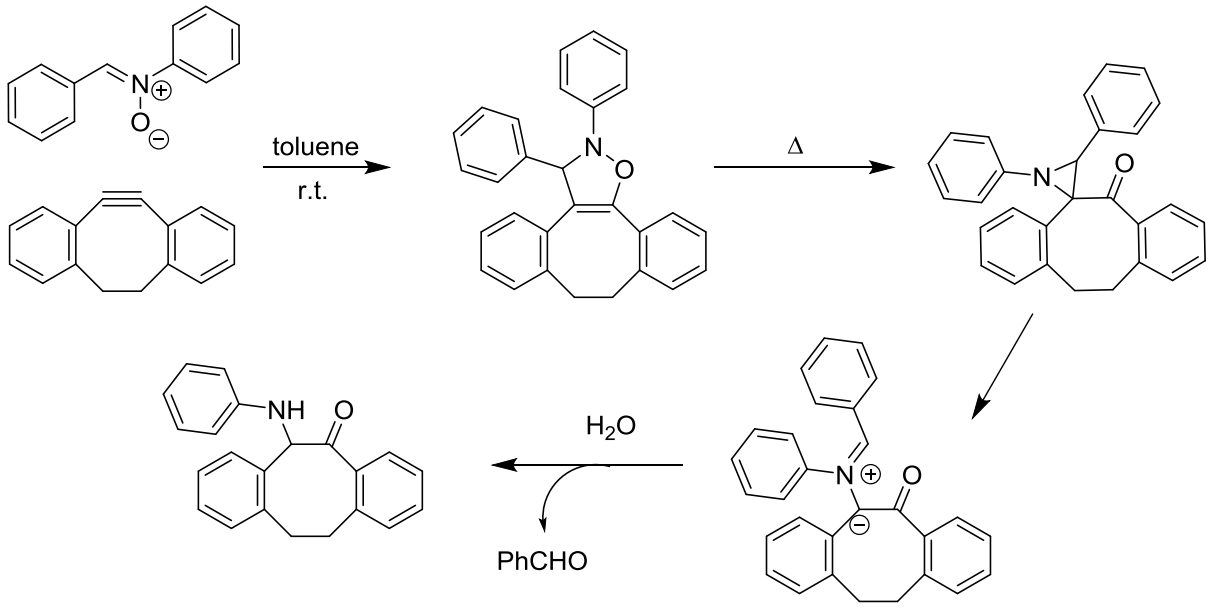

Scheme 1.2 – Thermal rearrangement of isoxazoline product after SPANC with *N*-phenylbenzylimine *N*-oxide and dibenzylcycloocytne (DBCO).[17,39] Aziridine ring-opening followed by hydrolysis and expulsion of benzaldehyde leads to the formation of a β-amino ketone.

Second-order rate constants of up to 58.8 $M^{-1}s^{-1}$ have been observed for SPANC reactions with BARAC, more than a 60-fold increase over the analogous reaction with benzyl azide.[37,40] Other strained alkynes such as 4-dibenzocyclooctynol (DIBO) and bicyclo[6.1.0]nonyne (BCN) have also been shown to react more rapidly with strained nitrones than with benzyl azide.[17,38,41] The increased reaction rates, stereoelectronic flexibility, and the bioorthogonality of SPANC reactions merit their position in the chemical biology toolbox and predicate that further evaluation of these reactions will elucidate the utility of SPANC as a click reaction in both biological and non-biological settings.

'Double-Click' Labelling

As with classical 'click' reactions used for materials preparation, certain bioorthogonal reactions are also orthogonal to each other, allowing for the simultaneous or sequential dual labelling of biomolecules. In 2011, Nguyen *et al* showed site-specific dual labelling of a recombinant calmodulin protein in E. *coli* expressing a Threonine→Cysteine mutation and an unnatural amino acid (UAA) bearing a protected aminothiol moiety. The UAA was incorporated at an amber stop codon site using an evolved aminoacyl *t*RNA synthetase/$tRNA_{CUA}$ pair. The recombinant protein was first labelled at the Cysteine site with a maleimide derivative of a rhodamine dye before the UAA was freed and condensed with a 2-Cyanobenzothiazole fluorescein dye. SDS-PAGE revealed the site-specific incorporation of both the Rhodamine dye and Fluorescein, confirming that the recombinant protein was in fact dual labelled.[42] This approach relies on a protection and deprotection strategy to achieve dual labelling - a principle that 'click' chemistry attempts to avoid. Other, more efficient strategies are therefore more desirable.

Schoch *et al* have demonstrated that CuAAC and *trans*-Cyclooctene/Tetrazine ligations are mutually orthogonal by modifying DNA oligonucleotides with both *trans*-Cyclooctene and

terminal alkynes and introducing both a fluorophore-modified azide (and accompanying Cu(I) catalyst) and tetrazine simultaneously.[43] No observable cross-reactivity was reported, presumably due to the opposing electronic nature of the dieneophile/dipolarophiles used. Alkynes that are highly reactive in CuAAC reactions tend to have low HOMO energy levels which are undesirable in inverse electron demand cycloadditions due to the inherently large energy gap between the HOMO of the dieneophile/dipolarophile and the LUMO of the diene/dipole. When the dual-functionalized DNA oligonucleotides were reacted with only *trans*-Cyclooctene or an azide under catalytic copper conditions no dual labelling was observed, indicating that *trans*-Cyclooctene/Tetrazine ligation is mutually orthogonal with CuAAC reactions, and that duplex labelling where two biomolecules are independently labelled with either *trans*-Cyclooctene/Tetrazine or CuAAC reagents and reacted with the appropriate complementary molecules could report on the location or interaction of two biomolecules simultaneously.

Simultaneous Labelling of Multiple Biomolecules

To show the potential of bioorthogonal and mutually orthogonal click chemistry to label and monitor multiple biomacromolecules in living systems, Karver *et al* reported the simultaneous multi-target fluorescent labelling of two co-cultured cancer cell lines by mutually orthogonal click reactions in 2011.[44] The group pre-targeted each cell line with fluorescent antibodies that were modified in vitro to bear either a *trans*-Cyclooctene reactive group or Dibenzylcyclooctyne (DBCO). Once decorated with antibodies, the cells were incubated with a mixture of tetrazine-fluorophore and azide-fluorophore conjugates which allowed the observation of specific cell-surface labelling of each cell line by fluorescent imaging at spectrally distinct channels. This study shows the mutual orthogonal nature of *trans*-Cyclooctene/tetrazine and SPAAC ligations

in a live-cell environment, as well as a method to selectively incorporate a highly reactive reporter tag into one cell type within a mixture. Although the pre-targeting of biomolecules by antibody complexation is limited to biomacromolecules, pre-targeting with antibodies followed by *in vivo* click reactions have shown to be useful in whole-organism radiolabelling experiments, particularly in tumour imaging.[45,46]

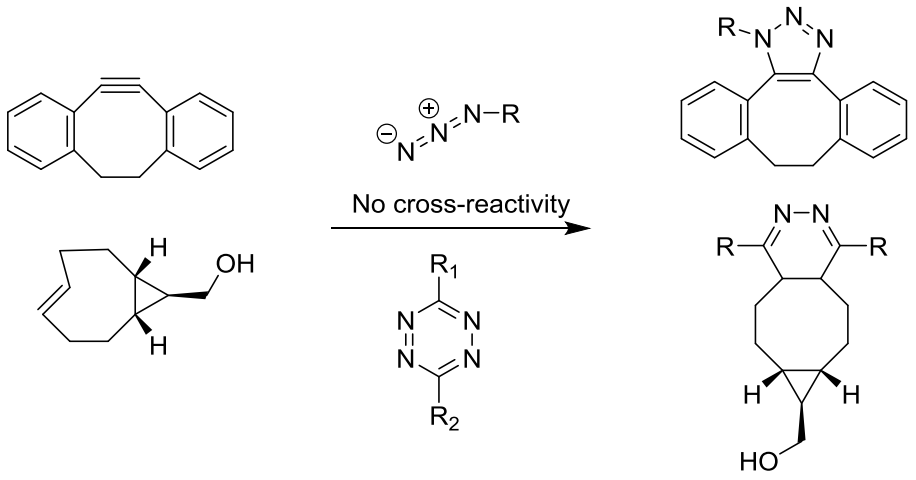

Scheme 1.3 – Mutual orthogonality in simultaneous SPAAC and *trans*-Cyclooctene/Tetrazine ligation reported by Karver *et al*. No evidence of DBCO/tetrazine or *trans*-cyclooctene/azide was observed.[44]

Multiplex bioorthogonal labelling has been extended as far as labelling three distinct molecular targets in a two-stage approach. Staudinger ligation, norbornene/tetrazine ligation, and CuAAC have been employed by Willems *et al* to label the three catalytic subunits (β_1, β_2, and β_5) of the mammalian 20S proteasome.[47] Three activity-based probes (ABP), each containing a reactive group specific for one subunit as well as a bioorthogonal reporter molecule were synthesized based on subunit-specific inhibitors. Human embryonic kidney (HEK) cell extracts were incubated with a mixture of all three probes followed by simultaneous treatment with a mixture of the complementary click functionalities (triaryl phosphine, tetrazine, and azide with a copper catalyst) conjugated to a fluorescent dye or biotin, and the labelling results were evaluated by SDS-PAGE. High levels of background fluorescence were observed when using copper sulfate and it was determined that under the conditions used, tetrazines are not compatible with CuAAC conditions. The Willems group then modified their approach to incubate the cell lysates with all three probes and perform the Staudinger ligation and norbornene/tetrazine ligation simultaneously, followed by a buffer exchange and subsequent CuAAC. With this two-stage approach, all three catalytic subunits of the 20S proteasome were effectively labelled and the first example of triple bioorthogonal ligation was reported.

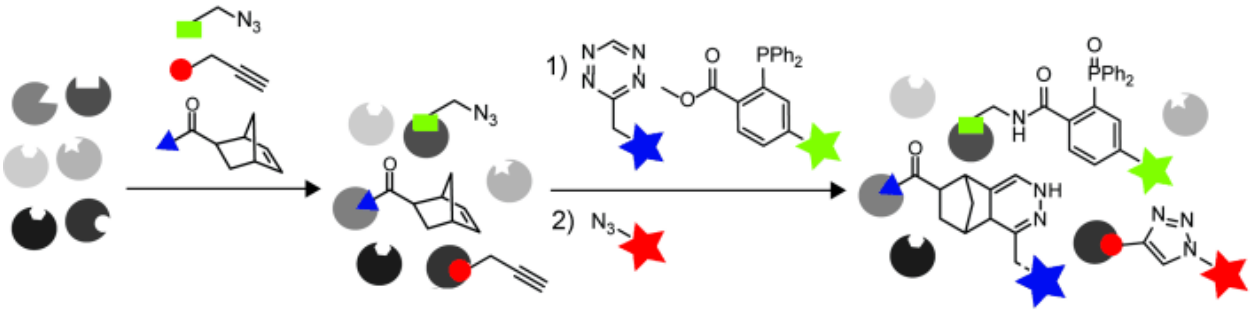

Scheme 1.4 – Triple ligation strategy used *in-vitro* to label three catalytic subunits of the mammalian 20S proteasome employing three mutually orthogonal and bioorthogonal labelling methods. *Trans* cyclooctene/tetrazine ligation was carried out in concert with traceless Staudinger ligation followed by CuAAC. Adapted from reference 47.

To date, research pertaining to dual and multiplex labelling of biomolecules has focused on developing methods that are orthogonal to each other as well as the biological system. Tuning of bioorthogonal reactions has largely been limited to achieving increasingly large second-order rate constants, while understandably so, less emphasis has been placed on reactions that proceed more slowly. Given that a diverse series of 1,3-dipoles can be generated based on the high degree of stereoelectronic flexibility of nitrones, and the recent progress in gaining access to strained dipolarophiles, it is reasonable that optimal dipole/dipolarophile pairs could be realised. Classic physical organic chemistry methods can offer insight into the fundamental reactivity in strain-promoted cycloadditions, particularly in SPANC where both reaction components are capable of being tuned to elicit selective reactivity. Altering one parameter at a time and conducting linear free-energy relationship studies will allow for the identification of reactivity patterns that could ultimately lead to the design of mutually orthogonal SPANC reactions and multiplex labelling of biomolecules within one system of reactivity using one set of reaction conditions.

Two-stage bioorthogonal ligation, when used in conjunction with classical biochemical studies shows great potential to be used in gaining information about biological processes that cannot be obtained through classical studies alone. Careful examination of the factors governing the reactivity of these 'click' reactions will provide the information necessary to evolve the chemistry and develop a wider array of tools. While increased reactivity will often lead to decreased selectivity, developing the flexibility of 'near-perfect' reactions will give researchers a greater ability to select the right tool for the application, allowing for more efficient progress in challenging fields of study. Performing fundamental reactivity studies will lead to finding the balance between reactivity and selectivity in SPANC chemistry, while creative application of

these tools will lead to novel materials, pharmaceuticals, and a greater understanding of biological systems at the chemical level.

Outline of Work

This work has focused on probing the reactivity of SPANC with BCN by physical organic methods and exploiting the observed reactivity trends that can be used in duplex bioorthogonal labelling experiments. A competition experiment of simultaneous SPANC reactions is offered as a proof-of-principle, as well as live-cell imaging of bacterial cultures to exemplify the potential applications of this technology.

References

(1) Kolb, H. C.; Finn, M. G.; Sharpless, K. B. *Angewandte Chemie International Edition* **2001**, *40*, 2004.

(2) Bohacek, R. S.; McMartin, C.; Guida, W. C. *Medicinal Research Reviews* **1996**, *16*, 3.

(3) Huisgen, R.; Knorr, R.; Möbius, L.; Szeimies, G. *Chemische Berichte* **1965**, *98*, 4014.

(4) Hoyle, C. E.; Bowman, C. N. *Angewandte Chemie International Edition* **2010**, *49*, 1540.

(5) Iha, R. K.; Wooley, K. L.; Nyström, A. M.; Burke, D. J.; Kade, M. J.; Hawker, C. J. *Chemical Reviews* **2009**, *109*, 5620.

(6) Ennist, J. H.; Gobrogge, E. A.; Schlick, K. H.; Walker, R. A.; Cloninger, M. J. *ACS Applied Materials & Interfaces* **2014**, *6*, 18087.

(7) Lutz, J.-F. *Angewandte Chemie International Edition* **2007**, *46*, 1018.

(8) Zong, H.; Goonewardena, S. N.; Chang, H.-N.; Otis, J. B.; Baker Jr, J. R. *Bioorganic & Medicinal Chemistry* **2014**, *22*, 6288.

(9) McKay, Craig S.; Finn, M. G. *Chemistry & Biology* **2014**, *21*, 1075.

(10) Carroll, L.; Evans, H. L.; Aboagye, E. O.; Spivey, A. C. *Organic & Biomolecular Chemistry* **2013**, *11*, 5772.

(11) Zhang, X.; Zhang, Y. *Molecules* **2013**, *18*, 7145.

(12) Prescher, J. A.; Bertozzi, C. R. *Nat Chem Biol* **2005**, *1*, 13.

(13) Sletten, E. M.; Bertozzi, C. R. *Angewandte Chemie International Edition* **2009**, *48*, 6974.

(14) Jewett, J. C.; Bertozzi, C. R. *Chemical Society Reviews* **2010**, *39*, 1272.

(15) Hofmann, K.; Finn, F. M.; Kiso, Y. *Journal of the American Chemical Society* **1978**, *100*, 3585.

(16) Blackman, M. L.; Royzen, M.; Fox, J. M. *Journal of the American Chemical Society* **2008**, *130*, 13518.

(17) McKay, C. S.; Moran, J.; Pezacki, J. P. *Chemical Communications* **2010**, *46*, 931.

(18) Moran, J.; McKay, C. S.; Pezacki, J. P. *Canadian Journal of Chemistry* **2011**, *89*, 148.

(19) Hao, Z.; Hong, S.; Chen, X.; Chen, P. R. *Accounts of Chemical Research* **2011**, *44*, 742.

(20) Shimomura, O.; Johnson, F. H.; Saiga, Y. *Journal of Cellular and Comparative Physiology* **1962**, *59*, 223.

(21) Chalfie, M.; Tu, Y.; Euskirchen, G.; Ward, W.; Prasher, D. *Science* **1994**, *263*, 802.

(22) Dzeng, R. K.; Jha, H. C.; Lu, J.; Saha, A.; Banerjee, S.; Robertson, E. S. *Molecular Oncology* **2014**, *9*, 365.

(23) Zornetta, I.; Brandi, L.; Janowiak, B.; Dal Molin, F.; Tonello, F.; Collier, R. J.; Montecucco, C. *Cellular Microbiology* **2010**, *12*, 1435.

(24) Zheng, S.; Zhang, G.; Li, J.; Chen, P. R. *Angewandte Chemie International Edition* **2014**, *53*, 6449.

(25) Saxon, E.; Luchansky, S. J.; Hang, H. C.; Yu, C.; Lee, S. C.; Bertozzi, C. R. *Journal of the American Chemical Society* **2002**, *124*, 14893.

(26) Saxon, E.; Armstrong, J. I.; Bertozzi, C. R. *Organic Letters* **2000**, *2*, 2141.
(27) Saxon, E.; Bertozzi, C. R. *Science* **2000**, *287*, 2007.
(28) Kennedy, D. C.; McKay, C. S.; Legault, M. C. B.; Danielson, D. C.; Blake, J. A.; Pegoraro, A. F.; Stolow, A.; Mester, Z.; Pezacki, J. P. *Journal of the American Chemical Society* **2011**, *133*, 17993.
(29) Kennedy, D. C.; Lyn, R. K.; Pezacki, J. P. *Journal of the American Chemical Society* **2009**, *131*, 2444.
(30) Worrell, B. T.; Malik, J. A.; Fokin, V. V. *Science* **2013**, *340*, 457.
(31) Agard, N. J.; Prescher, J. A.; Bertozzi, C. R. *Journal of the American Chemical Society* **2004**, *126*, 15046.
(32) Garcia-Hartjes, J.; Dommerholt, J.; Wennekes, T.; van Delft, F. L.; Zuilhof, H. *European Journal of Organic Chemistry* **2013**, *2013*, 3712.
(33) Chigrinova, M.; McKay, C. S.; Beaulieu, L.-P. B.; Udachin, K. A.; Beauchemin, A. M.; Pezacki, J. P. *Organic & Biomolecular Chemistry* **2013**, *11*, 3436.
(34) Liu, F.; Liang, Y.; Houk, K. N. *Journal of the American Chemical Society* **2014**, *136*, 11483.
(35) Selvaraj, R.; Fox, J. M. *Current Opinion in Chemical Biology* **2013**, *17*, 753.
(36) McKay, C. S.; Blake, J. A.; Cheng, J.; Danielson, D. C.; Pezacki, J. P. *Chemical Communications* **2011**, *47*, 10040.
(37) McKay, C. S.; Chigrinova, M.; Blake, J. A.; Pezacki, J. P. *Organic & Biomolecular Chemistry* **2012**, *10*, 3066.
(38) MacKenzie, D. A.; Pezacki, J. P. *Canadian Journal of Chemistry* **2014**, *92*, 337.
(39) MacKenzie, D. A.; Sherratt, A. R.; Chigrinova, M.; Cheung, L. L. W.; Pezacki, J. P. *Current Opinion in Chemical Biology* **2014**, *21*, 81.
(40) Gordon, C. G.; Mackey, J. L.; Jewett, J. C.; Sletten, E. M.; Houk, K. N.; Bertozzi, C. R. *Journal of the American Chemical Society* **2012**, *134*, 9199.
(41) Dommerholt, J.; Schmidt, S.; Temming, R.; Hendriks, L. J. A.; Rutjes, F. P. J. T.; van Hest, J. C. M.; Lefeber, D. J.; Friedl, P.; van Delft, F. L. *Angewandte Chemie International Edition* **2010**, *49*, 9422.
(42) Nguyen, D. P.; Elliott, T.; Holt, M.; Muir, T. W.; Chin, J. W. *Journal of the American Chemical Society* **2011**, *133*, 11418.
(43) Schoch, J.; Staudt, M.; Samanta, A.; Wiessler, M.; Jäschke, A. *Bioconjugate Chemistry* **2012**, *23*, 1382.
(44) Karver, M. R.; Weissleder, R.; Hilderbrand, S. A. *Angewandte Chemie International Edition* **2012**, *51*, 920.
(45) Rossin, R.; Robillard, M. S. *Current Opinion in Chemical Biology* **2014**, *21*, 161.
(46) Rossin, R.; van Duijnhoven, S. M. J.; Läppchen, T.; van den Bosch, S. M.; Robillard, M. S. *Molecular Pharmaceutics* **2014**, *11*, 3090.
(47) Willems, L. I.; Li, N.; Florea, B. I.; Ruben, M.; van der Marel, G. A.; Overkleeft, H. S. *Angewandte Chemie International Edition* **2012**, *51*, 4431.

2. Kinetic Studies of SPANC with Strained Alkyne BCN

Introduction

In the recent literature regarding SPAAC reactions, a large emphasis has been placed on obtaining increasingly large second-order rate constants in order to minimize the concentration of labelling reagents in cellular imaging experiments.[1-5] This in turn minimizes the potential perturbation of the native functions of the biological system by the exogenous reagents. The second-order rate constant of SPAAC reactions depend heavily on the strain energy imposed on the cyclooctyne and on the electronic nature of any substituents located at the propargyl position. Increased strain energy is often achieved through benzanulation and minimizing the number of sp^3-hybridized atoms in the cyclooctyne core. Due to the lack of sp^3-hybridized atoms, benzanulated cyclooctynes (DIBO, DIBAC, BARAC, etc.) possess high levels of conjugation and relatively low electron density at the alkyne which results in a lowered LUMO energy level when compared to the unsubstituted cyclooctyne (OCT). Conjugated electron-withdrawing groups or inductive electron withdrawing groups located at the propargyl position also contribute to this effect and to increasing the rate constant of SPAAC reactions. The majority of reported strained alkynes share this rigid electron deficiency.

BCN, however, displays k_2 values in SPAAC reactions with benzyl azide that are comparable to other strained alkynes while lacking benzanulation and propargylic electron withdrawing groups. Aside from the two *sp*-hybridized carbon atoms of the alkyne, BCN is also comprised entirely of sp^3-hybridized atoms. These features collectively lead to a higher density functional theory (DFT) calculated LUMO energy than DIFO, DIBO, DIBAC, or BARAC and therefore would be expected to show reduced rate constants in comparison.[6] Fusion of the cyclopropane ring is

responsible for maintaining the competitive rate constants of BCN. These competitive rates, taken together with the unique stereoelectronic structure have the potential to impart reactivity patterns that are distinct from other highly activated strained alkynes and prompt the study of BCN's reactivity in additional strain-promoted cycloadditions.

Table 2.1 – DFT calculated LUMO energy levels and measured rate constants with benzyl azide for select strained alkynes

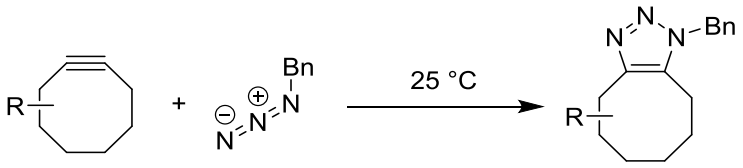

Cyclooctyne	LUMO (kcal/mol)[6]	k_2 ($M^{-1}s^{-1}$) [solvent]
OCT	43.5	0.0012 [CD_3CN][1]
DIFO	36.2	0.076 [CD_3CN][7]
BCN	38.2	0.19-0.29 [1:2 CD_3CN/D_2O][3]
DIBO	36.1	0.057 [CH_3OH][8]
DIBAC	35.2	0.31 [CD_3OD][9]
BARAC	34.6	0.96 [CD_3CN][10]

Previously, strain-promoted 1,3-dipolar cycloadditions employing nitrones rather than azides were reported independently by our lab[11] and the van Delft group[3] for metabolic labelling applications. In our lab, the reactivity of DIBO and BARAC in cycloadditions with nitrones have been evaluated,[11,12] finding that the second-order rate constants (k_2) obtained in SPANC reactions are as much as 120 times greater than those observed in SPAAC reactions,[13] BARAC has been shown to be insensitive towards electronic substituent effects of the nitrone component, presumably due to the delocalization of electron density around the alkyne as well as the low LUMO energy. The alkyne of BCN is more electron rich, has localized electron density around the alkyne, and has a higher calculated LUMO energy level than BARAC. These features may

sensitize BCN to the substituent effects of the 1,3-dipole in cycloadditions. One second-order rate constant for a SPANC reaction involving BCN and an electron-deficient acyclic nitrone in a mixture of acetonitrile and water was reported in the initial account of BCN;[3] however, the reaction has not been thoroughly explored by physical organic methods.

Hypothesis

The relatively high calculated LUMO energy and localized electron density within the alkyne of BCN, in comparison to other strained alkynes, will increase the sensitivity of BCN toward electronic changes of the 1,3-dipole in SPANC reactions. Exploring the BCN SPANC reaction will allow for the design of an optimal nitrone reacting partner to achieve a highly selective cycloaddition with rapid reaction kinetics that may find new utility in metabolic labelling experiments.

Results and Discussion

The unique stereoelectronic properties of BCN in addition to the large second-order rate constant (k_2) in reaction with benzyl azide and one acyclic nitrone prompted the systematic investigation of BCN's reactivity with acyclic and endocyclic nitrones. To explore the trends in reactivity, a series of structurally similar but electronically distinct acyclic nitrones was therefore prepared and the second-order rate constant of each reaction was determined. The reactivity of BCN with endocyclic nitrones was also explored to probe the influence of nitrone conformation on the reaction rates of cycloadditions involving BCN. After determining what factors affect the largest change in the rate constant of these SPANC reactions, hypotheses regarding how best to exploit the observed reactivity trends for use in metabolic labelling experiments could then be formulated. To this end, BCN was first prepared according to the protocol published by Dommerholt *et al*[3] as outlined in Scheme 2.1.

Commercially available 1,5-cyclooctadiene was reacted with ethyl diazoacetate under rhodium (II) acetate-catalyzed conditions, resulting in a mixture of **2.1a exo** and **2.1a endo** which were carefully separated by flash column chromatography. **2.1a exo** was stored and used for other projects, while the ester moiety of **2.1a endo** was reduced to the corresponding alcohol before preparing the vicinal dibromide and performing two elimination reactions with potassium tert-butoxide, resulting in endo BCN (**2.1**) as a pale yellow waxy solid. This two-step, four-stage synthetic procedure makes BCN more synthetically accessible than some other strained alkynes (DIBO, or BARAC for example) and increases its appeal as a convenient reagent for strain-promoted cycloadditions.

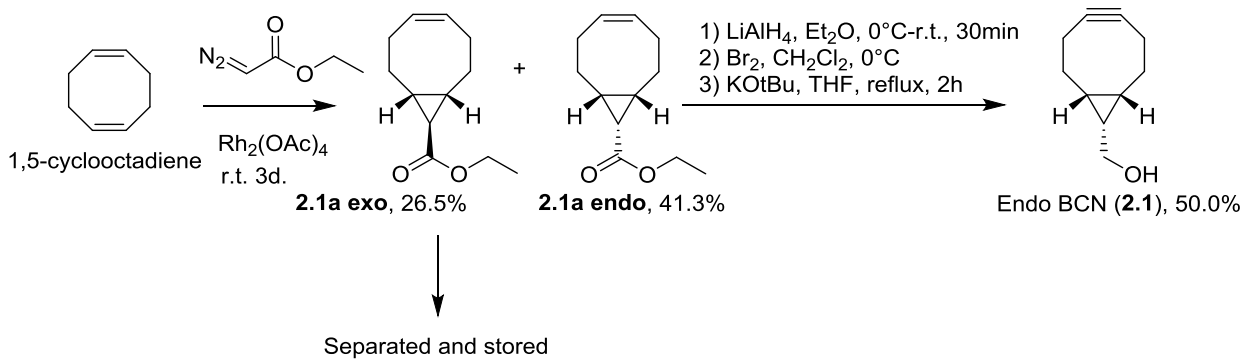

Scheme 2.1 – Synthetic procedure for preparing BCN from 1,5-Cyclooctadiene. Yields reported reflect the isolated yields obtained for each step after chromatography.

Kinetic Studies and Methodology – Acyclic nitrones

Second-order rate constants (k_2) of SPANC reactions involving BCN and acyclic nitrones **2.2-2.8** were determined by ^{1}H NMR under second-order reaction conditions. Stock solutions of both BCN and each nitrone were prepared in deuterated Methanol and combined in an NMR tube to achieve an equal initial concentration of each reagent. Each reaction was incubated at 25˚C in the NMR spectrometer where successive ^{1}H NMR spectra were recorded until the reaction was >95% complete.

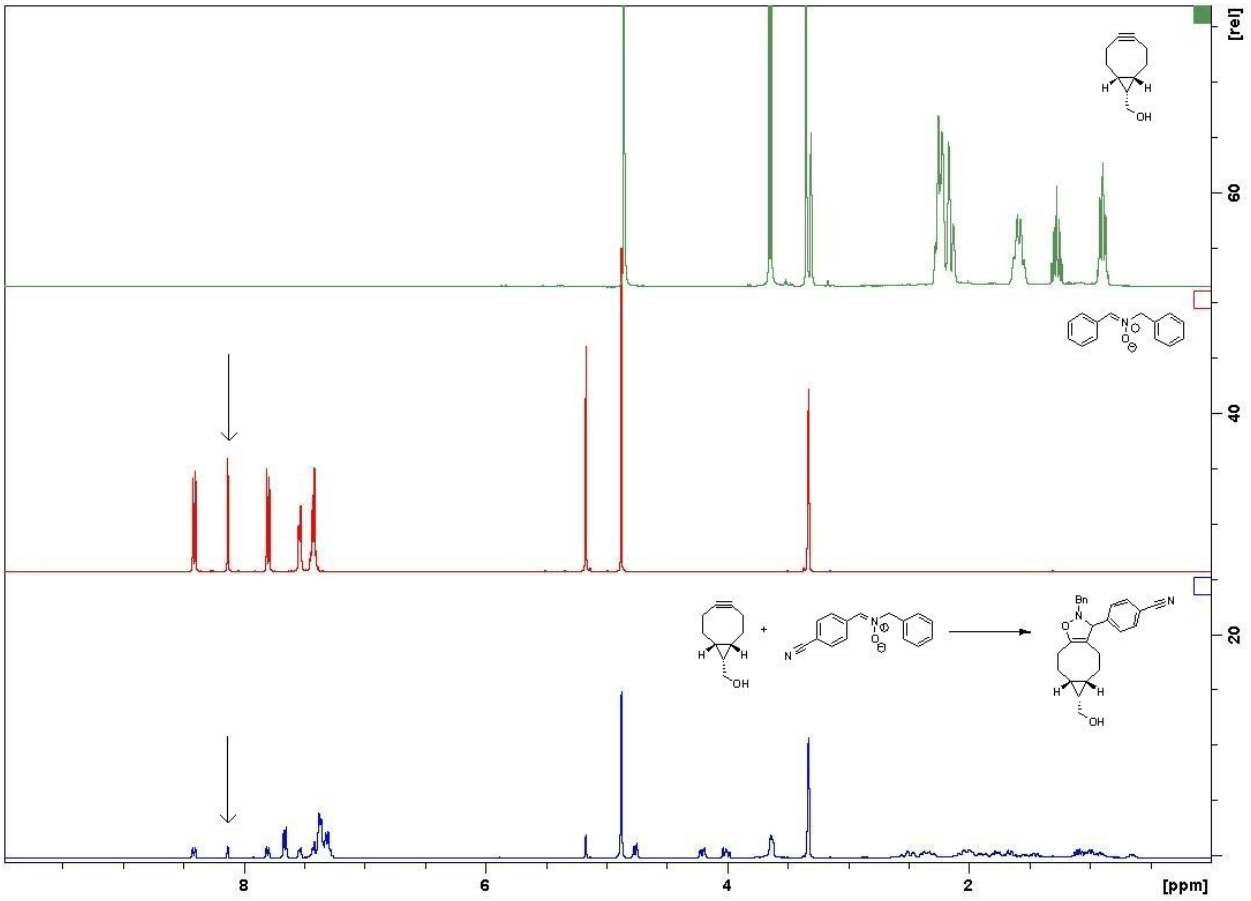

Figure 2.1 – SPANC reaction progress monitored by the decay in characteristic ^{1}H NMR signals. The vertical arrows point to the signal resulting from the proton on the nitrone α-carbon, highlighting the decay of this signal as the reaction proceeds. Samples were dissolved in deuterated Methanol.

The declining concentration of the nitrone starting material was monitored by the integration of the signal corresponding to the proton of the nitrone α carbon. The integration value of this signal was multiplied by the initial concentration of nitrone in the reaction mixture to obtain the instantaneous concentration of the remaining nitrone. The resulting instantaneous concentrations were then entered into the linear approximation of the integrated second-order rate law and plotted as a function of time.

Second-Order Rate Law: *Integrated Second-Order Rate Law:*

$rate = k_2[\text{Alkyne}][\text{Nitrone}]$ $1/[A] = 1/[A]_0 + kt$

When the initial concentration of the alkyne is equal to the initial concentration of the nitrone and each reagent is consumed at the same rate, the integration of the rate law is simplified and the following linear relationship can be obtained:

$$1/[\text{Nitrone}] - 1/[\text{Nitrone}]_0 = k_2 t$$

After plotting $1/[\text{Nitrone}] - 1/[\text{Nitrone}]_0$ versus time in seconds, the slope of the resulting trend line represents the second-order rate constant (k_2 in $M^{-1}s^{-1}$) for the SPANC reaction at 25 °C. Rate constants were measured by ^{1}H NMR to allow for the use of high reagent concentrations so these SPANC reactions could be completed on the minutes-hours timescale rather than the days-weeks required by more sensitive methods. A 1:1 molar ratio of nitrone:alkyne was used in accordance with the procedure carried out by Bertozzi *et al* in the initial report of SPAAC in 2004.[14] Although this method is less accurate in terms of the true rate constant value than rate measurement under pseudo-first order conditions or by using substantially different initial reagent concentrations, it offered a more direct rate comparison to those initially reported for

SPAAC and simplified the calculations required to obtain the second-order rate constants and identify the reactivity trends of SPANC reactions with BCN.

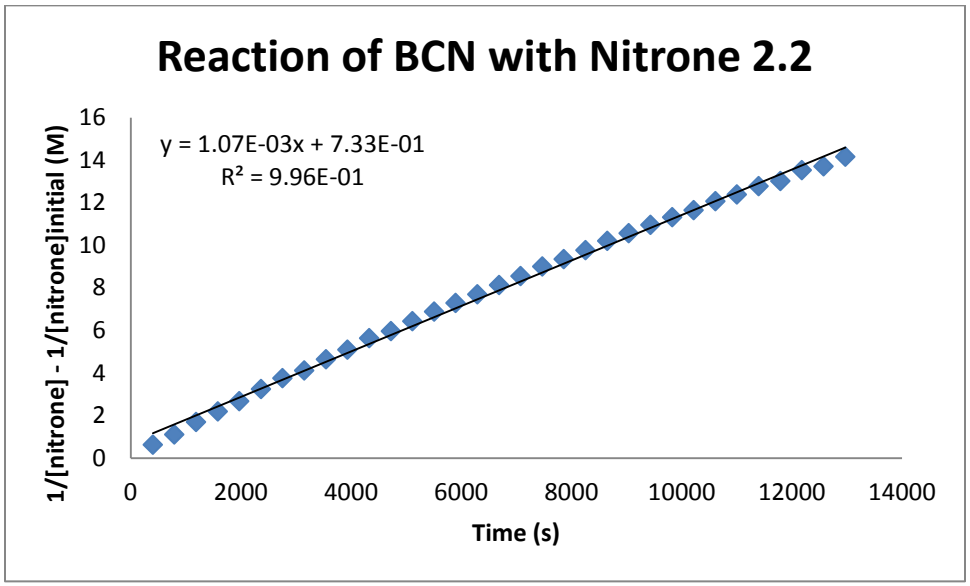

Figure 2.2 – Graphical determination of the second-order rate constant (k_2) of the SPANC reaction between BCN and nitrone 2.2. Slope of the trendline indicates the second-order rate constant.

SPANC of BCN with acyclic nitrones

A series of acyclic nitrones varying in the electronic nature of the functional group located at the *para* position of the aromatic ring conjugated to the C=N double bond of the nitrone were prepared in order to evaluate the effect of electronic changes of the nitrone component on the rate of SPANC reactions with BCN. Nitrones **2.2-2.5, 2.7,** and **2.8** were prepared by micelle catalyzed condensation of N-Benzyl-hydroxylamine with the corresponding benzaldehyde, while nitrone **2.6** was prepared in a similar fashion without catalysis. Magnesium sulfate was employed to scavenge the water produced during the condensation reaction and drive the nitrone formation to completion. Nitrones **2.2-2.5, 2.7,** and **2.8** were obtained in pure form from Dr. Craig McKay.

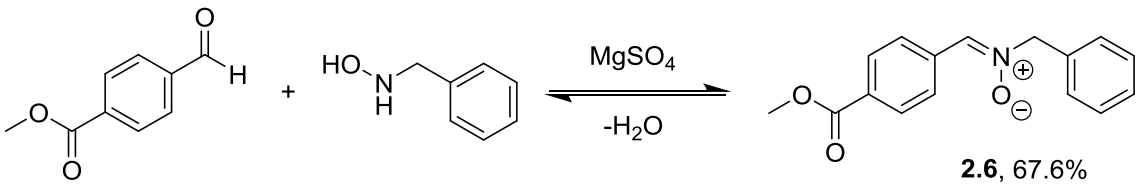

Equation 2.1 - Synthetic procedure for the preparation of acyclic nitrone 2.6. Nitrones 2.2-2.8 can be prepared in this fashion from substituted benzaldehydes and *N*-benzylhydroxylamine using magnesium sulfate as a water scavenger to prevent the reverse reaction.

Stock solutions of each nitrone in deuterated Methanol were prepared and combined with a stock solution of BCN in equimolar reaction concentrations in a clean and dry NMR tube. The reactions were monitored by ^{1}H NMR at 25˚C and the gradual decline of the nitrone α-C proton signal was observed.

Table 2.2 – Second-order rate constants (k_2) and Hammett σ_p values for acyclic nitrones in SPANC reactions. Second-order rate constants were measured by ^{1}H NMR spectroscopy while σ_p values were obtained from reference 15.

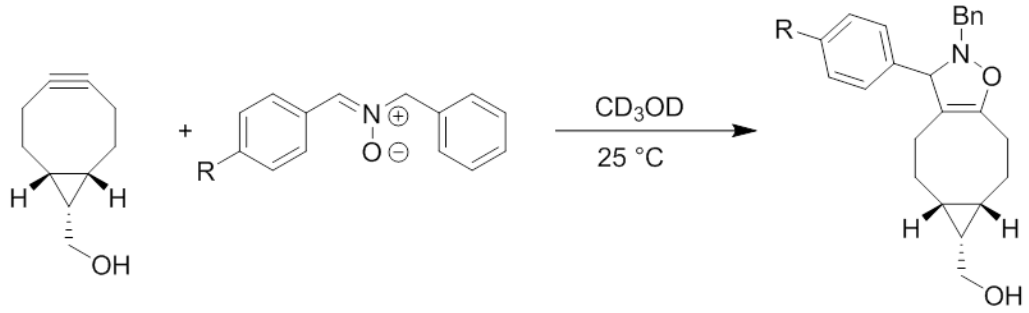

Nitrone	Structure	σ_p[15]	k_2 ($M^{-1}s^{-1}$)	log(k_{2X}/k_{2H})
2.2	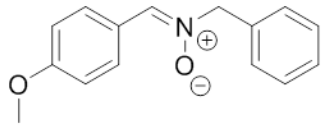	-0.268	0.00107	-0.436
2.3	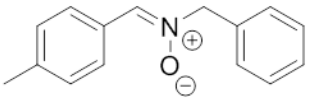	-0.170	0.00225	-0.113
2.4	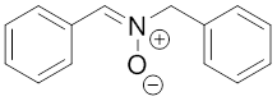	0	0.00292	0
2.5	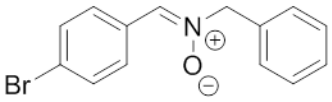	0.232	0.00648	0.346
2.6	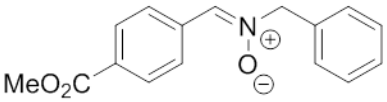	0.402	0.0107	0.564
2.7	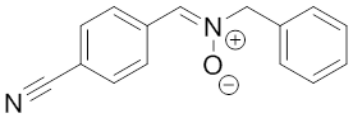	0.660	0.0210	0.857
2.8	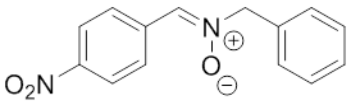	0.778	0.0291	0.999

The electron-deficient nitrone **2.8** showed a 27-fold rate enhancement over the electron-rich nitrone **2.2**, indicating that BCN is sensitive to the electronic effects of substituents on the nitrone in SPANC reactions. To further quantify the result of this linear free-energy relationship study, a Hammett plot was constructed (figure 2.3).

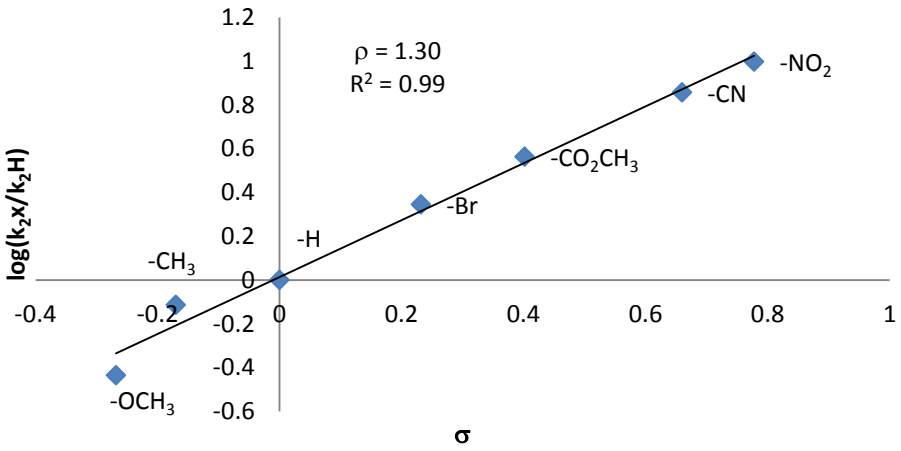

Figure 2.3 – Hammett Plot depicting the electronic sensitivity of SPANC reactions involving BCN and acyclic nitrones. Electron-withdrawing groups on the nitrones involved accelerate the reaction by reducing the build-up of negative charge in the transition state.[16]

A ρ value of 1.30 was obtained, indicating that there is a modest build-up of negative charge during the transition state. From this information, we can conclude that SPANC reactions involving BCN will proceed at much higher rates when electron-deficient nitrones are employed when compared to electron-rich nitrones. Previously in our lab, a Hammett plot depicting the electronic substituent effects of acyclic nitrones on the rates of SPANC reactions involving BARAC was prepared.

The ρ value obtained in SPANC reactions with BARAC (ρ = 0.25) [12] is lower than that observed with BCN (ρ = 1.30) ,[16] indicating that there is a greater negative charge buildup in the transition state in BCN SPANC reactions. This is likely due primarily to the higher LUMO energy and increased electron density of the alkyne of BCN.

Kinetic Studies and Methodology – Endocyclic Nitrones

Previously, our lab has reported increased reaction rates in SPANC reactions when endocyclic nitrones are employed.[11] We sought to increase the rates of SPANC reactions involving BCN, and to observe whether the electronic sensitivity of BCN is conserved across reactions with endocyclic nitrones. In order to explore the reactivity of BCN with endocyclic nitrones in SPANC reactions, nitrones **2.9-2.11** were prepared and the second-order rate constants (k_2) were measured. Since endocyclic nitrones display larger rate constants than their acyclic counterparts, these reactions were monitored by UV-Visibleibleible spectrophotometry under pseudo first-order conditions. UV-Visibleibleible spectrophotometry is a much more sensitive technique than ^{1}H NMR and therefore allows reactions to be monitored at lower reagent concentrations. The declining nitrone concentrations were monitored by the decrease in absorption at the characteristic wavelengths as a function of time. Measurement of k_2 under pseudo first-order conditions is more reliable than the direct measurement of second-order rate constants because the measurements are less affected by minute discrepancies in the initial concentrations of the reagents.

Second-Order Rate law:

$$rate = k_2[\text{Alkyne}][\text{Nitrone}]$$

When one reagent in a binary reaction is present in very large excess, its concentration remains effectively constant throughout the course of the reaction and can be incorporated as a constant in the rate equation. Performing a second-order reaction under these conditions simplifies the rate equation and allows for the determination of a series of *pseudo* first-order rate constants (k_{obs}) at different concentrations of excess reagent, which allows the reaction to be treated mathematically as if it were a first-order reaction.

Pseudo First-Order Rate Law:

$$rate = k_{obs}[\text{Nitrone}]$$

After obtaining k_{obs} at several significantly (≥10%) different concentrations of excess reagent a plot of k_{obs} vs excess reagent concentration will reveal the second-order rate constant (k_2) for the binary reaction as the slope of the trend line.

Table 2.3 – Kinetic rate measurement of SPANC reaction involving BCN and nitrone 2.9 in Methanol at 25 ± 0.1°C. k_{obs} values were measured by UV-Visibleible spectrophotometry based on the nitrone absorption at a characteristic wavelength.

Nitrone	Structure	[BCN] (mM)	k_{obs} (s^{-1})
2.9	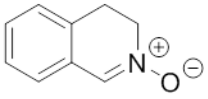	5	3.20×10^{-3}
		4.5	2.92×10^{-3}
		4	2.68×10^{-3}
		3.5	2.21×10^{-3}
		3	1.91×10^{-3}

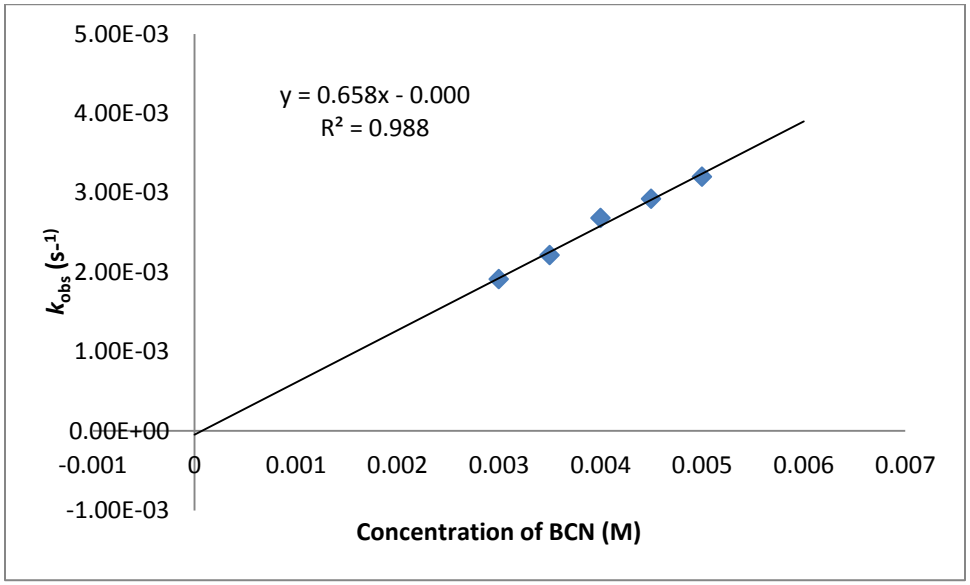

SPANC of BCN with endocyclic nitrones

Nitrone **2.9** was prepared by direct oxidation of the secondary amine 1,2,3,4-tetrahydroisoquinoline by Oxone® in a biphasic medium and was obtained from Mariya Chigrinova in the Pezacki group. 5,5-Dimethyl-1-pyrroline *N*-oxide **2.10** was commercially available, while nitrone **2.11** was prepared according to the following synthetic scheme:

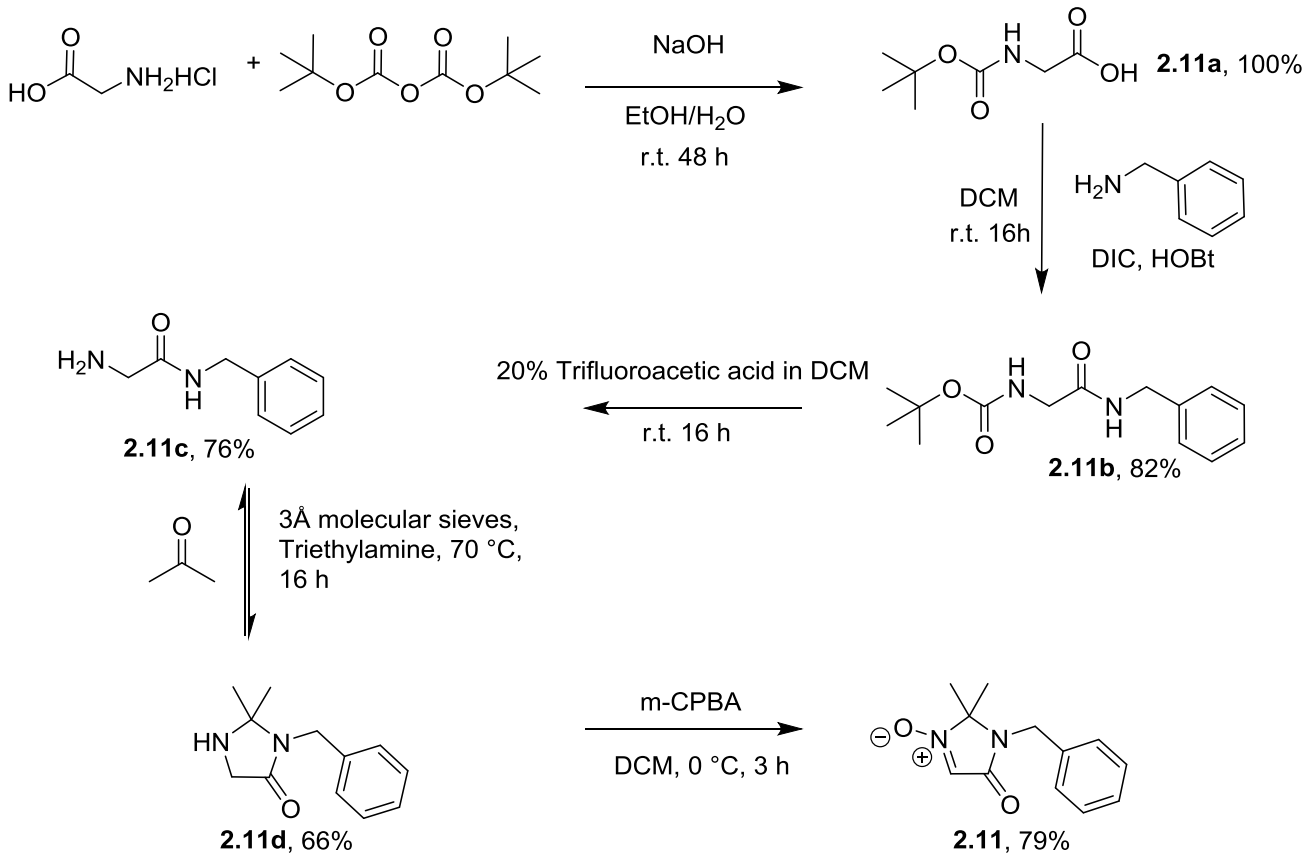

Scheme 2.2 – Synthesis of nitrone 2.11. The amino group of Glycine hydrochloride was Boc protected under basic aqueous conditions and coupled to benzylamine. Trifluoroacetic acid was employed to cleave the Boc group, leading to the primary amine 2.11c. Condensation with acetone followed, scavenging water with molecular sieves to prevent the reverse reaction. The resultant cyclic amine was then oxidized with *meta*-Chloroperoxybenzoic acid. Adapted from reference 20.

Stock solutions of BCN and each nitrone were prepared in Methanol and equilibrated to 25˚C prior to each kinetic trial. In each case, BCN was used as the excess reagent due to its low UV light absorbance. At least five reactions were performed for each cycloaddition beginning with BCN in 100-fold excess and decreasing the excess concentration by 10% in each subsequent trial. The pseudo first-order rate constant was obtained by plotting *ln*(abs) vs time and taking the slope of the trend line as $k_{obs.}$ The five k_{obs} values were then plotted against the concentration of BCN for each trial and the second-order rate constant (k_2) was determined by the slope of the resulting trend line. Treating each of three endocyclic nitrones similarly, it was determined that SPANC reactions with BCN in Methanol could be up to 40 times faster than the analogous SPAAC reaction with benzyl azide. The second-order rate constants observed with BCN are much lower than those observed with BARAC (1.49 $M^{-1}s^{-1}$ versus 46.5 $M^{-1}s^{-1}$ for SPANC with endocyclic nitrones); however, a greater sensitivity to electronic changes of the nitrone component is observed with BCN in SPANC reactions involving either endocyclic or acyclic nitrones. The increased electronic sensitivity of BCN is evidenced by the greater Hammett rho value (1.30 for BCN vs 0.25 for BARAC) and by the near 30-fold rate enhancement observed through the electronic modification of endocyclic nitrones. This shows that while BARAC is more reactive than BCN overall, BCN may be more susceptible to stereoelectronic tuning of SPANC conditions. Since the rate of SPANC reactions involving BCN are strongly influenced by the electronic character of the nitrone, and the reactions appear to be irreversible, the product distribution is likely influenced by the electronic character of the nitrone as well.

Table 2.4 – Second-order rate constants of SPANC reactions with endocyclic nitrones with comparison to SPAAC with benzyl azide. SPANC rate constants were measured under pseudo-first order conditions by UV-Visibleible spectrophotometry with BCN in at least 60-fold excess. Second-order rate constant for SPAAC with BCN in Methanol was measured by ^{1}H NMR under second-order conditions.

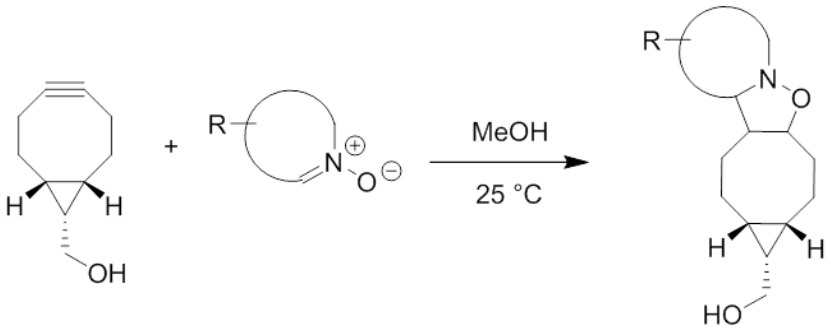

Nitrone	Structure	k_2 ($M^{-1}s^{-1}$)	k_{rel} (Benzyl Azide)
2.9	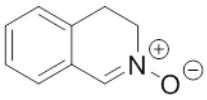	0.65	16
2.10	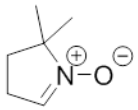	0.050	1.3
2.11	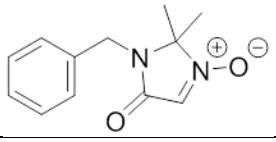	1.5	37
Benzyl Azide (in MeOD by ^{1}H NMR)	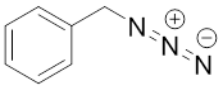	0.040	1.0

The trend observed in the reactivity of BCN in SPANC reactions is consistent with the symmetry-allowed interaction of the alkyne HOMO (Ψ_1) and the nitrone LUMO (Ψ_3).

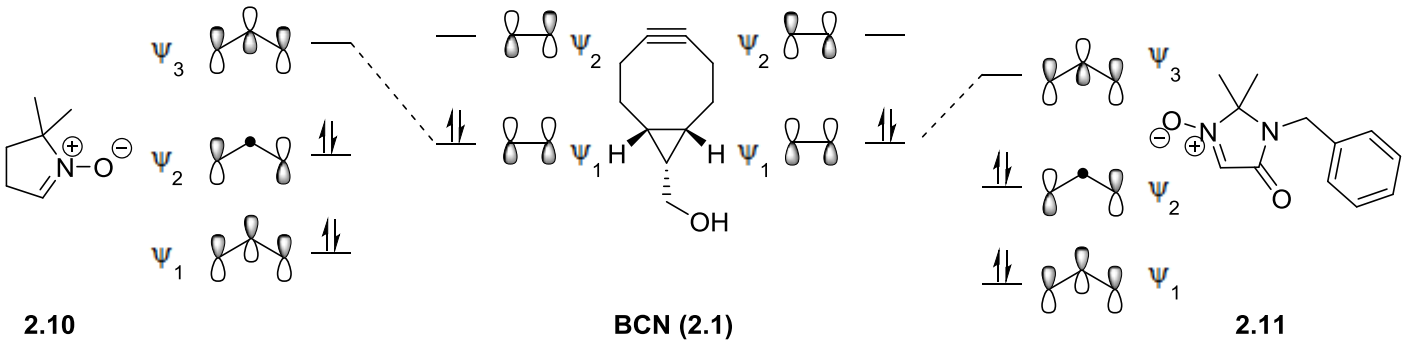

Figure 2.4 – Frontier-molecular orbital analysis of SPANC reactions involving BCN and nitrones with differing electronic nature. Rate accelerations were observed with increasingly electron-deficient nitrones caused by a lowering of the nitrone LUMO energy level, indicating the inverse electron demand nature of SPANC cycloadditions involving BCN.

Product distribution in one-pot SPANC reactions involving BCN

The contrast observed in the second-order rate constants of BCN SPANC reactions is primarily due to the electronic properties of the reacting nitrones. Lowering the Ψ_3 energy level of the nitrone through the introduction of electron-withdrawing groups will result in a smaller energy gap between the reactive frontier orbitals. Conversely, increasing the Ψ_3 energy level of the nitrone will widen the energy gap between the reactive orbitals and lead to a decrease in the observed rate constant. It is reasonable to assume that if a limiting amount of BCN were to react with an equal excess of two electronically different nitrones, the difference in rate constants of each cycloaddition would be reflected in the distribution of cycloadducts.

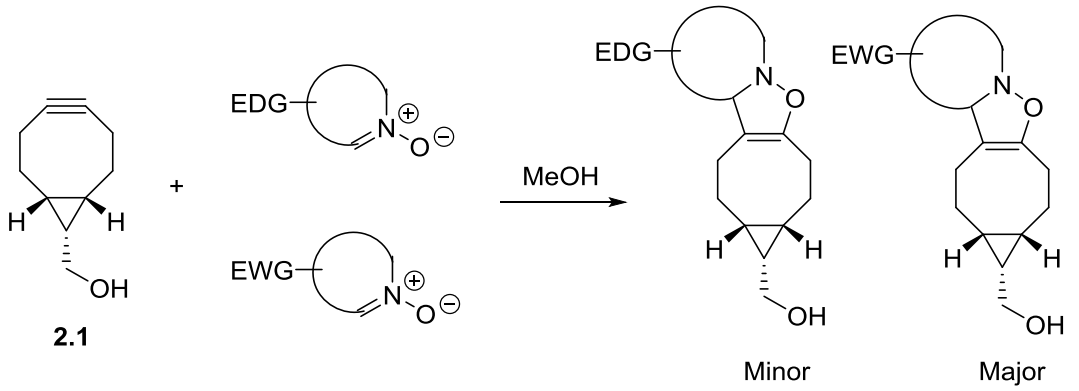

Equation 2.2 – Hypothetical proportions of BCN cycloadducts in a competitive cycloaddition. Since the SPANC reaction is irreversible, the distribution of products should reflect the relative rate constants of the independent cycloadditions that can take place.

The same reactivity trend has been observed in SPANC reactions involving BARAC and DIBO, though to a lesser extent than BCN. Since BARAC and DIBO have lower LUMO energy levels than BCN and show only modest rate enhancements in reactions with electron-deficient nitrones, their cycloaddition rate constants with electron rich nitrones are significantly larger than those of BCN. The rate law indicates that the distribution of products in a mixed cycloaddition reaction should also reflect the relative rate constants of each SPANC reaction. Therefore, in a mixed SPANC reaction with BCN, a benzanulated cyclooctyne and two nitrones that vary in electronic character, we predict that BCN will primarily react with the electron-deficient nitrone while the benzanulated cyclooctyne will primarily react with the electron-rich nitrone, and that these tendencies will be reflected in the distribution of products.

To evaluate this hypothesis, a solution of BCN and DIBO in equal concentrations was combined with a solution of nitrones **2.10** and **2.11** of the same concentration. DIBO was chosen for this experiment because of its low calculated LUMO energy level (36.1 kcal/mol versus 38.2

kcal/mol calculated for BCN) and its similar second-order rate constant with benzyl azide in Methanol (k_2 = 0.057 $M^{-1}s^{-1}$ for DIBO versus k_2 = 0.040 $M^{-1}s^{-1}$ for BCN). The reaction was monitored by LCMS and since the resulting products displayed similar potential for ionization and significantly different absorption profiles, the distribution of products was quantified by comparing the integration values for each product in the total ion chromatogram LCMS trace.

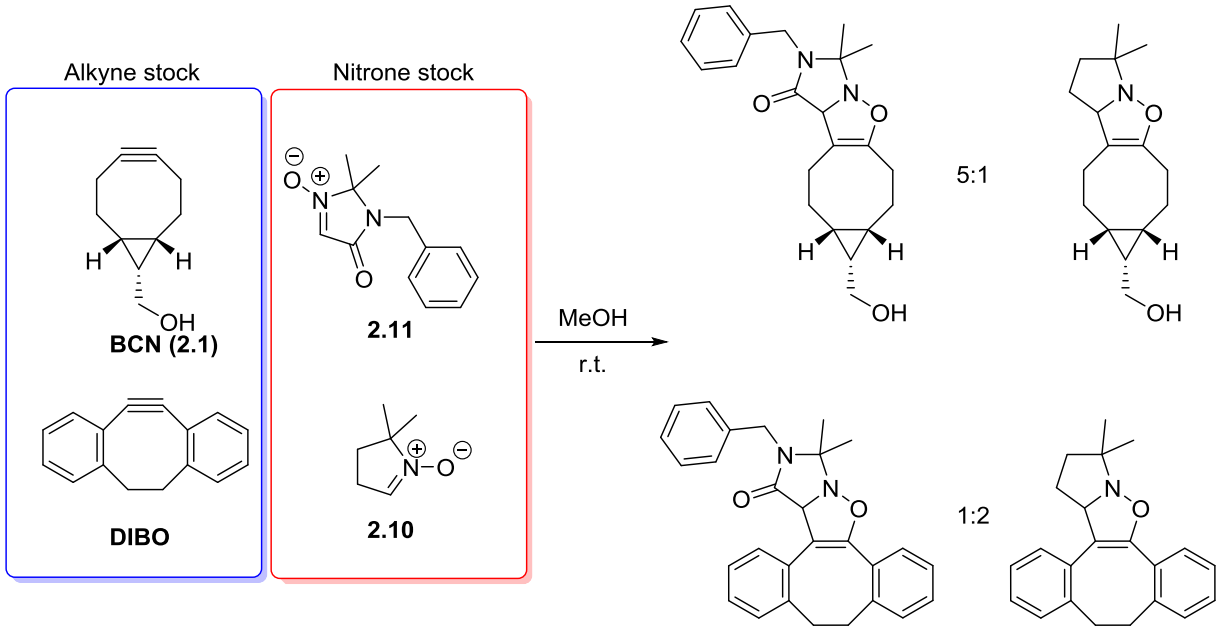

Scheme 2.3 – Product distributions observed in a one-pot competitive SPANC experiment with endocyclic nitrones. The distribution of cycloadducts formed from BCN reflect the difference in second-order rate constants observed for the individual SPANC reactions. In the presence of a competing alkyne (DIBO), this trend is conserved.

Each alkyne can potentially produce two cycloadducts (and isomers thereof). The integration values of both cycloadducts were compared individually for each alkyne in order to determine the cycloadduct distribution with respect to the alkyne. After this evaluation, it was found that BCN showed a 5:1 selectivity for the electron deficient nitrone **2.11** over the electron rich nitrone **2.10**. This result is expected since BCN has shown sensitivity to electronic changes of the nitrone in SPANC reactions. The 30-fold increase in second-order rate constant (k_2) therefore translates to a 5:1 product distribution when there is a competing cycloaddition present. At the same time, DIBO displayed a modest 2:1 selectivity for the electron rich nitrone **2.10** over the electron deficient nitrone **2.11** when the competing BCN SPANC reaction was present. This result is also expected since the benzanulated cyclooctynes have displayed only a modest increase in rate constants in SPANC reactions with electron-deficient nitrones.

These results indicate that due to the comparatively high LUMO energy of BCN, cycloadditions between BCN and nitrones proceed through the symmetry-allowed interaction of the Ψ_1 HOMO orbital of the alkyne and the Ψ_3 LUMO orbital of the nitrone. The benzanulated alkynes tested in SPANC reactions so far show a modest preference to proceed through the same interaction; however, the energy differences between this forward electron demand process are likely very similar to the inverse electron demand process in which the Ψ_2 LUMO of the alkyne interacts with the Ψ_2 HOMO of the nitrone.

Conclusion

BCN is a unique cycloalkyne structure in which the alkyne displays an increased electron density and subsequently higher LUMO energy level than other common bioorthogonal cyclooctynes while retaining a comparable second-order rate constant in strain-promoted azide-alkyne cycloadditions with benzyl azide. Due to these features, the rate constants of strain-promoted

alkyne-nitrone cycloadditions involving BCN show a dependence on the electronic properties of the nitrone reagent, with the largest rate constants being obtained with electron-deficient endocyclic nitrones. This tendency to react more rapidly with electron-deficient nitrones implies that SPANC reactions involving BCN proceed in an inverse electron-demand fashion through the symmetry-allowed interaction of the Ψ_1 HOMO of the alkyne with the Ψ_3 LUMO of the nitrone. The rate constants of SPANC reactions involving benzanulated cyclooctynes DIBO and BARAC have shown little dependence on the electronic properties of the nitrone, implying that these cycloadditions are able to proceed by either inverse electron-demand through the orbital interactions described above, or by normal electron-demand through interaction of the Ψ_2 LUMO of the alkyne and the Ψ_2 HOMO of the nitrone. Strained cyclooctynes with similarly low LUMO energy levels are expected to display a similar indifference toward the nitrone electronics because the energy gaps of the symmetry-allowed orbital interactions are similar for either normal- or inverse-electron demand cycloaddition with nitrones. As an extrapolation of the observed trends, cyclooctynes displaying LUMO energy levels lower than those of BARAC and DIBO are expected to proceed primarily in a forward electron demand fashion. Since BCN shows a disposition toward inverse-electron demand cycloadditions with nitrones, the selection of nitrone in these cycloadditions bears a more substantial impact on the second-order rate constant than in cycloadditions with benzanulated cyclooctynes. By selecting nitrones and cyclooctynes of opposing electronic nature, product distribution can be modulated in competing SPANC reactions. This concept should prove valuable in metabolic labelling experiments by allowing access to simultaneous selective conjugation reactions and the potential for duplex labelling within one bioorthogonal system.

Materials and Experimental Details

Equipment and reagents

Chemical reagents were purchased from Sigma-Aldrich unless otherwise stated and used without further purification. Deuterated solvents were purchased from Cambridge Isotope laboratories. Thin layer chromatography (TLC) was carried out on Analtech Uniplate® silica gel plates (60 Å F_{254}, layer thickness 250μm) using UV light and $KMnO_4$ stainto visualize. Flash column chromatography was performed using silica gel (60 Å, particle size 40-63μm). Mass spectrometry was performed on a Micromass ZQ2000 mass spectrometer equipped with pneumatically assisted electrospray ionization source in both positive and negative ionization modes. LC-MS traces were obtained using a Waters Alliance 2795 liquid chromatograph equipped with a Waters 996 photodiode array detector connected to the above mentioned mass spectrometer. LC-MS samples were eluted with a gradient of acetonitrile (+0.1% formic acid) and water (+0.1% formic acid) on a Waters SunFire C18 (2.1 x 100mm, 3.5μm) column with a flow rate of 0.2mL.min. ^{1}H NMR and ^{13}C NMR spectra were obtained using a 400 MHz Bruker NMR spectrometer. Chemical shifts are reported as δ referenced to residual solvent and coupling constants (*J*) are reported in Hz with splitting patterns reported using conventional methods. UV-Visibleible kinetic data was obtained on a Varian Cary 3 UV-Visibleibleible spectrophotometer equipped with a Cary temperature controller.

Synthesis of Reagents

Bicyclo[6.1.0]nonyne

(1*R*,8*S*,9*r*,Z)-Ethyl bicyclo[6.1.0]non-4-ene-9-carboxylate (2.1a exo), and (1*R*,8*S*,9*s*,Z)-ethyl bicyclo[6.1.0]non-4-ene-9-carboxylate (2.1a endo):

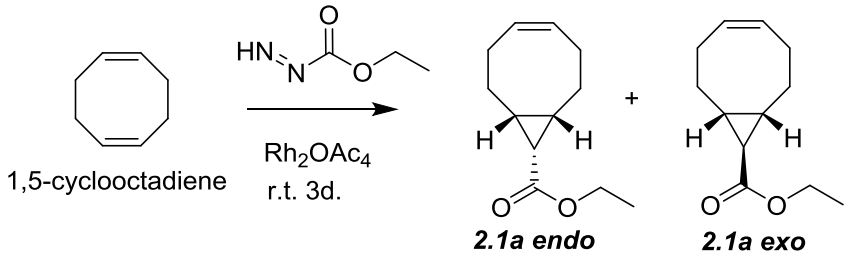

Procedure:

An oven-dried round-bottom flask was charged with 0.15 g of dirhodium tetraacetate and purged with Argon. 30.0 mL (26.5 g, 0.245 mol) was added via syringe and cooled to 0˚C. 3.60 mL (3.91 g, 34.3 mmol) was added dropwise over 2 h. The reaction was warmed to room temperature and stirred for 3 d. Purified by column chromatography (1-2.5% ether in hexanes) to afford 2.75 g (14.2 mmol, 41.3% yield) of **2.1a** *endo* as a clear oil and 1.76 g (9.06 mmol, 26.5% yield) of **2.1b** *exo* as a clear oil. ^{1}H NMR (400 MHz, $CDCl_3$) DM-01-085 *endo*: 5.64-5.57 (m, 2H), 4.11 (q, J=7.1 Hz, 2H), 2.54-2.46 (m, 2H), 2.25-2.15 (m, 2H), 2.10-2.01 (m, 2H), 1.87-1.78 (m, 2H), 1.70 (t, J=8.8 Hz, 1H), 1.43-1.34 (m, 2H), 1.26 (t, J=7.1 Hz, 3H DM-01-085 *exo*: 5.67-5.59 (m, 2H), 4.10 (q, J=7.2 Hz, 2H), 2.33-2.26 (m, 2H), 2.23-2.15 (m, 2H), 2.12-2.04 (m, 2H), 1.59-1.54 (m, 2H), 1.52-1.43 (m, 2H), 1.25 (t, J=7.1 Hz, 3H), 1.18 (t, J=4.8 Hz, 1H). ^{13}C NMR spectra match those reported in the literature.[3]

(1R,8S,9s)-Bicyclo[6.1.0]non-4-yn-9-ylMethanol (2.1):

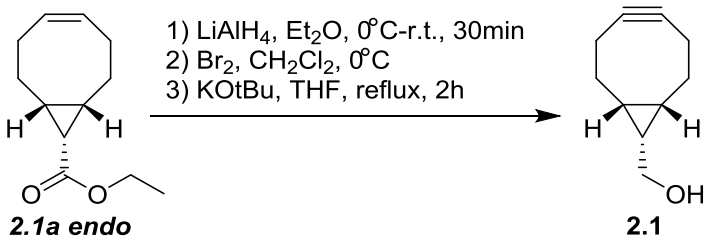

2.1a endo **2.1**

Procedure:

$LiAlH_4$ (0.210 g, 4.52 mmol) was suspended in dry ether (13.4 mL) and cooled to 0℃ in an oven-dried flask under Argon. **2.1a** endo (0.700 g, 3.60 mmol) was dissolved in dry ether (3 mL) and added dropwise to the suspension and warmed to room temperature after addition. The reaction was monitored by TLC and upon completion (~30 minutes) the reaction was cooled in an ice bath and the excess $LiAlH_4$ was quenched with distilled water. Na_2SO_4 was then added, and the reaction was filtered through cotton and rinsed with ether (~100 mL). A clear oil was obtained and used directly in the next step. Rf = 0.08 (5% EtOAc in Hexanes)

The alcohol was dissolved in dry DCM (2.70 mL), placed under Argon and cooled to 0℃. Elemental Bromine was dissolved in DCM and added dropwise to the reaction until a deep yellow colour persisted. The reaction was stirred for an additional 30 minutes, quenched with $Na_2S_2O_3$ and stirred until the colour faded. The product was extracted with DCM (3x20 mL), dried over Na_2SO_4, filtered and concentrated. A white solid was obtained and used directly in the next step.

The solid product was dissolved in dry THF (20 mL) and cooled to 0℃. KOtBu (1 M in THF, 11.0 mL, 11.0 mmol) was added dropwise. After addition, the ice bath was removed and the reaction was heated to reflux for 2 h, monitoring by TLC. The reaction was quenched with

ammonium chloride, extracted with DCM, dried over Na_2SO_4, filtered, concentrated, and purified by column chromatography (1:1 EtOAc in hexanes) to afford **2.1**, 0.270 g (1.80 mmol, 50.0% yield over 3 steps) as a pale yellow waxy solid. Rf = 0.53.

Acyclic Nitrones

***N*-[(4-Methoxyphenyl)methylene]-benzenemethanamine *N*-oxide:**

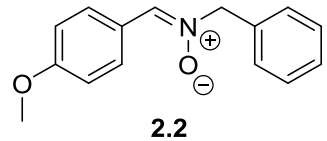

2.2

Nitrone **2.2** was obtained from Dr. Craig McKay in the Pezacki group. Synthesis and characterization has been previously described in the literature.[17]

***N*-[(4-Methylphenyl)methylene]-benzenemethanamine *N*-oxide:**

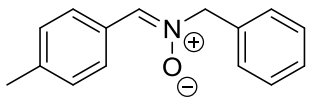

2.3

Nitrone **2.3** was obtained from Dr. Craig McKay in the Pezacki group. Synthesis and characterization has been previously described in the literature.[17]

***N*-(Phenylmethylene)-benzenemethanamine *N*-oxide:**

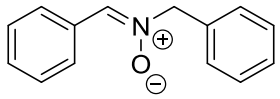

2.4

Nitrone **2.4** was obtained from Dr. Craig McKay in the Pezacki group. Synthesis and characterization has been previously described in the literature.[17]

***N*-[(4-Bromophenyl)methylene]-benzenemethanamine *N*-oxide:**

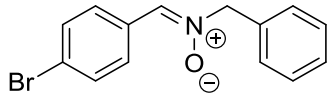

2.5

Nitrone **2.5** was obtained from Dr. Craig McKay in the Pezacki group. Synthesis and characterization has been previously described in the literature.[17]

4-[[Oxido(phenylmethyl)imino]methyl]-benzoic acid methyl ester:

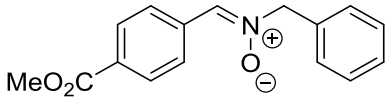

2.6

Nitrone **2.6:** *N*-Benzylhydroxylamine hydrochloride (0.082 g, 0.510 mmol) was dissolved in dry DCM (dried over 3 Å molecular sieves, 2.00 mL). Magnesium sulfate (0.078g, 0.650 mmol) was added to the mixture, followed by Methyl-4-formylbenzoate (0.077 g, 0.47 mmol) and 2.00 mL of additional DCM. The reaction was stirred at room temperature over-night and filtered. The filtrate was concentrated and purified by column chromatography (1:1 EtOAc:Hexanes).

0.086 g of a white powder was obtained (67.5% yield). Rf = 0.28. ^{1}H and ^{13}C NMR match the literature spectra.[18]

4-[[Oxido(phenylmethyl)imino]methyl]-benzonitrile:

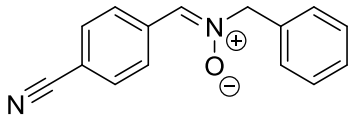

2.7

Nitrone **2.7** was obtained from Dr. Craig McKay in the Pezacki group. Synthesis and characterization has been previously described in the literature.[17]

***N*-[(4-Nitrophenyl)methylene]-benzenemethanamine *N*-oxide:**

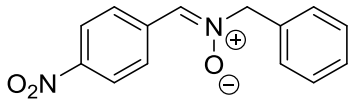

2.8

Nitrone **2.8** was obtained from Dr. Craig McKay in the Pezacki group. Synthesis and characterization has been previously described in the literature.[17]

Endocyclic Nitrones

3,4-Dihydroisoquinoline 2-oxide:

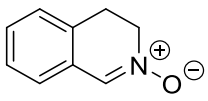

2.9

Nitrone **2.9** was obtained from Mariya Chigrinova in the Pezacki group. Synthesis and characterization has been previously described in the literature.[19]

5,5-Dimethyl-1-pyrroline *N*-oxide:

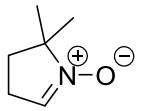

2.10

Nitrone **2.10** was commercially available and was purchased from Sigma-Aldrich.

2,3-Dihydro-2,2-dimethyl-3-(phenylmethyl)-4H-imidazol-4-one-1-oxide:

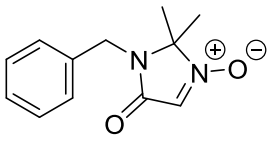

2.11

Nitrone **2.11** was synthesized according to the procedure previously published by Dai *et al* from glycine hydrochloride as follows:

***N*-[(1,1-Dimethylethoxy)carbonyl]-glycine (2.11a):**

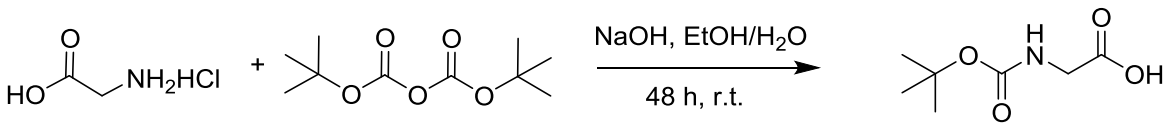

2.11a

Procedure:

Glycine hydrochloride (6.00 g, 53.8 mmol) was dissolved in a 1:1 mixture of ethanol and water to which Sodium hydroxide (4.30 g, 108 mmol) was added. The mixture was stirred for 15 minutes at room temperature before adding Di-tert-butyl-dicarboxylate (12.9 g, 59.2 mmol), and stirred for 48 hours. The ethanol was evaporated, and the aqueous solution was washed with ether (3x20 mL) and acidified to pH~3. The acidified aqueous phase was extracted with ethyl acetate (3x20 mL). The combined organic phases were dried over anhydrous Magnesium sulfate, filtered, and concentrated. 9.42 g of white solid was obtained (quantitative). ^{1}H and ^{13}C NMR match those previously reported in the literature.[20]

***N*-[2-Oxo-2-[(phenylmethyl)amino]ethyl]-carbamic acid, 1,1-dimethylethyl ester (2.11b):**

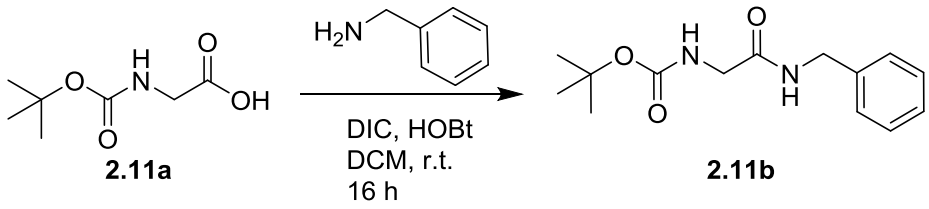

Procedure:

N-[(1,1-Dimethylethoxy)carbonyl]-glycine (0.700 g, 4.00 mmol) and Hydroxybenztraizole monohydrate (0.540 g, 4.00 mmol) were dissolved in dry DCM (dried over 3 Å molecular sieves, 15 mL) to which *N*,*N*'-Diisopropylcarbodiimide (0.620 mL, 4.00 mmol) and Benzyl amide (0.429 g, 4.00 mmol) were added at room temperature. The reaction was stirred overnight under argon. The mixture was washed with 1 M HCl (3x15 mL) followed by saturated Sodium bicarbonate. The organic layer was dried over anhydrous sodium sulfate, filtered, and concentrated. Purified by column chromatography (1:1 EtOAc/Hexanes). 0.866 g obtained as a colourless oil (81.9% yield). Rf = 0.26. ^{1}H and ^{13}C NMR match those previously reported in the literature.[21]

2-Amino-*N*-(phenylmethyl)-acetamide (2.11c):

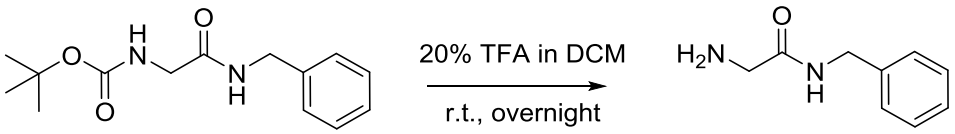

2.11b **2.11c**

Procedure:

N-[2-Oxo-2-[(phenylmethyl)amino]ethyl]-carbamic acid,1,1-dimethylethyl ester (0.866 g, 3.27 mmol) was dissolved in dry DCM (dried over 3Å molecular sieves, 6.40 mL) to which trifluoroacetic acid (1.60 mL, 9.42 mmol) was added dropwise and placed under argon. The reaction was stirred overnight at room temperature. The product was concentrated *in vacuo* and distilled as an azeotrope from Methanol. 0.514 g of an off-white solid was obtained (95.6% yield). ^{1}H NMR (400 MHz, $CDCl_3$): 7.58 (br s, 1H), 7.36-7.27 (m, 5H), 4.48, (d, J=5.9 Hz), 3.41 (s, 2H). ^{13}C NMR spectrum matches that previously reported in the literature.[20]

2,2-Dimethyl-3-(phenylmethyl)-4-imidazolidinone (2.11d):

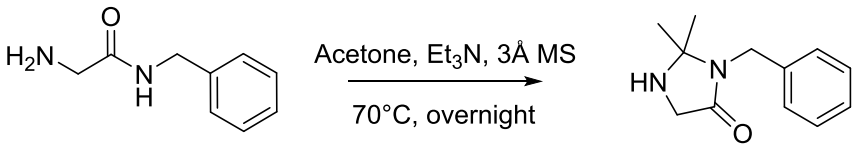

2.11c **2.11d**

Procedure:

A flame-dried round bottom flask was charged with 2-Amino-*N*-(phenylmethyl)-acetamide (0.200 g, 1.22 mmol). 3 Angstrom molecular sieves (0.700 g) were added, followed by Acetone (0.900 mL, 12.2 mmol) and Triethylamine (0.850 mL, 6.10 mmol). The flask was fitted with a reflux condenser, purged with argon, and stirred at 70˚C overnight. The reaction was cooled to

room temperature and filtered through Celite. The filtrate was concentrated and purified by column chromatography (0-5% MeOH in DCM). 0.164 g of a pale yellow semi-solid was obtained (65.7% yield). Rf = 0.33. ^{1}H NMR (400 MHz, $CDCl_3$): 7.30-7.28 (m, 3H), 7.27-7.25 (m, 2H), 4.43 (s, 2H), 3.54 (s, 2H), 1.25 (s, 6H). ^{13}C spectrum matches that previously reported in the literature.[20]

2,3-Dihydro-2,2-dimethyl-3-(phenylmethyl)-4H-imidazol-4-one 1-oxide (2.11):

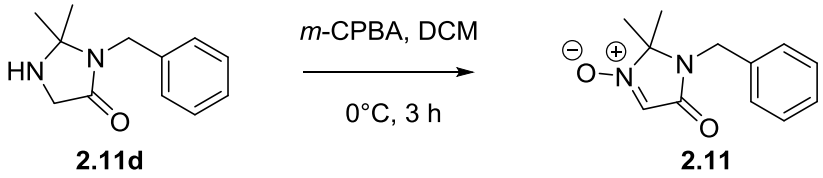

Procedure:

2,2-Dimethyl-3-(phenylmethyl)-4-imidazolidinone (0.137 g, 0.670 mmol) was dissolved in dry DCM (dried over 3Å molecular sieves, 3.00 mL) and cooled to 0˚C. *Meta*-Chloroperoxybenzoic acid (0.300 g, 1.68 mmol) was added and the reaction was stirred for 3 hours before concentrating *in vacuo* and purifying by column chromatography (5% MeOH in DCM). ^{1}H and ^{13}C NMR spectra match those previously reported in the literature.[20]

References

(1) Prescher, J. A.; Bertozzi, C. R. *Nat Chem Biol* **2005**, *1*, 13.

(2) Sletten, E. M.; Bertozzi, C. R. *Angewandte Chemie International Edition* **2009**, *48*, 6974.

(3) Dommerholt, J.; Schmidt, S.; Temming, R.; Hendriks, L. J. A.; Rutjes, F. P. J. T.; van Hest, J. C. M.; Lefeber, D. J.; Friedl, P.; van Delft, F. L. *Angewandte Chemie International Edition* **2010**, *49*, 9422.

(4) Jewett, J. C.; Bertozzi, C. R. *Chemical Society Reviews* **2010**, *39*, 1272.

(5) Gordon, C. G.; Mackey, J. L.; Jewett, J. C.; Sletten, E. M.; Houk, K. N.; Bertozzi, C. R. *Journal of the American Chemical Society* **2012**, *134*, 9199.

(6) Garcia-Hartjes, J.; Dommerholt, J.; Wennekes, T.; van Delft, F. L.; Zuilhof, H. *European Journal of Organic Chemistry* **2013**, *2013*, 3712.

(7) Baskin, J. M.; Prescher, J. A.; Laughlin, S. T.; Agard, N. J.; Chang, P. V.; Miller, I. A.; Lo, A.; Codelli, J. A.; Bertozzi, C. R. *Proceedings of the National Academy of Sciences* **2007**, *104*, 16793.

(8) Poloukhtine, A. A.; Mbua, N. E.; Wolfert, M. A.; Boons, G.-J.; Popik, V. V. *Journal of the American Chemical Society* **2009**, *131*, 15769.

(9) Debets, M. F.; van Berkel, S. S.; Schoffelen, S.; Rutjes, F. P. J. T.; van Hest, J. C. M.; van Delft, F. L. *Chemical Communications* **2010**, *46*, 97.

(10) Jewett, J. C.; Sletten, E. M.; Bertozzi, C. R. *Journal of the American Chemical Society* **2010**, *132*, 3688.

(11) McKay, C. S.; Moran, J.; Pezacki, J. P. *Chemical Communications* **2010**, *46*, 931.

(12) McKay, C. S.; Chigrinova, M.; Blake, J. A.; Pezacki, J. P. *Organic & Biomolecular Chemistry* **2012**, *10*, 3066.

(13) MacKenzie, D. A.; Sherratt, A. R.; Chigrinova, M.; Cheung, L. L. W.; Pezacki, J. P. *Current Opinion in Chemical Biology* **2014**, *21*, 81.

(14) Agard, N. J.; Prescher, J. A.; Bertozzi, C. R. *Journal of the American Chemical Society* **2004**, *126*, 15046.

(15) Hammett, L. P. *Journal of the American Chemical Society* **1937**, *59*, 96.

(16) MacKenzie, D. A.; Pezacki, J. P. *Canadian Journal of Chemistry* **2014**, *92*, 337.

(17) McKay, C. PhD Thesis, University of Ottawa, 2012.

(18) Evans, D. A.; Song, H.-J.; Fandrick, K. R. *Organic Letters* **2006**, *8*, 3351.

(19) Chigrinova, M. M.Sc. Thesis, University of Ottawa, 2014.

(20) Dai, X.; Miller, M. W.; Stamford, A. W. *Organic Letters* **2010**, *12*, 2718.

(21) Li, N.; Lim, R. K. V.; Edwardraja, S.; Lin, Q. *Journal of the American Chemical Society* **2011**, *133*, 15316.

3. Applications of Tunable SPANC Reactions in Biological Context

Introduction

Incorporating unnatural chemical functionality into the biomolecules of living systems is the cornerstone of metabolic labelling, which can provide insight into the nature of metabolic pathways, biosynthesis, and molecular interactions that are not directly obvious through product isolation experiments. In order for rapid click reactions to be used in metabolic labelling experiments, one of the click reagents must be incorporated into a probe that will mimic or modify the natural substrate being studied. Staudinger ligation is most well-known for being applied to the metabolic labelling of cell-surface glycans through the design of azide-derivitazed sugars capable of cellular uptake and expression on cell surfaces.[1] Azides and alkynes have since been incorporated into viral capsids,[2] peptides and nucleotides,[3] sterols,[4] and unnatural amino acids[5-8] for copper-catalyzed or strain-promoted cycloadditions with great success. Without a covalent linkage to an appropriate biomolecule, bioorthogonal click reactions would simply result in organic couplings without any particular biological significance. Developing methods to incorporate functional bioorthogonal groups into biologically relevant substrates is therefore crucial to applying any chemistry as a labelling strategy.

SPANC reactions have been applied to biological labelling experiments by modifying proteins to bear nitrone functional groups. Acyclic nitrones have been incorporated into proteins through oxidation of an N-terminal serine residue by sodium periodate to produce an aldehyde, followed by condensation with a hydroxylamine, resulting in a nitrone-tagged polypeptide.[9,10] Subsequent SPANC reactions have allowed the fluorescent labelling of proteins in solution with the sole requirement of an *N*-terminal cysteine residue. Human epidermal growth factor (EGF) has also

been modified to bear an endocyclic nitrone, allowing for fluorescent SPANC labelling of mammalian cell surfaces expressing EGF receptors.[11] Thus, SPANC reactions are predisposed to applications in metabolic labelling.

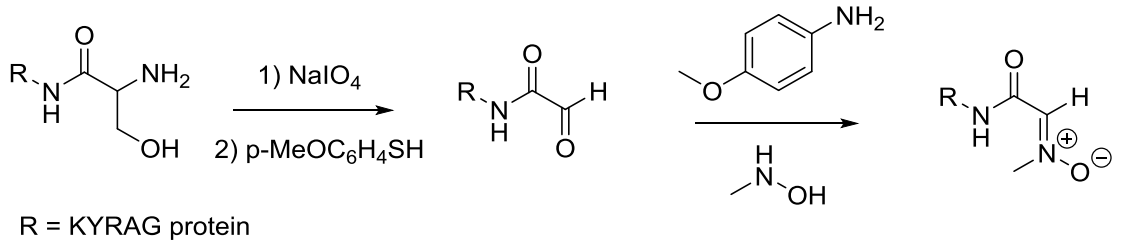

Equation 3.1 – Nitrone installation on to a protein through oxidation of a terminal serine residue followed by condensation with a hydroxylamine. This strategy, reported by the van Delft group can be applied to incorporate an acyclic nitrone into any protein possessing an *N*-terminal serine residue. Adapted from reference 9.

Recently, an endocyclic nitrone-modified variant of 3-Deoxy-D-manno-octulosonic acid (KDO) has been shown to be readily incorporated into *E. coli* cell surface lipopolysaccharides (LPS) by highly selective biosynthetic enzymes.[12] This incorporation and subsequent labelling by a modified Kinugasa reaction marks the first metabolic incorporation of an endocyclic nitrone in bacteria.

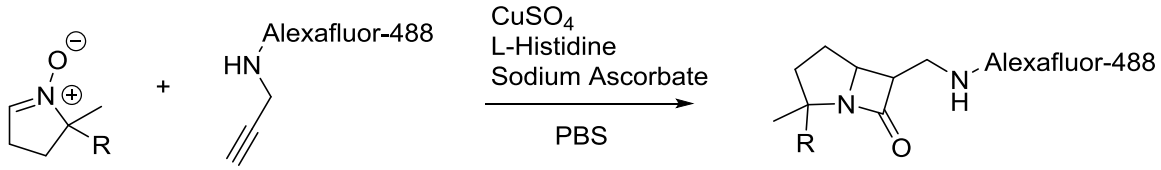

Equation 3.2 – Biocompatable Kinugasa reaction employing endocyclic nitrones under copper (I) catalytic conditions, used to fluorescently label cell-surface LPS in *E. coli*. *L*-His is used as the ligand source to minimize cytotoxicity and metabolic influence of the catalyst. Adapted from reference 12.

Live-cell fluorescent imaging of bacterial cell wall peptidoglycan (PG) using fluorescent or azide-bearing unnatural D-amino acids has appeared in the literature over the last few years.[6-8] Incorporation of unnatural amino acids into gram positive bacterial PG appears to hinge primarily on the stereochemistry of the amino acid, and incorporation of bulky fluorescent molecules has been reported.[6] Since bacteria use D-amino acids to cross-link layers of PG to form a mesh-like sacculus surrounding the cell membrane,[13] and since D-amino acids are rarely employed in any other kingdom of life, this unique bacterial trait represents a substantial focal point of antibiotic research. Extensive *in-vitro* studies have been performed on PG in order to determine its composition in various bacterial cell lines, and Bertozzi *et al* have performed novel labelling experiments in which PG is fluorescently labelled after phagocytosis by mammalian macrophages,[7] but PG dynamics have only recently begun to be studied with the help of bioorthogonal click chemistry.

Hypothesis

The tendency of bacterial PG to incorporate a variety of unnatural D-amino acid analogues represents a rich opportunity to apply bioorthogonal click chemistry to the study of PG dynamics. Designing unnatural D-amino acid analogues bearing endocyclic nitrones will allow the visualization of bacterial growth via SPANC reactions. Given the previously defined sensitivity of BCN to the electronic properties of endocyclic nitrones in SPANC reactions[14], designing unnatural D-amino acid analogues bearing endocyclic nitrones of opposing electronic nature will allow duplex labelling of morphologically distinct gram positive bacteria in a binary bacterial culture.

Results and Discussion

Exploring nitrone incorporation into gram-positive bacterial PG required the design of appropriate metabolic probes that mimic a molecule naturally occurring in native PG synthesis. PG is composed of alternating amino sugars cross-linked by short peptides that make use of D- and L- amino acids. Cross-linking peptides often contain two successive D-Alanine residues - a moiety that is targeted by some modern antibiotics since the D-Ala-D-Ala motif is not observed in eukaryotic organisms.[13] Based on the importance of D-Alanine and other D-amino acids in PG cross-linking, and the recently reported incorporation of fluorescent[6] or azide-bearing[7,8] D-amino acids into bacterial PG, we modeled our nitrone-bearing metabolic probes after the amino acids commonly observed in PG cross-linking peptides. With these probes in hand, fluorescent labelling of bacterial PG could be explored via SPANC.

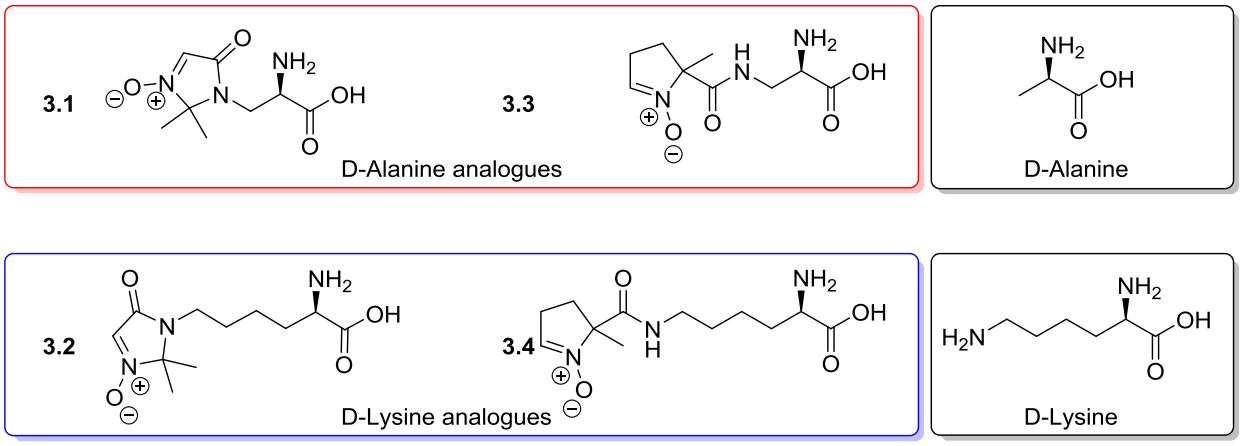

Figure 3.1 – D-amino acid based probes used for metabolic labelling of *E. coli, L. innocua,* and *L. lactis*. UAAs 3.1 and 3.3 are based on D-Alanine and are modified to bear the electronically opposing nitrones 2.11 and 2.10, respectively. UAAs 3.2 and 3.4 were designed in a similar fashion using D-Lysine as the model substrate.

Synthesis of unnatural D-amino acids

To investigate the potential incorporation of endocyclic nitrones into the PG of bacterial cell walls, a series of nitrone-containing unnatural D-amino acid were prepared. Unnatural amino acids (UAAs) **3.1** and **3.2** were designed to include D-amino acid center and the electron-deficient nitrone **2.11** while remaining as structurally similar to the parent D-amino acid as possible, while **3.3** and **3.4** were designed to include the electron-rich nitrone **2.10** in order to provide electronically contrasting UAAs. The general synthetic procedure for nitrones **3.1** and **3.2**, detailed in Scheme 3.1, is based on the synthesis of nitrone **2.11** originally reported by Dai *et al*.[15] Nitone **3.1** was synthesized from Boc-D-Dap-OH (purchased from Matrix Scientific) which was subjected to a series of protecting group installations in order to minimize side product formation and maximize the yield of the desired intermediates in this eight-step synthesis. In order to install a *tert*-Butyl protecting group on the carboxylic acid moiety to prevent its involvement in downstream amide bond-forming coupling reactions, it was necessary to install an orthogonal protecting group on the more nucleophilic primary amine. After installing the *tert*-Butyl protecting group on the carboxylic acid of **3.1a**, the Fmoc group was removed with Piperidine in DMF, and the primary amine was coupled to Fmoc-Glycine-OH under standard amide coupling conditions. Removal of the resultant Fmoc group lead to the formation of **3.1e**, which was then condensed with acetone, oxidized to the nitrone with *m*-CPBA, and treated with TFA to furnish the metabolic probe **3.1**. Nitrone **3.2** was synthesized in an analogous fashion from Boc-D-Lys-OH.

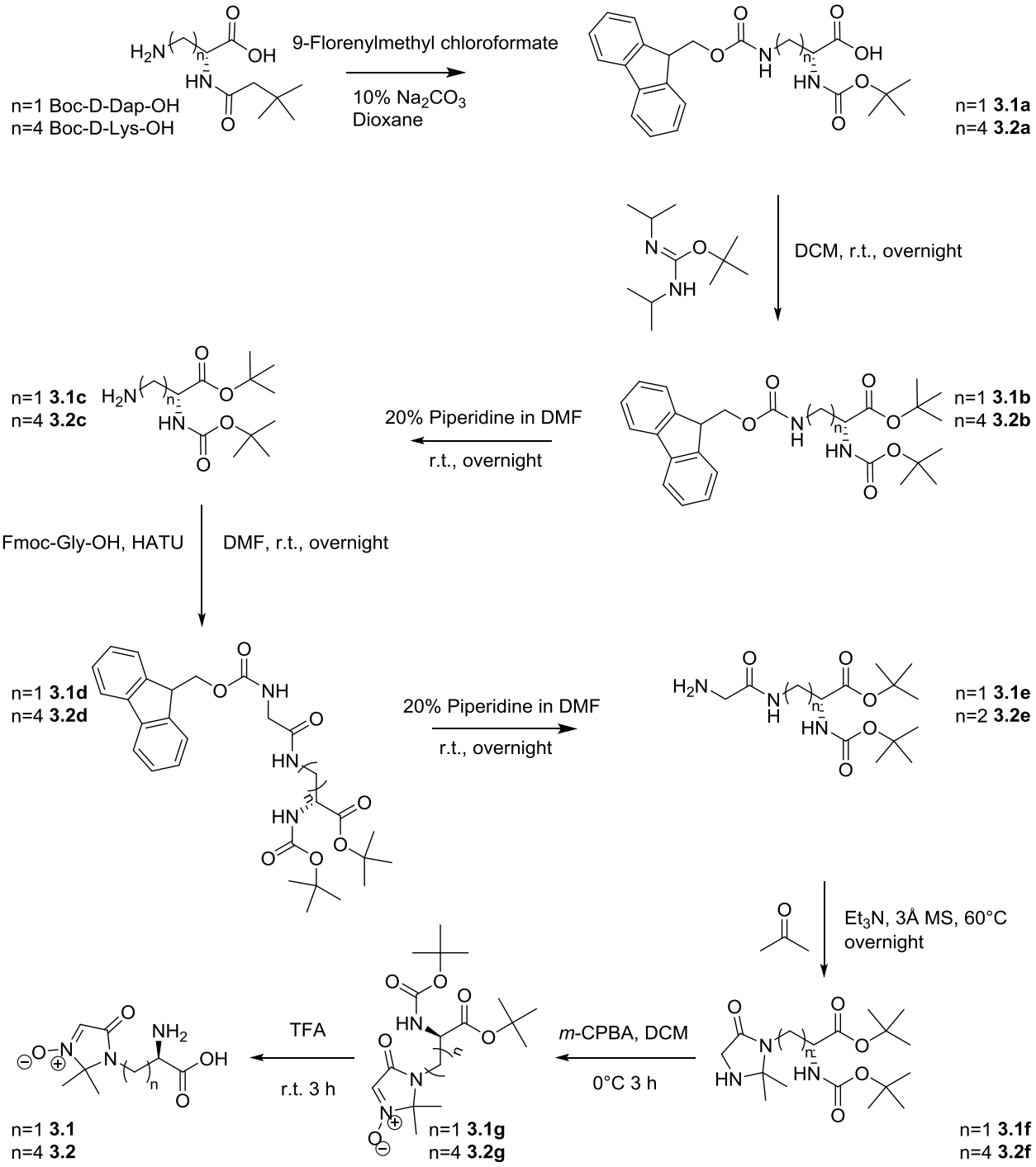

Scheme 3.1 – Synthetic procedure for nitrones 3.1 and 3.2. Boc-protected D-amino acids were purchased from Matrix Scientific. 2-*tert*-Butyl-1,3-diisopropylisourea used in the protection of 3.1a/3.2a was prepared from DIC and *tert*-Butanol according to the procedure described by Hodges *et al.*[16] Protection of the amino acid functionality was required to prevent self-coupling in subsequent amide coupling reactions. Synthesis is a variation of that used to prepare nitrone 2.11.[15]

Nitrones **3.3** and **3.4** were synthesized from intermediate protected D-amino acids **3.1c** and **3.2c** via an HATU-mediated amide coupling reaction followed by cleavage of the Boc and *tert*-Butyl protecting groups according to equation 3.3:

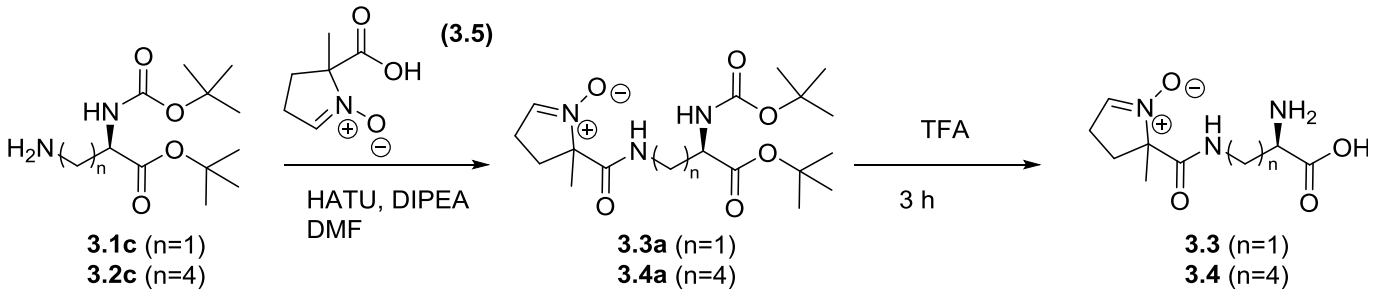

Equation 3.3 – Synthesis of UAA 3.3 and 3.4 from intermediates 3.1c and 3.2c, respectively. Nitrone 3.5 was synthesised in accordance to the procedure reported in reference 20 and coupled to 3.1c and 3.2c by an HATU-mediated amide bond-forming reaction. The resulting compounds 3.3a and 3.4a were treated with Trifluoroacetic acid to cleave the Boc and *tert*-Butyl protecting groups. UAA 3.3 and 3.4 were obtained in pure form from Mariya Chigrinova in the Pezacki group.

Gram-positive bacteria peptidoglycan labelling

With a series of UAA analogues bearing nitrone functionality in hand, the issue of metabolic incorporation could be addressed. *Listeria innocua* was chosen as a model organism for its non-infectious resemblance to the food-borne pathogen *L. monocytogenes*. *L. innocua* are gram-positive rod-shaped bacteria that thrive over a broad range of temperatures.[17,18] Gram-positive bacteria possess a thicker PG layer than gram-negative bacteria and do not require that labelling reagents cross the cell membrane before reaching the PG. These features make *L. innocua* an ideal model for PG labelling studies.

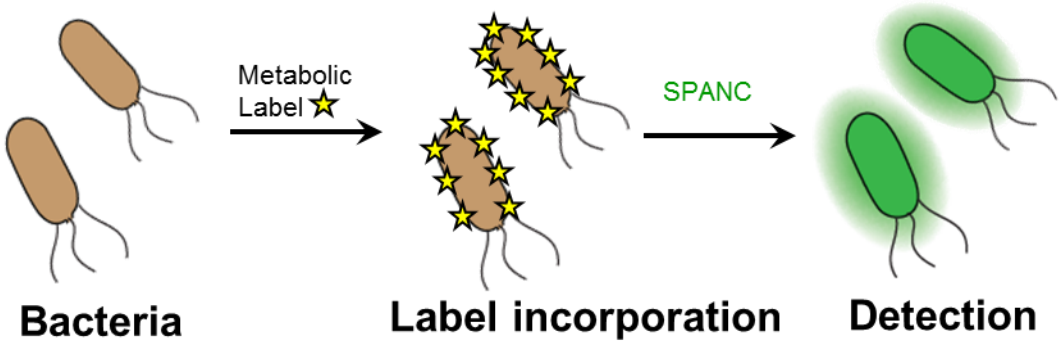

Equation 3.4 – General strategy for nitrone incorporation and fluorescent PG labelling via SPANC. Bacteria are incubated with a nitrone-bearing UAA probe during log-phase growth. After washing with PBS buffer to remove excess probe, the bacteria are incubated with a fluorophore-modified strained alkyne, washed again with PBS buffer to remove excess fluorophore, and visualized by fluorescence microscopy to detect labelled bacteria.

As a preliminary screen, cultures of *L. innocua* with an original optical density (OD_{600}) of 0.05 were incubated at 30˚C for 2 hours before being distributed into 1.50 mL Eppendorf tubes in 100 µL aliquots. Each aliquot was then incubated with either nitrone-modified UAA **3.3** (500 mM in DMSO) for 30 minutes, washed with PBS buffer, incubated with DIBO Alexafluor-488 conjugate (25.0 µM in DMSO) for 10 minutes at 37˚C, washed again with PBS buffer to remove excess fluorophore, and visualized by fluorescent microscopy.

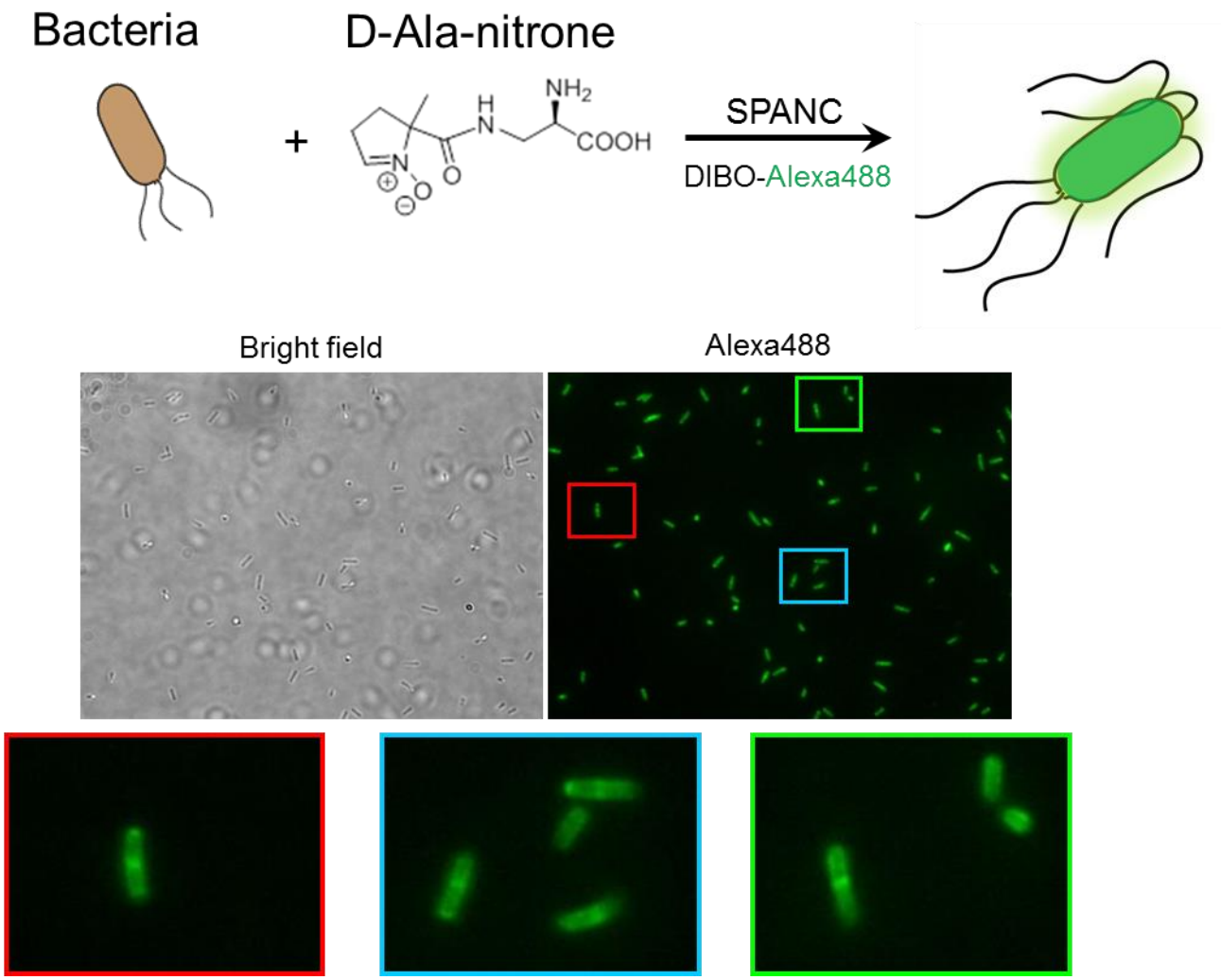

Figure 3.2 – Preliminary results showing fluorescently labelled PG in *L. innocua* as a result of the incorporation of UAA probe 3.3 and subsequent SPANC with fluorescently modified DIBO. Magnifications show increased fluorescence at sites of cell division where PG is newly synthesized. Images are corrected for background fluorescence.

The fluorescence observed in labelling experiments using nitrone-modified UAA probes was compared to that observed by incubating bacterial cultures with azido D-Alanine in place of the nitrone-modified UAA, since PG labelling with azide-modified D-amino acids has been previously reported.[7] Encouragingly, significant cell labelling was observed above background fluorescence with nitrone **3.3** via SPANC. Higher fluorescent intensity was observed at the midpoints of the cells, where cell division and active PG synthesis occur. Multiple incorporation mechanisms have the potential to occur simultaneously, however, increased fluorescence at cell division points suggests that the nitrone-modified UAA can be incorporated into newly synthesized PG. Motivated by this success, PG labelling was performed with nitrones **3.1, 3.2,** and **3.4**.

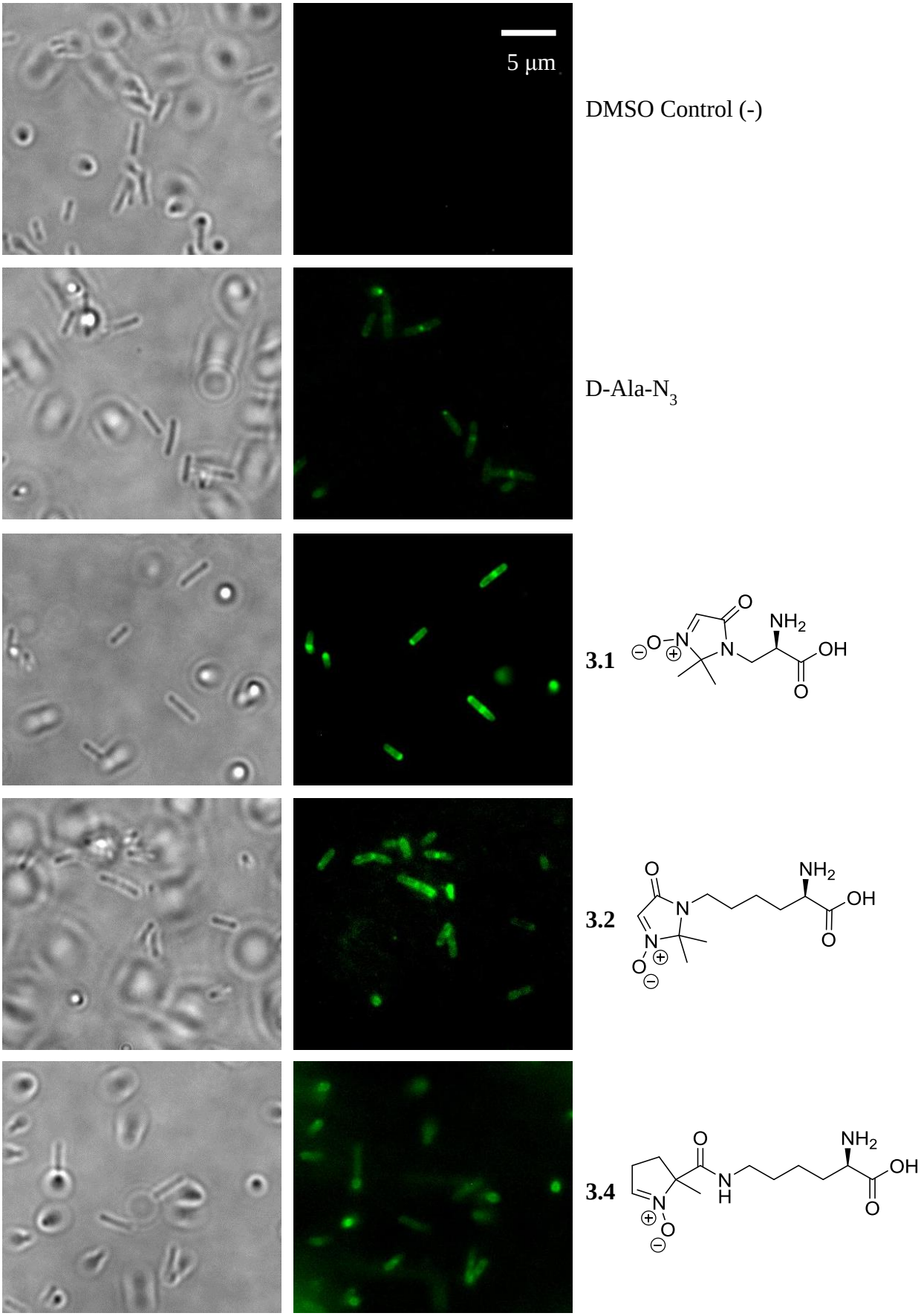

Figure 3.3 – Bright field (left) and fluorescent (right) imaging results of metabolic incorporation of modified D-amino acids by of *L. innocua* and subsequent SPANC with fluorophore-modified DIBO. Fluorescence observed for all UAA probes tested is corrected for background fluorescence. Results of metabolic labelling with nitrone 3.3 are shown in Figure 3.2.

DMSO vehicle was used as the negative control. All of the D-amino acids tested were able to effectively label the PG of *L. innocua* equally or more efficiently than the azido D-Alanine probe. The greatest resolution and brightest fluorescent images were obtained using nitrone **3.1**. PG labelling was not observed in the absence of a 'clickable' amino acid, indicating that the fluorescence observed is the direct result of amino acid incorporation and subsequent SPANC. Once ubiquitous PG labelling with nitrone-modified UAA was achieved in *L. innocua*, the potential PG labelling of another gram-positive species, *Lactococcus lactis,* was evaluated using similar labelling conditions with the exception that the bacteria were shaken during the incubation period with the metabolic probe, since *L. lactis* lack flagella. This gram-positive, lactic acid-producing bacterium is commonly used in the dairy industry and represents an industrial relevant species with the potential to co-exist on food samples with pathogenic *L. monocytogenes. L. lactis* was chosen for these labelling experiments for its industrial importance as well as its physiological traits, displaying a round, chain-forming morphology and a lack of motility in contrast to the singular, rod-shaped and motile *L. innocua*, making the two species visually distinct under bright field microscopy.

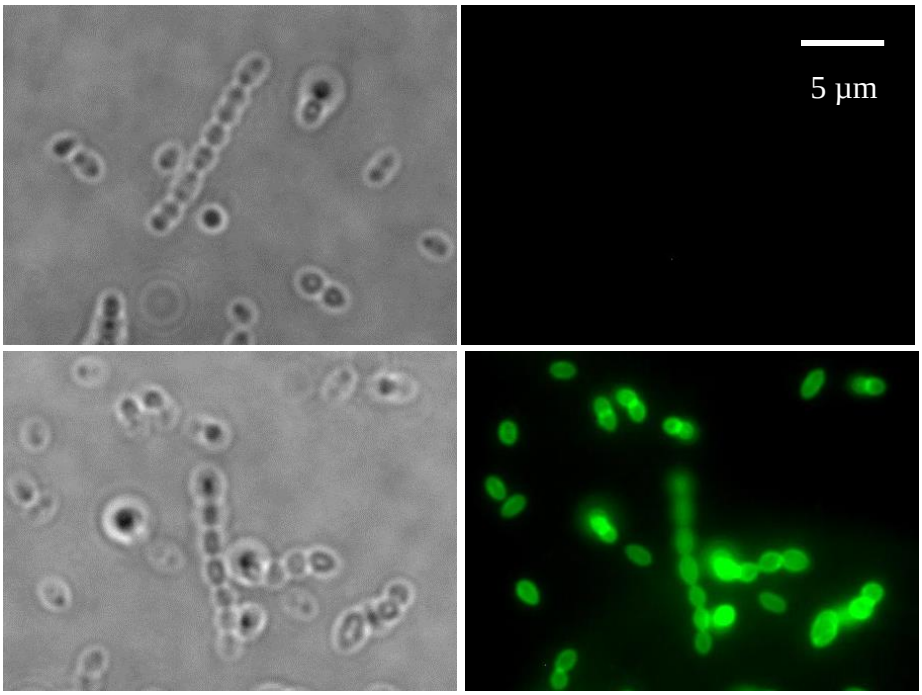

Figure 3.4 – Bright field (left) and fluorescent (right) imaging results of metabolic incorporation of nitrone 3.1 by *L. lactis* and subsequent SPANC with DIBO Alexafluor-488. Efficient PG labelling is achieved and under the conditions used, *L. lactis* remains visually distinct from *L. innocua* cultures visualized in previous experiments (Figure 3.3).

Fluorescent labelling of *L. lactis* PG was observed above background fluorescence with nitrone **3.1**, establishing SPANC as a functional method of labelling metabolically incorporated UAA bearing endocyclic nitrones.

Gram-negative bacteria peptidoglycan labelling

Nitrone-modified UAAs have shown to be readily incorporated into the PG of gram-positive bacteria of contrasting morphologies and motility. Gram-negative bacteria pose additional challenges to PG labelling. UAA probes would be required to pass through the outer cell membrane before reaching the PG where potential incorporation could occur. The PG layer of gram-negative bacteria is also less thick than that of gram-positive bacteria, providing fewer opportunities for UAA incorporation into cross-linking peptides. To evaluate the ability of nitrone-modified UAAs to penetrate the cell membrane and label the PG of gram-negative bacteria, K12 *Escherichia coli* were grown in LB broth until exhibiting mid-log phase growth and were incubated with amino acid probes **3.1** and **3.2** as described above, with comparison to azido D-Alanine and employing DMSO as a negative control. The fluorescence observed is comparable to azido D-Alanine, although much less prominent than the fluorescence observed in the PG labelling of gram-positive bacteria (Figure 3.2-3.4). The observation of fluorescent labelling of gram-negative *E. coli* suggests that the UAA probes are capable of penetrating bacterial cell membranes, supporting the hypothesis that these UAA are incorporated into newly synthesized PG or PG precursors. A similar result was observed by Bertozzi *et al* using alkyne-modified amino acids.[7]

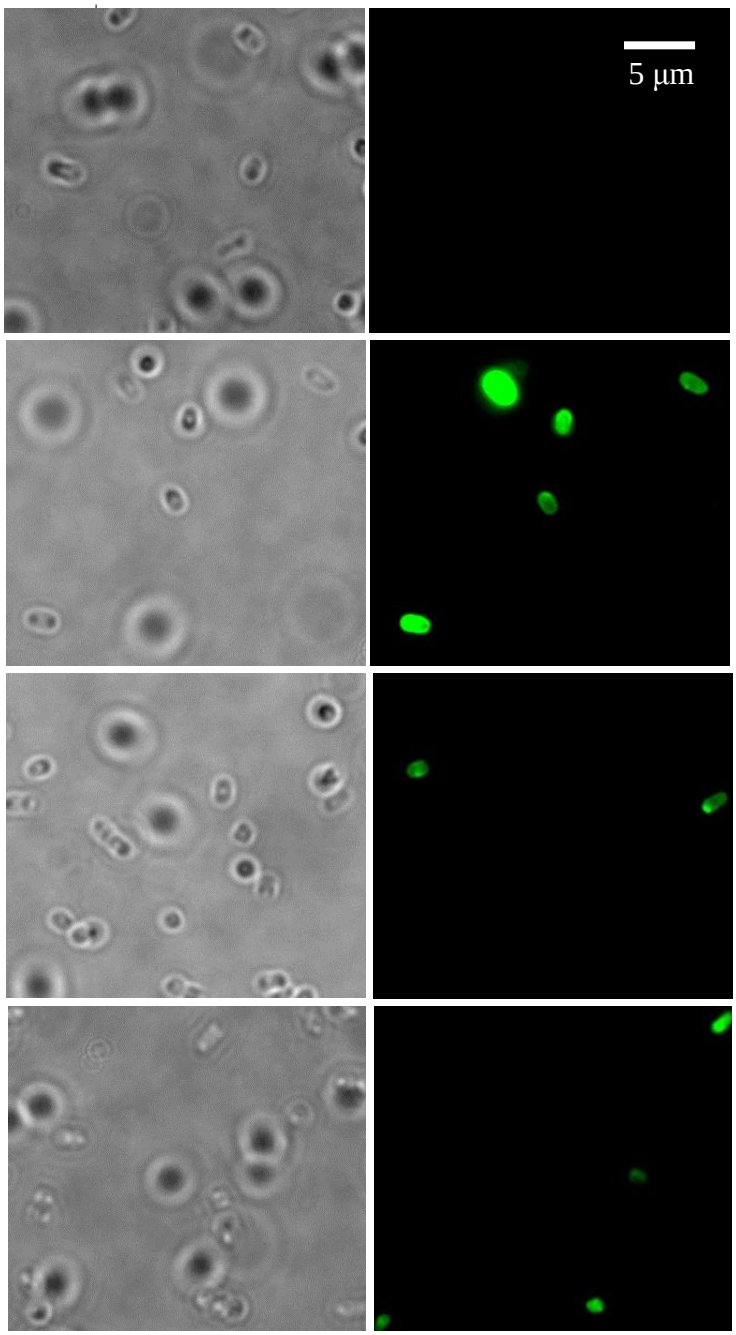

Figure 3.5 – Bright field (right) and fluorescent (left) imaging results of metabolic incorporation of D-amino acid probes by gram-negative *E. coli* and subsequent SPANC with DIBO Alexafluor-488. Though PG labelling appears less efficient than that observed in gram-positive bacteria, higher than background fluorescence is observed, suggesting the UAA probes are capable of penetrating cell membranes.

Labelling of PG with modified peptide-based antibiotics and visualization via SPANC

Once we had established SPANC as a visualization method for metabolically incorporated nitrone-bearing UAA probes for PG in gram-positive bacteria, we sought to explore alternate PG labelling methods that would expand the scope and potential applications of bioorthogonal SPANC. Recent literature has reported the use of vancomycin-functionalized magnetic nanoparticles as a non-covalent probe for capturing gram-positive bacteria.[19,20] Vancomycin is a pentapeptide glycoprotein antibiotic natural product that targets the D-Alanine-D-Alanine motif in gram-positive PG. Cell-surface fluorescent labelling of bacteria with vancomycin has not yet been reported using a two-stage 'click' chemistry method, although Bertozzi *et al* have also recently labelled nascent PG with a fluorescent BODIPY modified vancomycin.[7]

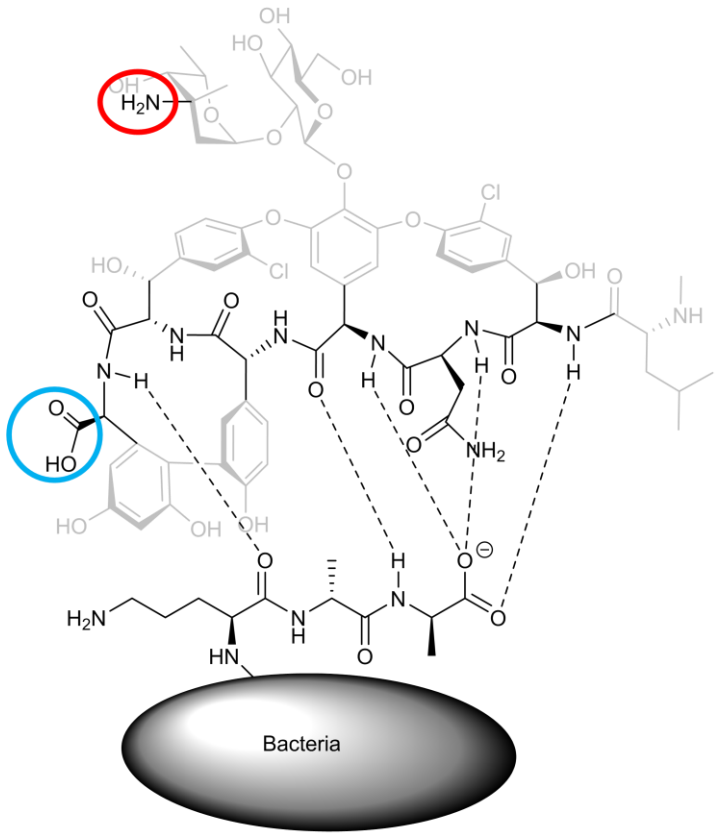

Figure 3.6 – Non-covalent interactions of the antibiotic polypeptide vancomycin with the D-Ala-D-Ala motif of cross-linked PG. Optimal and orthogonal chemical modification sites are circled in red and blue. Adapted from reference 19.

To address whether SPANC could be applied to labelling of non-covalent interactions between bacterial PG and small molecules, a nitrone-modified variant of vancomycin was prepared. The functionalization of vancomycin is simplified by the fact that there are two potential and mutually exclusive modification sites that are unlikely to disrupt the tertiary structure of the peptide. A primary amine located on the vancosamine sugar is ideal for standard coupling reactions with activated carboxylic acid moieties, while only one carboxylic acid is exposed as the rest of the amino acid functional groups exist as peptide bonds. Studies performed by Kell *et al* demonstrate that modification of vancomycin at the free carboxylic acid position causes the least perturbation of the antibiotic function.[19] We therefore sought to functionalize vancomycin with an endocyclic nitrone at the free carboxylic acid residue, using a polyethylene glycol (PEG) spacer to increase the accessibility of the nitrone to a strained alkyne reacting partner. Nitrone **3.5** was reacted with 4,7,10-trioxa-1,13-tridecanediamine in an HATU-mediated amide coupling reaction using the diamino PEG linker in large excess to avoid coupling two equivalents of nitrone **3.5** to each PEG unit. The PEG-modified nitrone was then coupled to vancomycin hydrochloride in a similar fashion. *L. lactis* were then cultured as described above, incubated with varying concentrations of **3.6**, reacted with DIBO Alexafluor-488 in a SPANC reaction, and visualized by fluorescent microscopy. Cell surface labelling was observed with concentrations as low as 20.0 μM in **3.6**, which displayed similar labelling at higher concentrations.

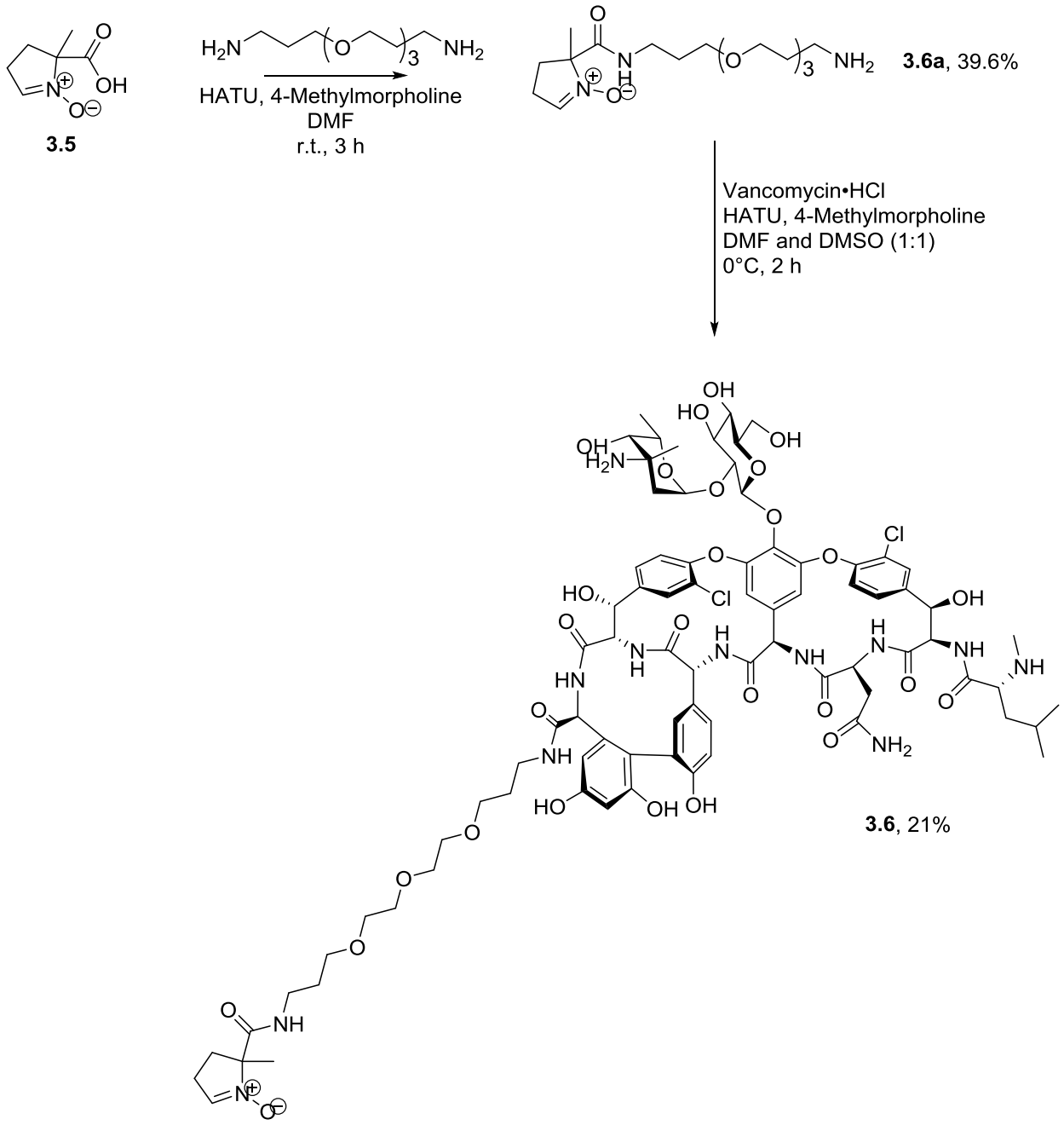

Scheme 3.2 – Synthesis of nitrone-modified vancomycin for gram-positive bacterial labelling. Nitrone 3.5 was treated with a stoichiometric excess of 4,7,10-Trioxa-1,13-tridecane diamine under HATU-mediated amide coupling conditions to prevent coupling to two equivalents of 3.5. Primary amine 3.6a was then coupled to the carboxylic acid residue of vancomycin; based on the findings of Kell *et al* on the efficiency of vancomycin-modified nanoparticles.[19]

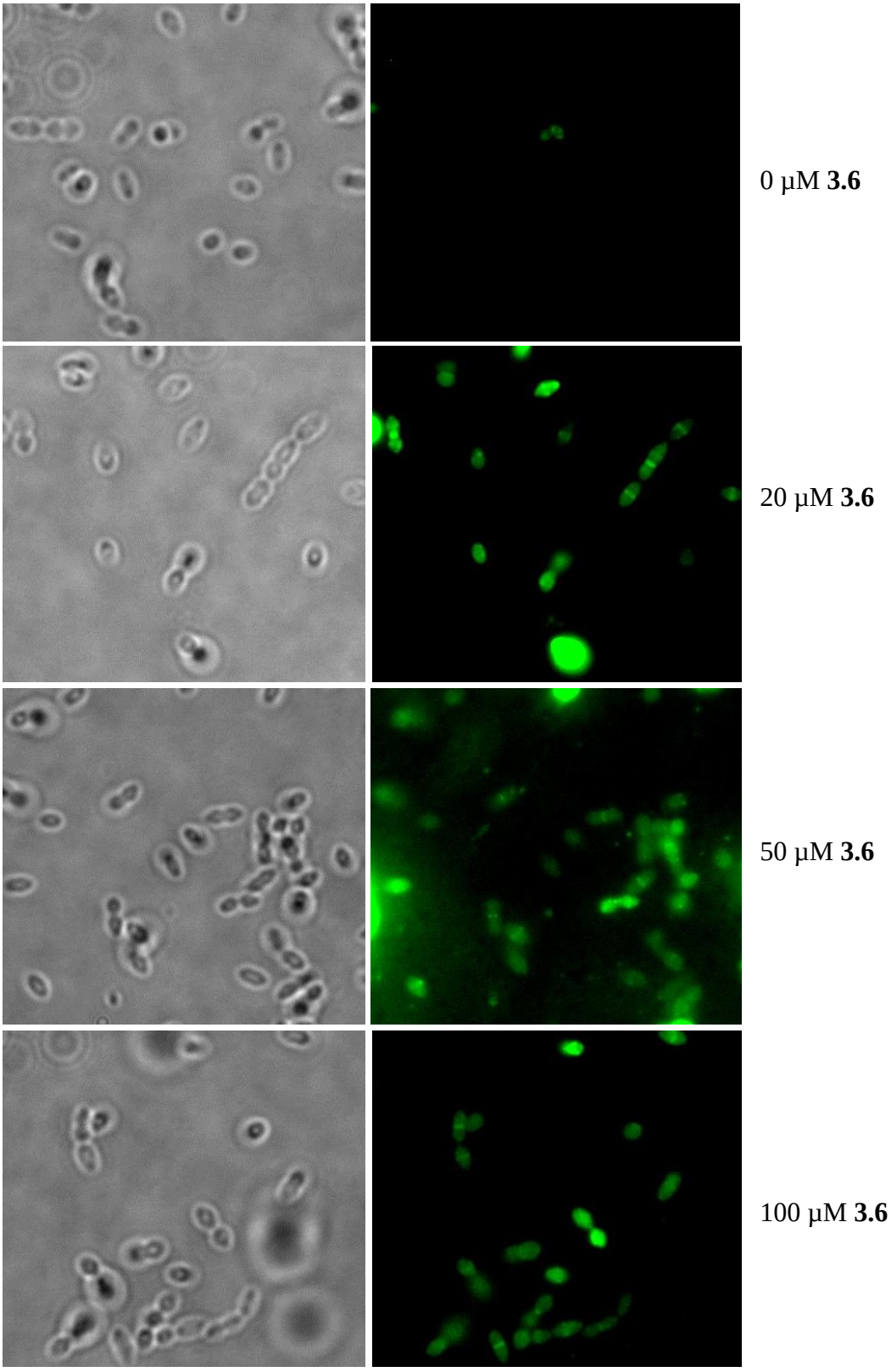

Figure 3.7 – Bright field (left) and fluorescent (right) imaging of *L. lactis* with nitrone-modified vancomycin probe 3.6 via SPANC with fluorophore-modified DIBO at varying probe concentrations. Cell-surface labelling is observed at concentrations of 3.6 as low as 20 µM.

Toward duplex bacterial labelling using nitrone-modified molecular probes

Duplex labelling in bacterial cultures has the potential to allow the identification novel molecular interactions and more in-depth study of known interactions by offering the ability to monitor two biologically relevant molecules simultaneously. The large variety of nitrone scaffolds that can be modified to mimic biomolecules and the unequal cycloadduct distribution in SPANC reactions employing different strained alkynes suggest that tuned SPANC reactions are likely capable of facilitating duplex biological labelling experiments. With a variety of nitrone-modified unnatural amino acid probes and a PG-interacting glyclopeptide antibiotic probe in hand, a strained alkyne reporter sensitive to stereoelectronic changes in nitrones was the sole missing requirement for evaluating SPANC as a duplex metabolic labelling strategy. To address this, BCN was synthesized as described previously and modified to bear a fluorescent molecule separated by a PEG linker according to Scheme 3.3.

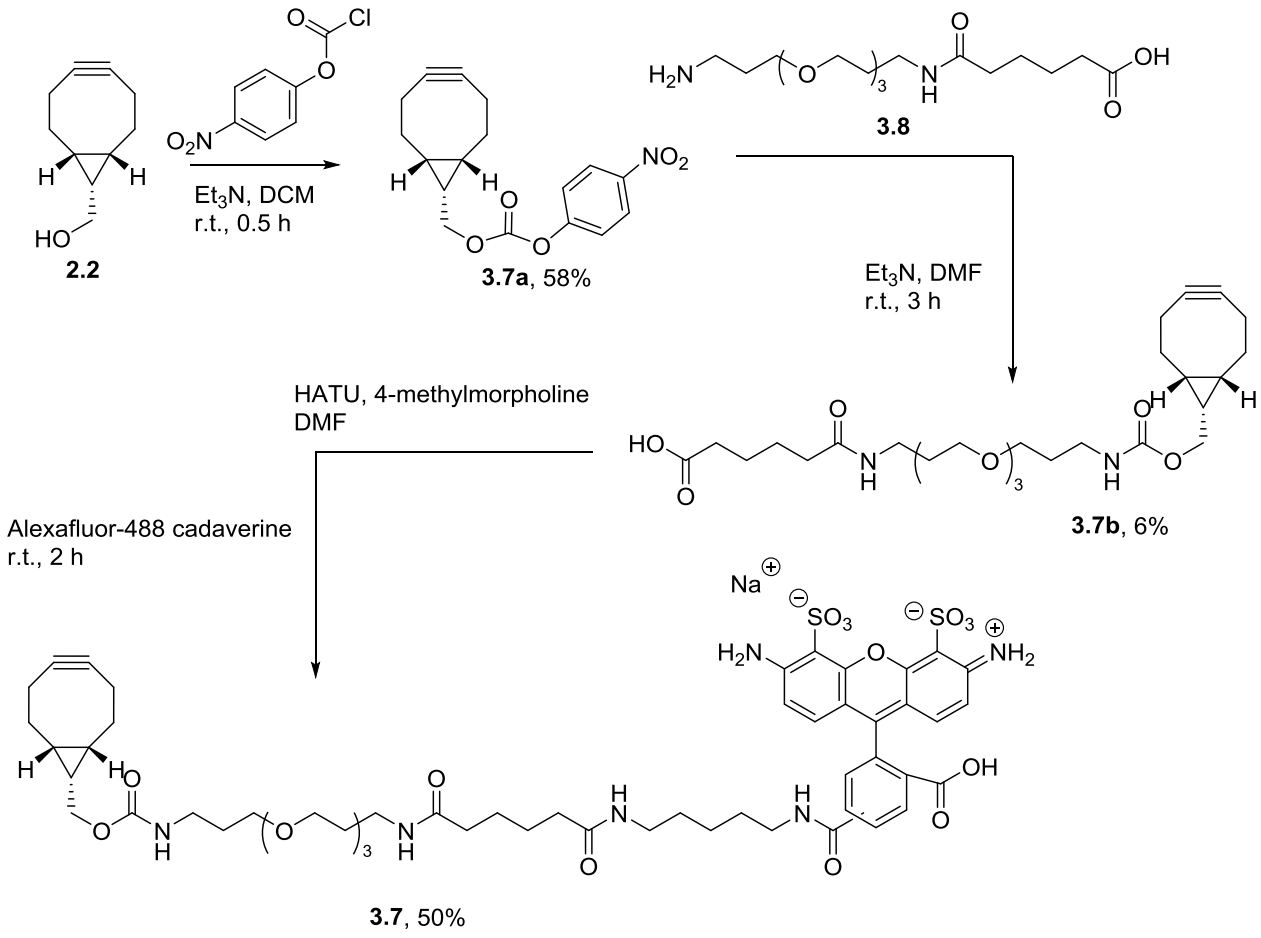

Scheme 3.3 – Synthesis of BCN Alexafluor-488 conjugate. Linker 3.8 was synthesized and used to displace the *para*-nitro carbonate of 3.7a by Alexafluor-488 cadaverine.

PEG linker **3.8** was synthesized from 4,7,10-Trioxa-1,13-tridecanediamine and Adipic acid in order to function as a nucleophile to displace the *p*-nitro phenyl group of the BCN carbonate ester, **3.7b**, while remaining reactive toward an HATU-mediated peptide coupling with Alexafluor-488 cadaverine. With **3.7** in hand, the efficiency of SPANC and SPAAC under a variety of conditions could be tested. Firstly, working with *L. innocua*, the viability of **3.7** was evaluated as a fluorescent reporter in systems that previously yielded metabolic PG labelling using DIBO Alexafluor-488 as the reporter.

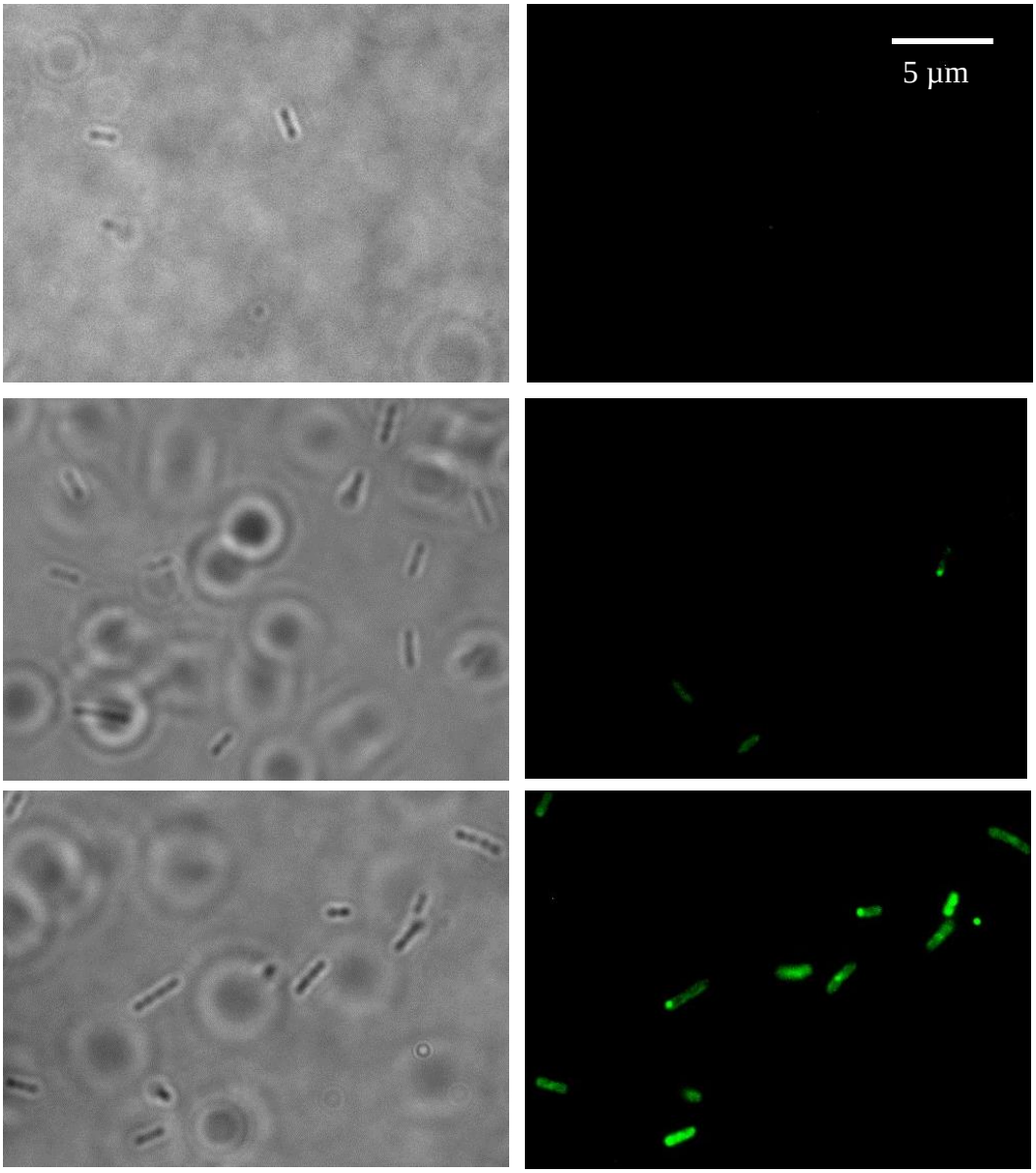

Figure 3.8 - Bright field (left) and fluorescent (right) imaging results of metabolic incorporation of UAA probes by *L. innocua* and subsequent SPANC or SPAAC by incubation with BCN reporter 3.7 for 10 minutes. Increased fluorescence is observed when nitrone 3.1 is employed, resulting from the greater second-order rate constant of the SPANC reaction versus the SPAAC reaction.

Interestingly, the PG labelling observed in *L. innocua* shows greater intensity when nitrone **3.1** is metabolically incorporated rather than azido D-Alanine. This increase in intensity follows the reactivity trends observed in our kinetic experiments discussed in chapter 2, suggesting that differences in second-order rate constant can lead to differences in fluorescent intensity. To further test this theory, a similar set of labelling experiments using DIBO Alexafluor-488 was performed using bacteria from the same cell culture. DIBO has been shown to be less selective in dipolar cycloadditions evidenced by the observed product distribution in the one-pot competitive SPANC reaction previously discussed (Scheme 2.3).[14] It is therefore expected that more uniform labelling will be observed, regardless of the dipole employed as the metabolic probe. Figure 3.9 summarizes the results of this experiment. Greater labelling efficiency is observed when nitrone **3.1** is employed; however, the difference in fluorescence observed between SPANC and SPAAC labelling methods is less extreme than that observed after labelling with alkyne **3.7**. From this, we can infer that azido D-Alanine may be incorporated into the PG of *L. innocua* in lower levels than nitrone **3.1**, although the unequal fluorescent intensity observed is partially due to the difference in the second-order rate constant of the SPANC reaction versus SPAAC.

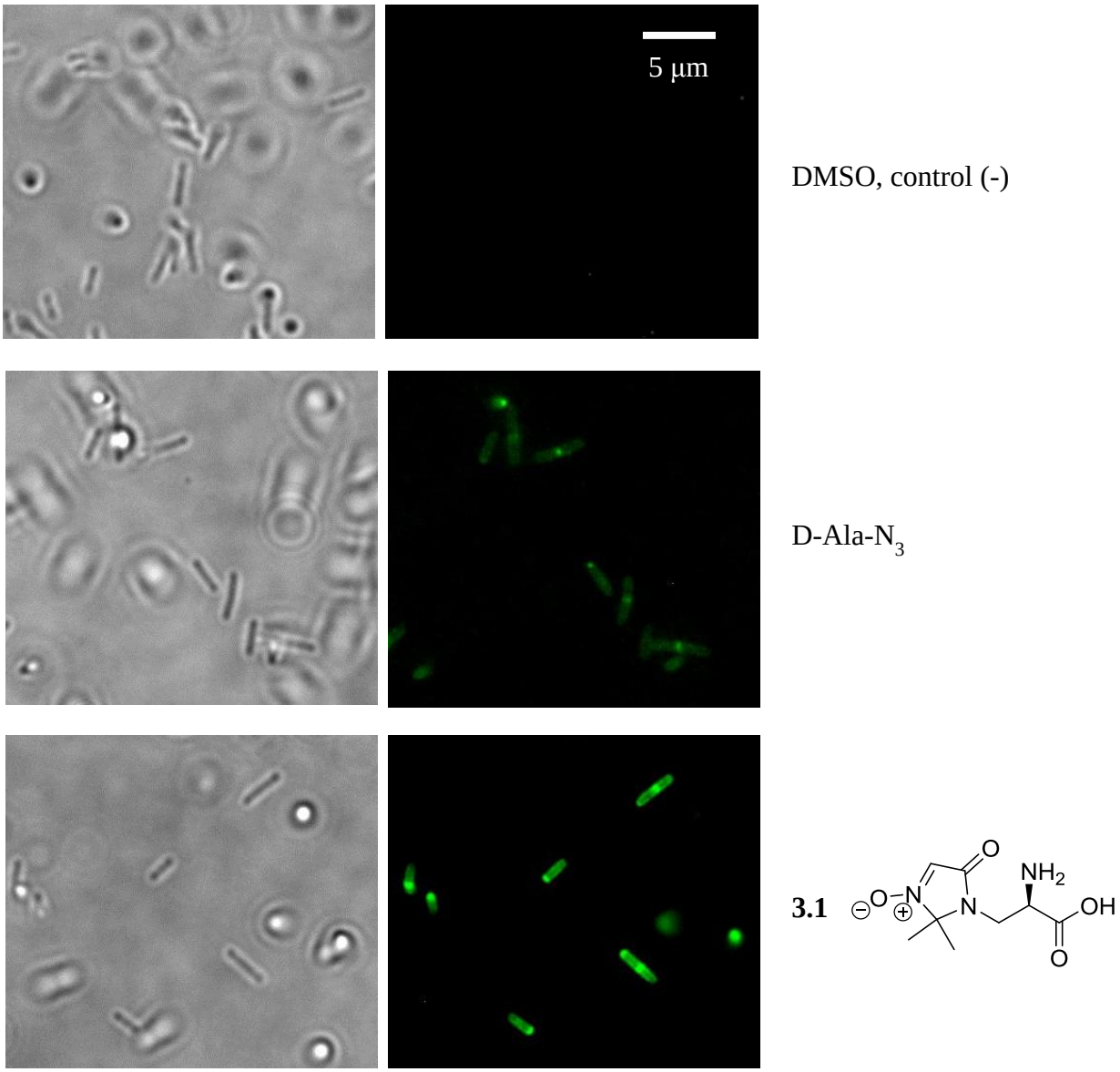

Figure 3.9 – Bright field (left) and fluorescent (right) imaging results of the metabolic incorporation of UAA probes by *L. innocua* via strain-promoted cycloaddition using DIBO Alexafluor-488. The observed contrast in fluorescent intensity is smaller than that observed when alkyne 3.7 is used as the chemical reporter (compare against Figure 3.8).

After observing unequal fluorescent intensities in metabolic PG labelling experiments based on the differences in rate constant of SPANC versus SPAAC with fluorescent alkyne **3.7**, it was envisaged that duplex labelling could be demonstrated by performing metabolic PG labelling in a mixed culture of two morphologically distinct bacteria using metabolic probes bearing nitrones that display significantly different second-order rate constants. Since we have shown that one-pot competitive SPANC reactions lead to unequal product distribution, we designed the metabolic labelling experiment outlined in Scheme 3.4 which could be performed with the gram-positive bacteria for which we have observed the metabolic incorporation of nitrone-bearing UAA probes to establish SPANC as a bioorthogonal duplex labelling strategy. To evaluate the potential of this experiment, we first performed PG labelling of *L. lactis* with D-Alanine azide and nitrone **3.1** and visualized the PG through SPANC with the fluorescent BCN **3.7**, analogous to the experiments performed with *L. innocua* previously.

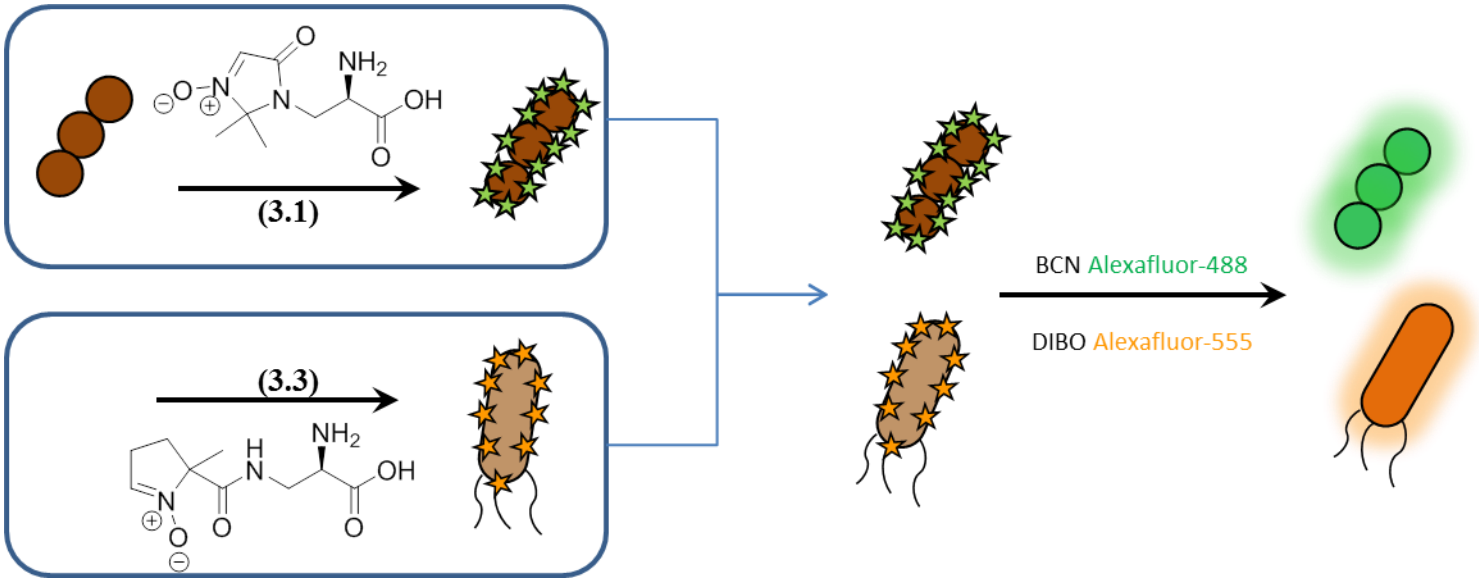

Scheme 3.4 – Experimental design of simultaneous orthogonal SPANC reactions used to fluorescently label gram-positive bacteria that have been independently incubated with nitrone-modified UAA probes 3.1 and 3.3. After probes 3.1 and 3.3 are incorporated into the PG of *L. lactis* and *L. innocua*, respectively, the two bacterial cultures are combined and treated simultaneously with fluorescent alkyne 3.7 (green) and Alexafluor-555 modified DIBO (orange). If mutual exclusivity is achieved, only orange fluorescent rod-shaped *L. innocua* and fluorescent green round *L. lactis* will be observed.

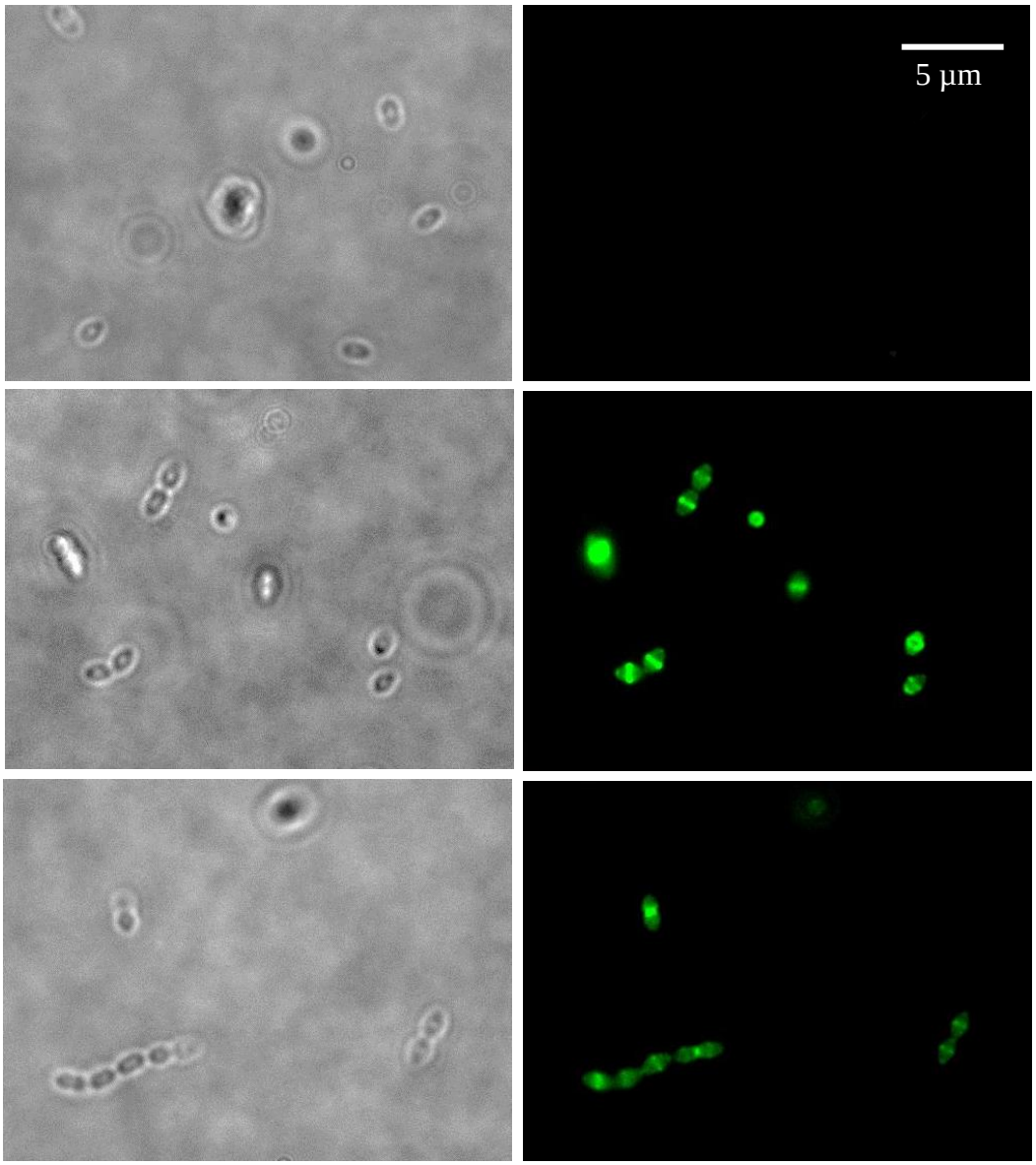

Figure 3.10 – Bright field (left) and fluorescent (right) imaging results of metabolic incorporation of UAA probes by *L. lactis* and subsequent SPANC or SPAAC with BCN Alexafluor-488. Greater fluorescent intensity is observed when the azido D-Alanine probe is used, despite the near 40-fold difference in second-order rate constants between benzyl azide and nitrone 2.11 with BCN.

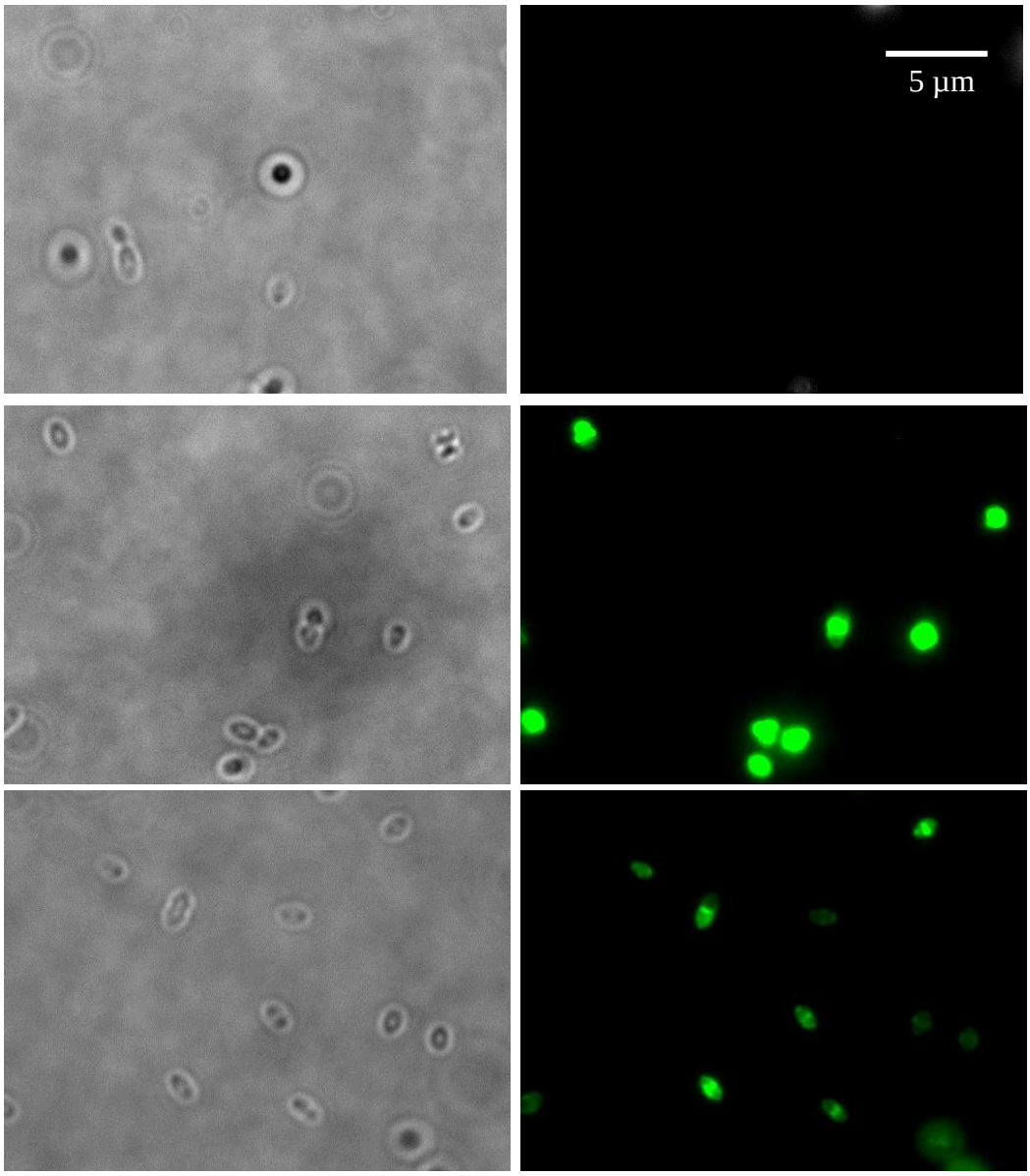

Figure 3.11 – Bright field (left) and fluorescent (right) imaging results of metabolic incorporation of UAA probes by *L. lactis* and subsequent SPANC or SPAAC with DIBO Alexafluor-488. Greater fluorescent intensity is observed with the azide-modified UAA probe. These results, along with those presented in Figure 3.10 suggest that D-Ala-N_3 is incorporated into the PG of *L. lactis* at greater concentrations than nitrone 3.1.

Surprisingly, the fluorescence observed for *L. lactis* is more intense in cycloadditions employing D-Alanine azide as the reactive dipole on the metabolic probe when either **3.7** or DIBO Alexafluor-488 is used for visualization. This observation leads us to believe that a greater concentration of azido D-Alanine in the PG of *L. lactis* is achieved over the UAA incubation period than can be achieved over the same incubation period with **3.1**. Efforts to evaluate this observation are currently underway.

Despite the apparent inequalities in the levels of azido D-Alanine and nitrone **3.1** between *L. innocua* and *L. lactis*, we sought to evaluate the duplex labelling potential of the non-optimized SPANC metabolic labelling strategy as described in Scheme 3.4. Presumably, since nitrone probes **3.1** and **3.3** are similar in structure and size, one probe will be incorporated into the PG of one bacterial culture as efficiently as the other probe. As a preliminary experiment to observe the ideal labelling scenario that would be achieved by mutually exclusive duplex labelling, *L. lactis* was incubated with nitrone **3.1** and visualized with fluorescent BCN, **3.7**. In parallel, a culture of *L. innocua* was incubated with nitrone **3.3** and visualized with DIBO Alexafluor-555, and the two bacterial cultures were combined. UAA probe **3.1** was successfully incorporated into *L. lactis* and visualized with **3.7**, however, no fluorescence was observed after attempting to visualize *L. innocua* incubated with **3.3** and visualizing with DIBO Alexafluor-555. To rule out the DIBO Alexafluor-555 as the cause of the problem, the same culture of *L. innocua* that had been incubated with nitrone **3.3** was then incubated with fluorescent BCN, **3.7**, also resulting in a lack of fluorescence. All subsequent attempts to metabolically label *L. innocua* with nitrone **3.3** have resulted in little to no fluorescent PG labelling.

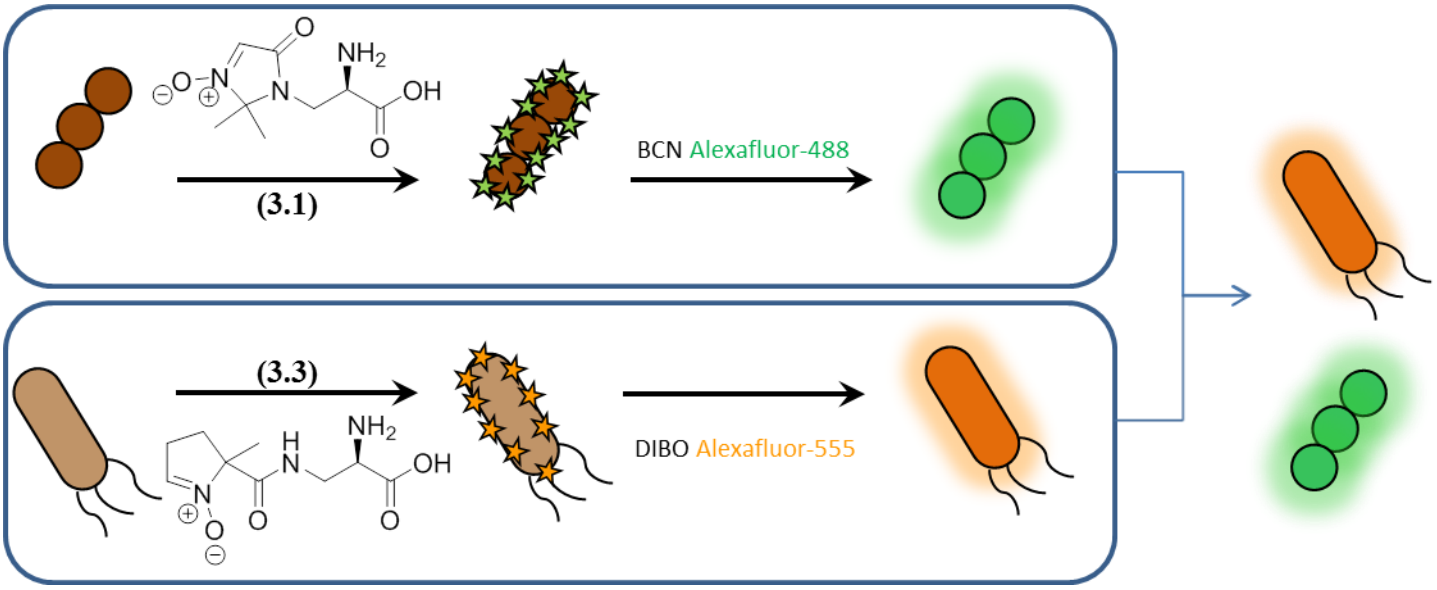

Scheme 3.5 – Representation of ideal mutually exclusive fluorescent labelling in a binary bacterial culture via SPANC. *L. lactis* (top) is metabolically labelled with UAA probe 3.1 and visualized with fluorescent BCN reporter 3.7. Separately, *L. innocua* (bottom) is metabolically labelled with UAA probe 3.3 and visualized with DIBO Alexafluor-555. The two fluorescently labelled cultures are then combined and visualized by fluorescence microscopy to provide a visual comparison for future duplex labelling experiments.

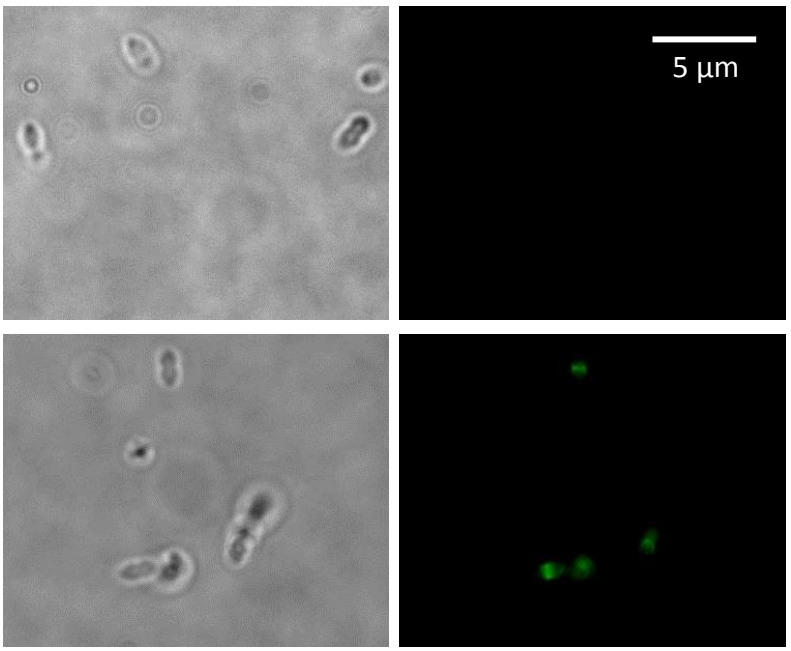

DMSO, control (-)

3.1

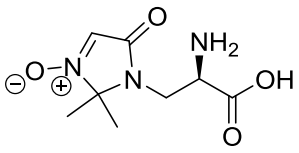

Figure 3.12 – Bright field (left) and fluorescent (right) imaging results of *L. lactis* incubated with nitrone 3.1 and visualized through subsequent SPANC with 2.5 µM fluorescent BCN, 3.7, as a systematic check in pursuit of a positive comparison for duplex SPANC labelling.

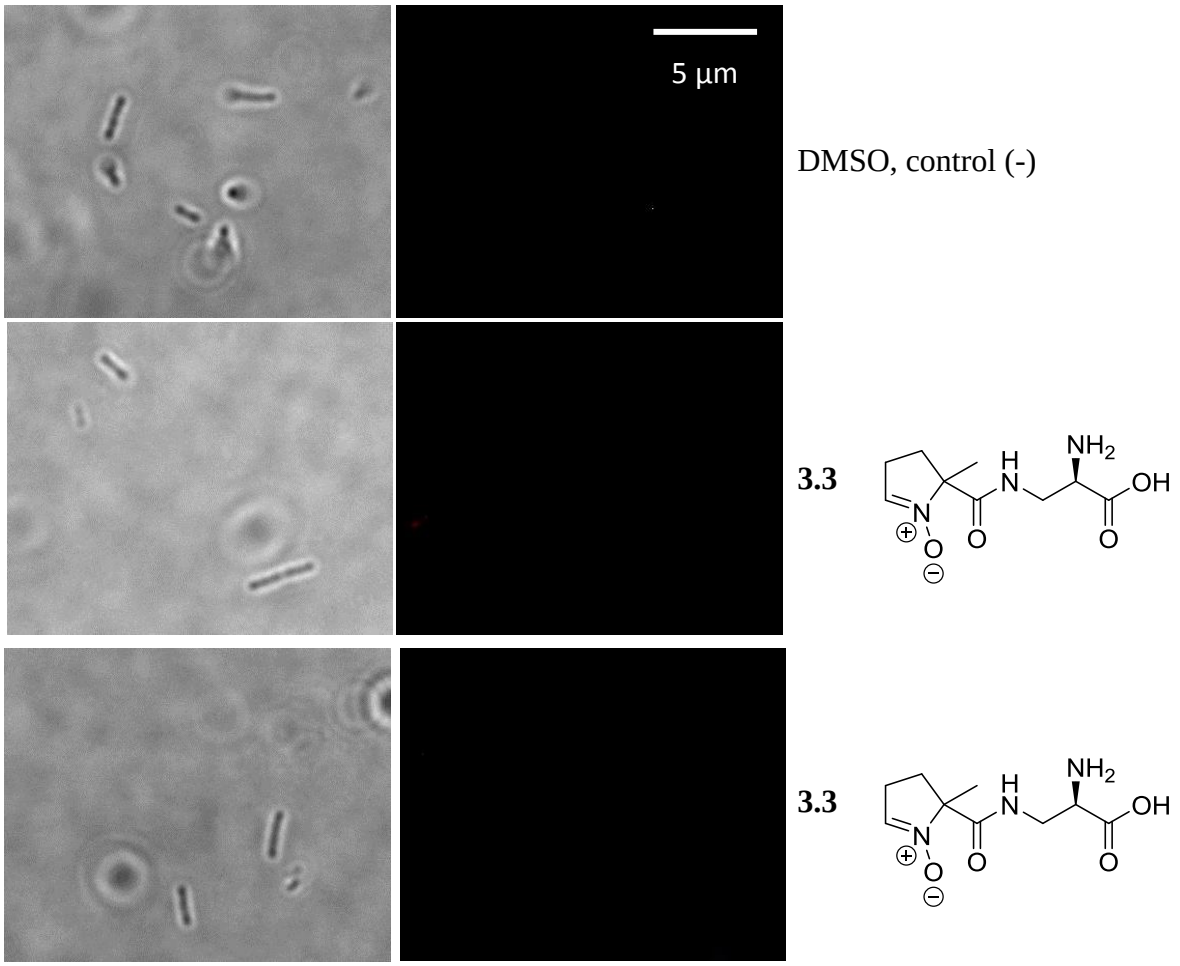

Figure 3.13 - Bright field (left) and fluorescent (right) imaging results of *L. innocua* incubated with nitrone 3.3 and visualized by SPANC with 2.5 µM DIBO Alexafluor-555 (middle) or 2.5 µM 3.7 (bottom). No fluorescence is observed, suggesting that nitrone 3.3 was not incorporated into the bacterial PG.

A similar experiment (Scheme 3.6) was also performed, inverting the fluorescent cyclooctynes used for imaging. The results of this experiment will serve as a reference, showing the level of labelling efficiency that can be expected from mismatched nitrone-cyclooctyne pairs. Since some cross-reactivity was observed in the one-pot competitive SPANC reaction (Scheme 2.3), low-levels of fluorescence are expected from the mismatched nitrone-cyclooctyne pairs, although lower levels than those observed in the experiment depicted in Scheme 3.5 are expected. With the results of these two reference experiments, we are able to qualitatively evaluate the efficiency of SPANC as a duplex metabolic labelling strategy for bacterial PG labelling.

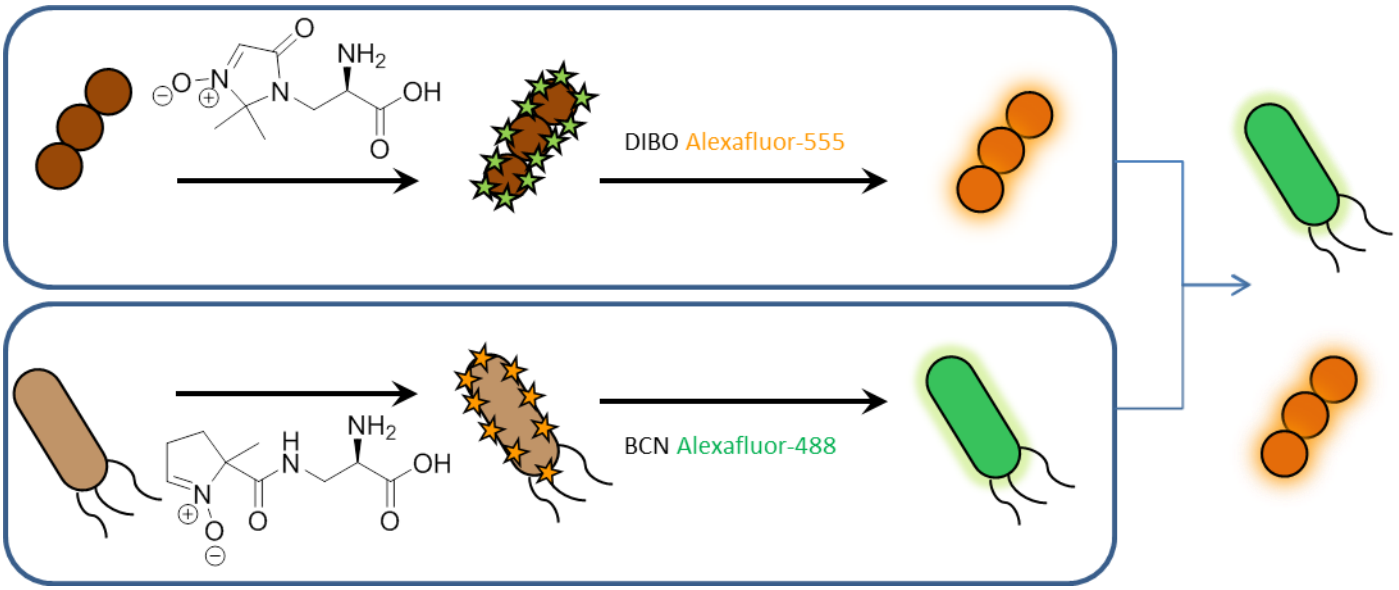

Scheme 3.6 - – Representation of mismatched nitrone-alkyne fluorescent labelling in a binary bacterial culture via SPANC. *L. lactis* (top) is metabolically labelled with UAA probe 3.1 and visualized with DIBO Alexafluor-555. Separately, *L. innocua* (bottom) is metabolically labelled with UAA probe 3.3 and visualized with fluorescent BCN, 3.7. The two fluorescently labelled cultures are then combined and visualized by fluorescence microscopy to provide a visual representation of the maximum level of fluorescence that can be expected from cross-reactivity in the duplex metabolic labelling experiment depicted in Scheme 3.4.

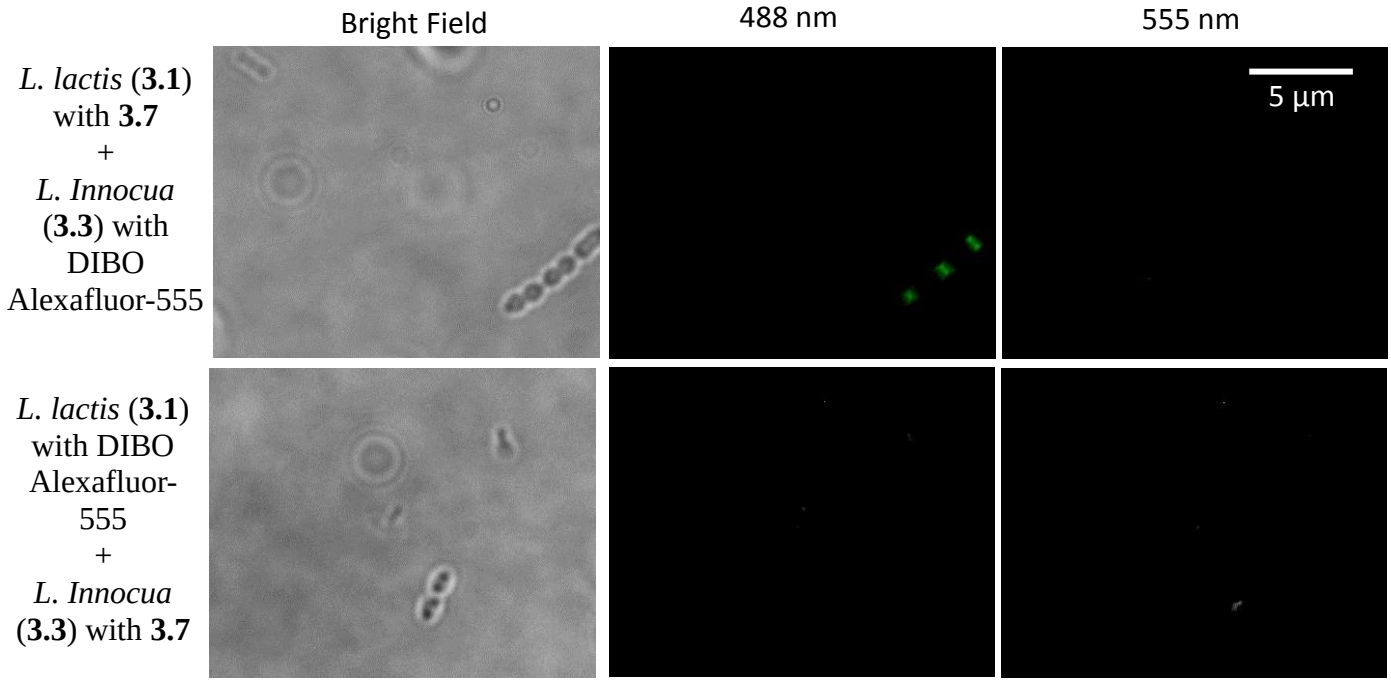

Figure 3.14 – Bright field (left), 488 nm fluorescent (middle) and 555 nm fluorescent imaging (right) results of individually labelled cultures of *L. lactis* and *L. innocua* that were combined after SPANC with 2.5 µM 3.7 or DIBO Alexafluor-555 as indicated. Top panels show imaging results for ideally matched nitrone-alkyne pairs, while the bottom panels show imaging results for mismatched nitrone-alkyne pairs.

Over the course of collecting the reference images, it was observed that the electron-rich nitrone-modified UAA probe **3.3** was poorly incorporated into the PG of *L. innocua* (Figure 3.13). This is a puzzling result given the initial success shown in Figure 3.2. Efforts to determine the source of the resistance to incorporation of **3.3** are currently underway.

With the reference experiments completed, duplex labelling as described in Scheme 3.4 was attempted. *L. lactis* was incubated with probe **3.1** while *L. innocua* was incubated with UAA probe **3.3**. Each culture was washed in PBS buffer before being combined together and incubated with fluorescent BCN conjugate **3.7** and DIBO Alexafluor-555 for 10 minutes, washed again in PBS and visualized by fluorescence microscopy (Figure 3.15). Interestingly, only labelling of *L. lactis* with **3.7** is observed. Labelling of *L. innocua* with **3.7** or DIBO Alexafluor-555 is not observed, nor is labelling of *L. lactis* with DIBO Alexafluor-555. Although it appears again as though **3.3** was not efficiently incorporated into the PG of *L. innocua*, this experiment demonstrates that DIBO Alexafluor-555 will not readily form visible conjugates with UAA probe **3.1** in the presence of fluorescent BCN **3.7**. This encouraging result suggests that cross-reactivity will be minimal or negligible when nitrone **3.3** is efficiently incorporated into the bacterial PG, lending support for the use of SPANC as a viable duplex labelling method in living systems.

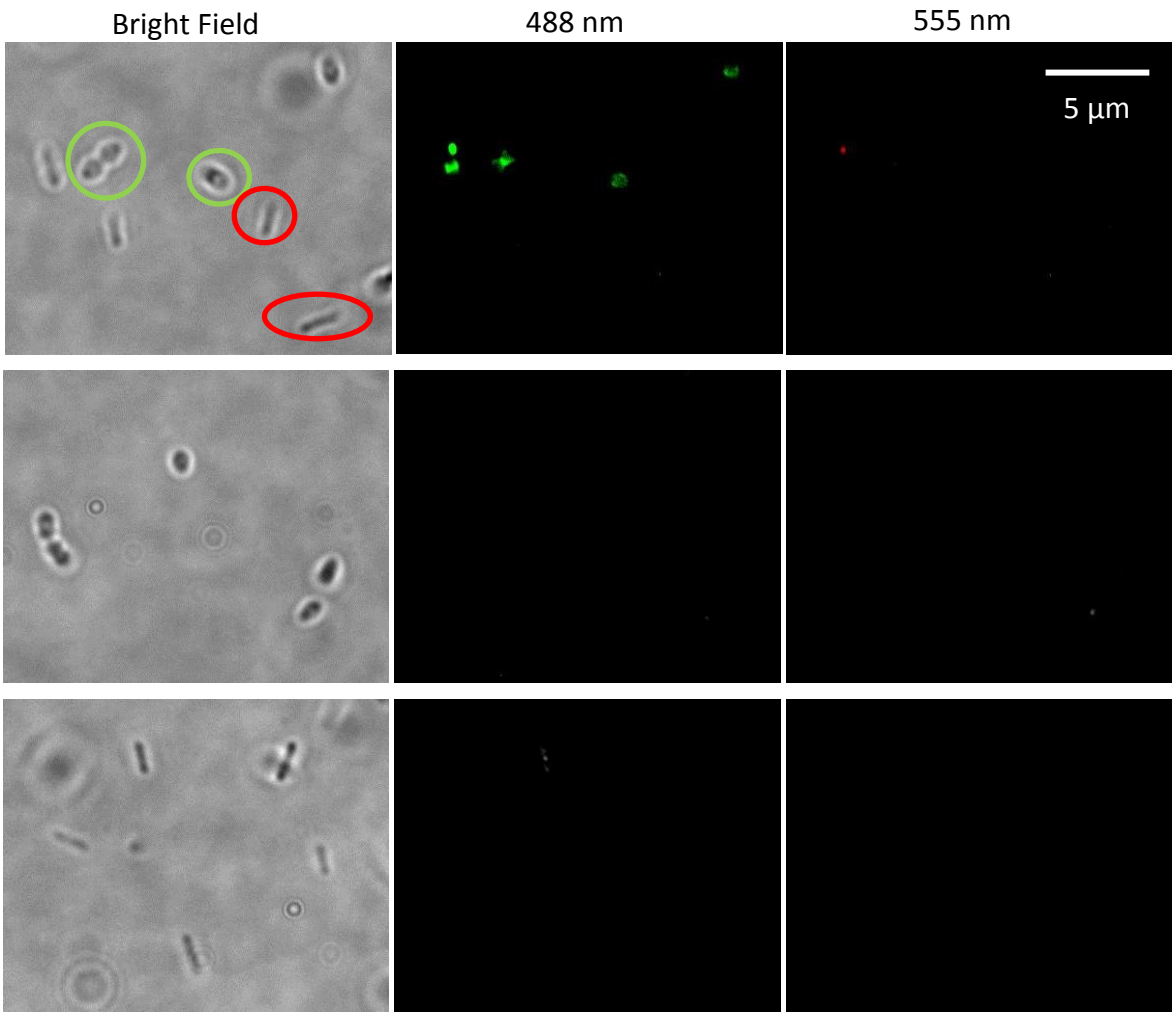

Figure 3.15 – Bright field (left), 488 nm fluorescent (middle) and 555 nm fluorescent (right) imaging results for non-optimized duplex SPANC labelling of PG in a binary mixture of bacteria. Row A represents the experimental condition where a mixture of *L. lactis* and *L. innocua* metabolically labelled with nitrone 3.1 or 3.3 were incubated with 2.5 µM each of 3.7 and DIBO Alexafluor-555 simultaneously for 10 minutes. Green circles highlight *L. lactis* and red circles highlight *L. innocua*. Rows B and C represent negative controls lacking UAA incorporation into *L. lactis* and *L. innocua*, respectively, while still being subject to incubation with the same mixture of fluorescent alkynes.

Conclusion

Nitrones can be incorporated into biomolecules by classical peptide coupling reactions or through the direct oxidation of amines existing or installed in the native biological substrates. Nitrone-bearing unnatural amino acid analogues synthesized in these ways are capable of metabolic incorporation into the peptidoglycan wall of both gram-positive and gram-negative bacteria. SPANC reactions of metabolically incorporated unnatural amino acids with fluorescently tagged cyclooctynes are a convenient method to visualize PG in live bacteria. Increased fluorescent intensity is observed at sites of active cell division where PG is newly synthesized. Taken together with the ability of nitrone-bearing UAA to be incorporated into PG of gram-negative bacteria, these observations suggest that the UAA tested are capable of crossing the cell membrane and are incorporated into the cross-linking peptides of nascent PG. Visualization of non-covalent molecular interactions can also be achieved on the surface of live bacteria via SPANC. Through careful choice of nitrone and alkyne structure in metabolic probes and reporters, product distribution can be controlled in live-cell environments with the potential to achieve mutual exclusivity. Though not all factors governing the metabolic incorporation of nitrone-modified UAA probes have been identified, we have shown that SPANC can be used to fluorescently label bacterial PG through the use of metabolically incorporated probes as well as non-covalent PG interactions. With multiple SPANC-based imaging methods at our disposal, it is anticipated that duplex metabolic labelling of live bacteria will soon be achieved.

Future Directions

Duplex metabolic labelling

Nitrone-bearing unnatural D-amino acid analogues have been shown to be incorporated into gram-positive bacterial PG and remain capable of fluorescent visualization through SPANC reactions with fluorescently modified strained cyclooctynes. The rate constants of SPANC reactions involving BCN have been shown to be sensitive toward electronic alterations of the nitrone component. The differences in rate constants have also been shown to lead to biased product distribution in a two-alkyne, two-nitrone, one-pot simultaneous SPANC competition experiment. Applying this principle to a biological setting could allow the simultaneous monitoring of multiple biomolecules allowing the visualization of potential synergistic effects in response to a stimulus. Preliminary experiments in bacteria have shown that the incorporation of nitrone-modified UAA probes into PG is not trivial, although, once the UAA probes are incorporated biased cycloadduct proportions are observed when fluorescent BCN **3.7** and DIBO Alexafluor-555 are employed as fluorescent reporters. These results support the hypothesis that SPANC reactions can be tuned, and tuned SPANC reactions have the potential to be used as a duplex reporter system.

The future needs of this project begin with identifying the factors that govern the incorporation of unnatural D-amino acid based probes into the PG of gram-positive bacteria. This can be achieved by modifying the temperatures at which the bacteria are incubated with the UAA probe, as well as the incubation time and concentration of UAA probe. Structure-activity relationship studies can also be performed to meet this requirement. Preparation of a series of UAA probes that differ in structure, size, charge, and location of the reactive dipole will allow the incorporation of a variety of substrates to be tested, providing insights toward the best, and least

tolerated aspects of the metabolic probe. Once the factors governing the metabolic incorporation of UAA probes are elucidated, duplex labelling can be attempted again as described in Scheme 3.4.

Improving reaction kinetics

BCN has been shown to react more rapidly with electron-deficient nitrones. In order to achieve greater selectivity in one-pot competitive SPANC reactions with BCN, greater electronic contrast in endocyclic nitrones is desired. This can be achieved through the design and synthesis of nitrones displaying a greater electronic deficiency. Nitrone **2.11** has shown the largest second-order rate constant in SPANC reactions with BCN, and serves as a logical starting point for the design of electron-poor nitrones. In the synthesis of nitrone **2.11**, the dehydrative cyclization conversion from **2.11c** to **2.11d** employs acetone as an electrophile. If more electrophilic ketones or aldehydes (substituted benzaldehyde or benzophenone derivatives, for example) were used in place of acetone, the resulting heterocycles would also be more electrophilic. Variation of the electrophile employed at this step of the synthesis could lead to a series of nitrones whose inductive electronic effects on the second-order rate constants of SPANC reactions could be studied.

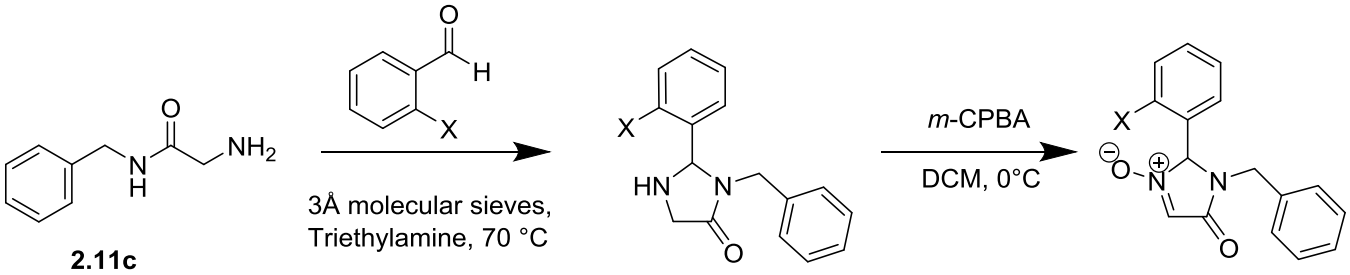

Equation 3.5 – Synthetic procedure for increasingly electron-deficient nitrones based on nitrone 2.11 that are likely to exhibit increased second-order rate constants in SPANC reactions with BCN.

Materials and Experimental Methods

Chemical reagents were purchased from Sigma Aldrich, Alfa Aesar, Acros Organics, or Matrix Scientific and used without further purification. Reactions were carried out under Argon atmosphere unless otherwise stated. Deuterated solvents were purchased from Cambridge Isotope laboratories. Thin layer chromatography (TLC) was carried out on Analtech Uniplate® silica gel plates (60 Å F_{254}, layer thickness 250 μm) using UV light and $KMnO_4$ stainto visualize. Flash column chromatography was performed using silica gel (60 Å, particle size 40-63 μm). ^{1}H NMR and ^{13}C NMR spectra were obtained using a 400 MHz Bruker NMR spectrometer. Chemical shifts are reported as δ referenced to residual solvent and coupling constants (*J*) are reported in Hz. Low-resolution mass spectral data were obtained using a Waters micromass ZQ mass spectrometer coupled to a Waters 2795 separations module liquid chromatograph equipped with a Waters 996 photodiode array detector.

Unnatural Amino Acid Synthesis: Electron-deficient D-Ala Derivative

(2R)-2-*tert*-Butoxycarbonylamino-3-(9H-fluoren-9-ylmethoxycarbonylamino)-propionic acid (3.1a):

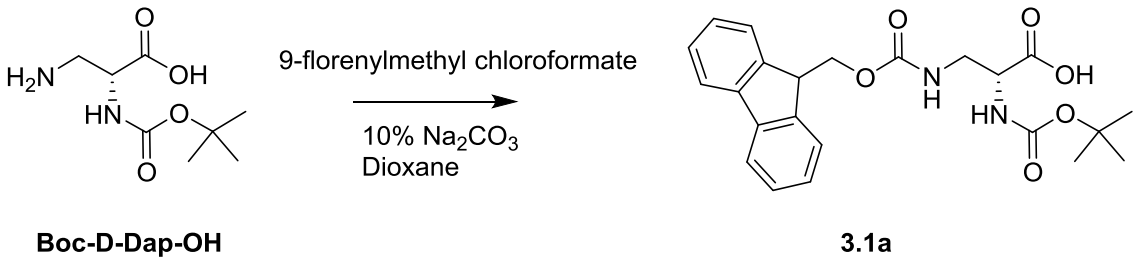

Boc-D-Dap-OH **3.1a**

Procedure: Boc-D-Dap-OH (2.08 g, 10.2 mmol) was partially dissolved in a 10% aqueous solution of Sodium carbonate and cooled to 0℃. A solution of 9-Florenylmethyl chloroformate (3.18 g, 12.3 mmol) in 32.0 mL of 1,4-Dioxane was added slowly. The reaction was stirred at 0℃ for 1 h, then diluted with distilled water and ether and separated. The aqueous phase was acidified to pH~1 with concentrated HCl and extracted with Ethyl acetate. Dried over Magnesium sulfate, filtered and concentrated to afford 4.34 g as a fluffy white solid, quantitative yield. RF = 0.05 (5% MeOH in DCM). ^{1}H NMR (400 MHz, $CDCl_3$): 9.76 (br s, 1H), 7.75 (d, J=7.5 Hz, 2H), 7.55 (d, J=7.4 Hz, 2H), 7.37 (t, J=7.2 Hz, 2H) 7.28 (t, J=7.2 Hz, 2H) 4.36 (m, 3H) 4.17 (t, J=6.7 Hz, 1H) 3.61 (m, 2H) 1.43 (s, 9H). ^{13}C (100 MHz, $CDCl_3$): 173.1, 156.2, 143.7, 141.3, 127.7, 127.1, 125.1, 120.0, 67.2, 47.1, 42.8, 28.3, 21.0, 14.2.

(2R)-2-*tert*-Butoxycarbonylamino-3-(9H-fluoren-9-ylmethoxycarbonylamino)-propionic acid *tert*-butyl ester (3.1b):

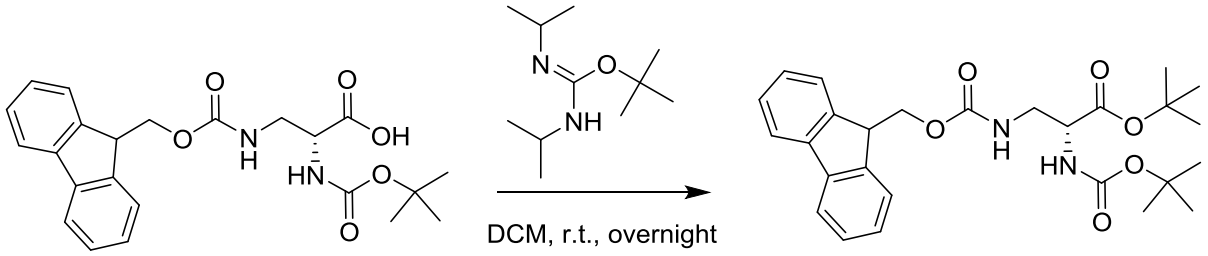

3.1a **3.1b**

Procedure: **3.1a** (0.700 g, 1.64 mmol) was dissolved in 10.0 mL of dry DCM (dried over 3 Å molecular sieves) and placed under Argon at room temperature. 2-*tert*-Butyl-1,3-diisopropylurea (2.94 g, 14.7 mmol) was added dropwise and stirred overnight at room temperature. Hexanes were added to precipitate the urea byproduct, which was then filtered off. The filtrate was concentrated, taken up in Ethyl acetate and distilled water. The organic layer was separated and washed with saturated Sodium bicarbonate (2x30 mL) and water (2x30 mL), then dried over Sodium sulfate, filtered, and concentrated. Purified by column chromatography (20% EtOAC in hexanes) to afford 0.542 g as a pale yellow oil (68.5% yield). RF = 0.16. ^{1}H NMR (400 MHz, $CDCl_3$): 7.76 (d, J=7.5 Hz, 2H), 7.58 (d, J=7.4 Hz, 2H), 7.40 (t, J=7.4 Hz, 2H), 7.31 (t, J=7.5 Hz, 2H), 4.37 (d, J=6.9 Hz, 2H), 4.29 (br s, 1H), 4.21 (t, J=7.0 Hz, 1H), 3.59 (m, 2H), 1.47 (s, 9H), 1.45 (s, 9H). ^{13}C(125MHz, $CDCl_3$): 169.6, 156.5, 143.9, 143.8, 141.3, 127.7, 127.1, 125.1, 120.0, 82.9, 80.2, 67.0, 54.4, 47.2, 43.4, 28.3, 27.9.

3-Amino-(2R)-2-*tert*-butoxycarbonylamino-propionic acid *tert*-butyl ester (3.1c):

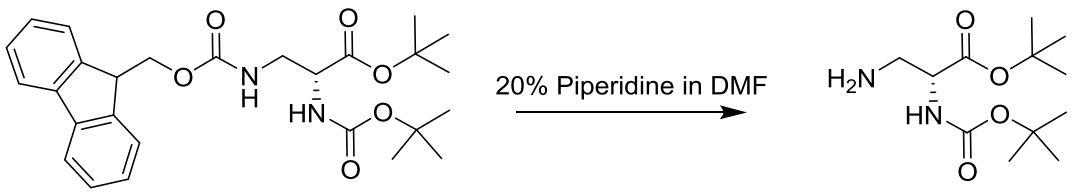

3.1b **3.1c**

Procedure: **3.1b** (0.542 g, 1.12 mmol) was dissolved in 20.0 mL of 20% (v/v) Piperidine in DMF and stirred at room temperature overnight. The reaction was concentrated *in vacuo* and purified by column chromatography (1:1 EtOAc : Hexanes, followed by 20% (v/v) EtOH in $CHCl_3$ + 1% Et_3N) to afford 0.239 g of a pale yellow oil (81.9% yield). RF = 0.57. ^{1}H NMR (400 MHz, $CDCl_3$): 5.48 (d, J=7.5 Hz, 1H), 3.36 (t, J=5.7 Hz, 1H), 3.19 (t, J=5.6 Hz, 1H), 1.35 (s, 9H), 1.32, (s, 9H). ^{13}C (125MHz, $CDCl_3$): 170.5, 155.6, 82.2, 79.8, 56.3, 44.2, 28.3, 28.0.

(2R)-2-*tert*-Butoxycarbonylamino-3-[2-(9H-fluoren-9-ylmethoxycarbonylamino)-acetylamino]-propionic acid *tert*-butyl ester (3.1d):

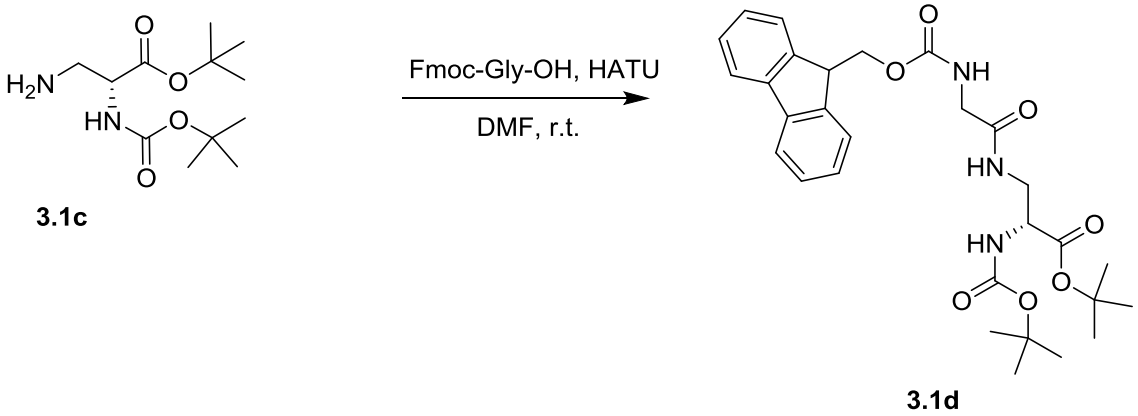

3.1c **3.1d**

Procedure: Fmoc-Gly-OH (0.262 g, 0.880 mmol) was dissolved in DMF (5.00 mL) to which HATU (0.335 g, 0.880 mmol) and 4-Methylmorpholine (0.107 mL, 0.970 mmol) at room temperature. The reaction was placed under Argon. **3.1c** (0.230 g, 0.880 mmol) was dissolved in DMF (5.00 mL) and added dropwise and stirred overnight. The reaction was diluted with DCM and distilled water. The organic phase was separated and washed with 1 M HCl, water, and saturated Sodium bicarbonate. Dried over Magnesium sulfate, filtered, concentrated, and purified by column chromatography (1:1 EtOAc : Hexanes) affording 0.375 g of a pale yellow oil, 79% yield. RF = 0.72. ^{1}H NMR (400 MHz, $CDCl_3$): 7.73 (d, J=6.4 Hz, 2H), 7.58 (d,J=7.2

Hz, 2H), 7.37 (t, J=7.4 Hz, 2H), 7.27 (t, J=6.9 Hz, 2H) 7.00 (br s, 1H), 5.90 (br s, 1H), 5.64 (d, J=6.7 Hz, 1H), 4.37 (d, J=7.0 Hz, 2H), 4.19 (t, J=7.0 Hz, 1H), 3.86 (br s, 2H), 3.62 (br s, 2H), 2.78 (s, 1H), 1.44 (s, 9H), 1.41 (s, 9H).

3-[(2R)-2-Amino-acetylamino]-2-tert-butoxycarbonylamino-propionic acid *tert*-butyl ester (3.1e):

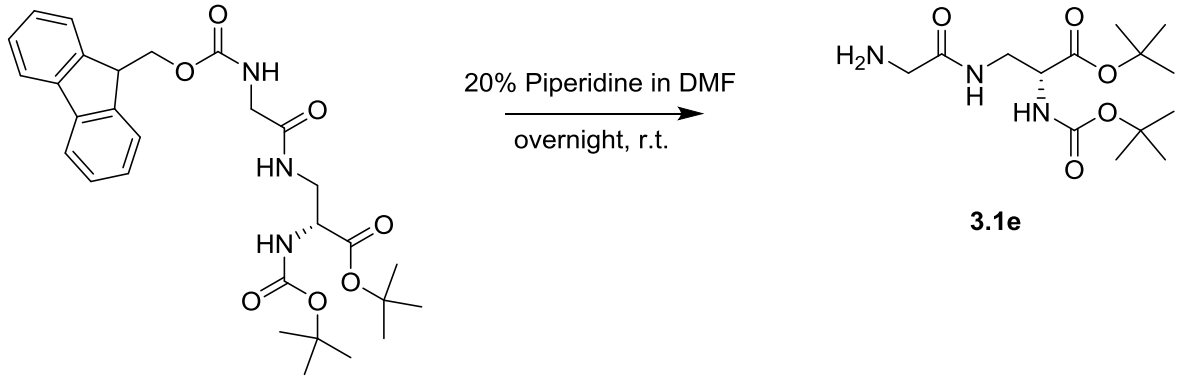

3.1d **3.1e**

Procedure: **3.1d** (0.375 g, 0.700 mmol) was dissolved in 20% (v/v) Piperidine in DMF and stirred under argon overnight. The reaction was concentrated and purified by column chromatography (1:1 EtOAc : Hexanes, followed by 2:8 EtOH : $CHCl_3$) affording 0.158 g of a pale yellow oil, 71.4% yield. RF = 0.08 (5% MeOH in DCM) ^{1}H NMR (400 MHz, $CDCl_3$): 7.64 (br s, 1H), 5.61 (d, J=6.9 Hz, 1H), 4.20 (br, 1H), 3.61-3.50 (m, 2H), 3.30 (s, 2H), 2.70 (br s, 2H), 1.39 (s, 9H), 1.36 (s, 9H). ^{13}C (125 MHz, $CDCl_3$): 173.1, 169.7, 155.7, 82.5, 79.8, 54.5, 44.4, 41.2, 28.2, 27.9.

(2R)-2-*tert*-Butoxycarbonylamino-3-(2,2-dimethyl-5-oxo-imidazolidin-1-yl)-propionic acid *tert*-butyl ester (3.1f):

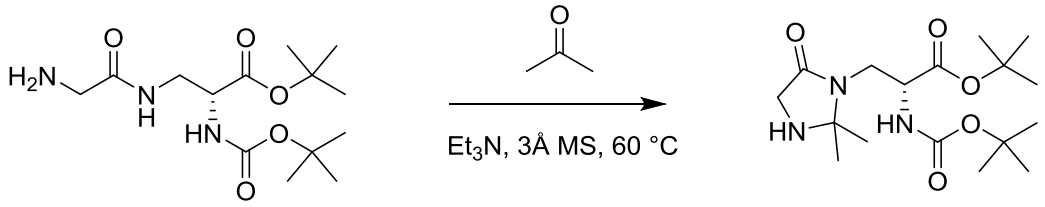

3.1e **3.1f**

Procedure: **3.1e** (0.158g, 0.50mmol) was dissolved in $CHCl_3$ and transferred to a flame-dried round-bottom flask and concentrated. 3Å molecular sieves (0.100 g) were added followed by acetone (0.370 mL, 5.00 mmol) and Et_3N (0.347 mL, 2.50 mmol). The reaction was stirred at 60℃ overnight and monitored by TLC. After completion, the mixture was cooled to room temperature and dissolved in Methanol, filtered through Celite, concentrated and purified by column chromatography (0-5% MeOH in DCM) to afford 0.117 g of a beige semi-solid (65.3% yield). ^{1}H NMR (400 MHz, $CDCl_3$): 5.57 (d, J=7.7 Hz, 1H), 4.27-4.21 (m, 1H), 3.55-3.45 (m, 1H), 3.40 (d, J=4.7 Hz, 1H) 3.36-3.30 (m, 1H), 1.42 (s, 9H), 1.41, (s, 3H), 1.38, (s, 9H), 1.34, (s, 3H). ^{13}C (125MHz, $CDCl_3$): 174.9, 169.4, 155.5, 82.4, 79.7, 78.5, 54.8, 48.0, 41.4, 28.3, 27.9, 26.3, 25.6.

(2R)-2-*tert*-Butoxycarbonylamino-3-(2,2-dimethyl-5-oxo-3-oxy-2,5-dihydro-imidazol-1-yl)-propionic acid *tert*-butyl ester (3.1g):

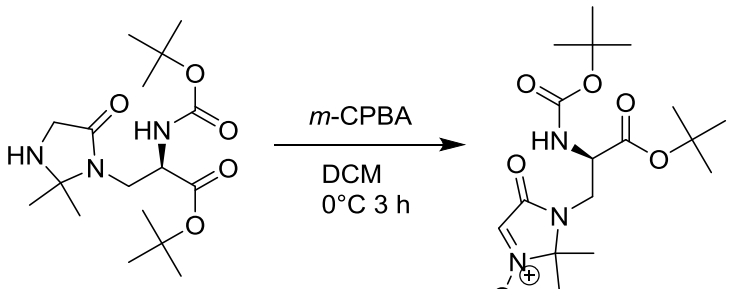

3.1f **3.1g**

Procedure: **3.1f** (0.058 g, 0.160 mmol) was dissolved in dry DCM (purchased from Sigma-Aldrich) and cooled to 0˚C, to which *m*-CPBA was added. The mixture was stirred for 3 hours, concentrated, and purified by column chromatography (40-50% EtOAc in Hexanes) affording 0.050 g of a translucent white semi-solid, 83.9% yield. RF (5% MeOH in DCM) = 0.31. ^{1}H NMR (400 MHz, $CDCl_3$): 7.02 (s, 1H), 5.45 (d, J=7.4 Hz, 1H), 4.37 (dd, J=7.5, 7.2 Hz, 1H), 3.78-3.67 (m, 2H), 1.68 (s, 3H), 1.67 (s, 3H), 1.46, (s, 9H), 1.42, (s, 9H). ^{13}C (125MHz, $CDCl_3$): 169.0, 162.8, 155.4, 123.4, 90.7, 83.1, 80.2, 53.7, 41.6, 30.1, 28.3, 27.9, 24.6.

(2R)-2-Amino-3-(2,2-dimethyl-5-oxo-3-oxy-2,5-dihydro-imidazol-1-yl)-propionic acid (3.1):

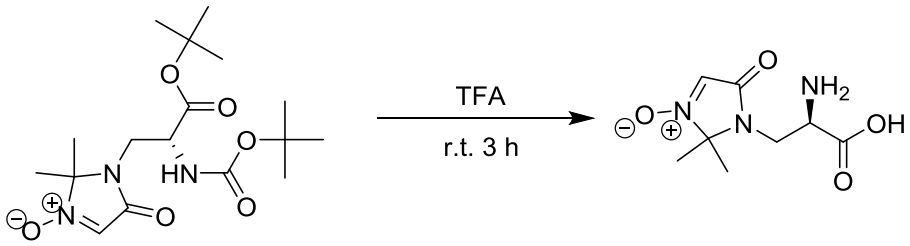

3.1g **3.1**

Procedure: Trifluoroacetic acid (1.24 mL, 16.1 mmol) was slowly added to **3.1g** (0.041 g. 0.110 mmol) and stirred for 3 hours. After completion, Methanol was added and the solvent was evaporated affording 0.024 g of a dark brown oil, quantitative. ^{1}H NMR (400 MHz, CD_3OD): 7.30 (s, 1H), 4.15 (br s, 1H), 3.96 (br s, 2H), 2.12 (s, 1H), 1.65 (s, 3H), 1.62 (s, 3H). ^{13}C NMR (100 MHz, CD_3OD): 165.0, 123.9, 91.1, 41.1, 23.0, 23.0.

Unnatural Amino Acid Synthesis: Electron-deficient *d*-lysine derivative

(2R)-2-*tert*-Butoxycarbonylamino-6-[2-(9H-fluoren-9-ylmethoxycarbonylamino)-acetylamino]-hexanoic acid *tert*-butyl ester (3.2b):

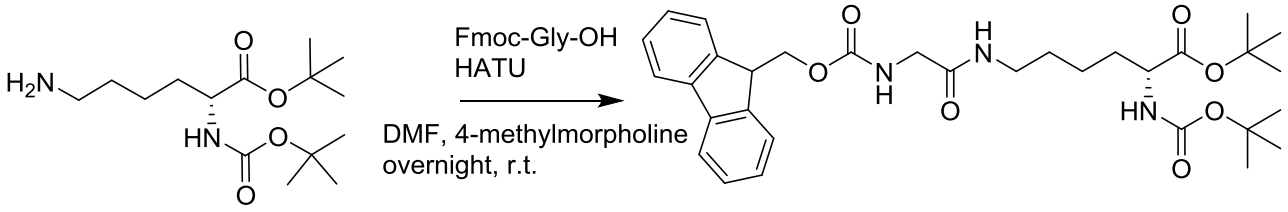

3.2a **3.2b**

N-2-[(1,1-dimethylethoxy)carbonyl]-1,1-dimethylethyl ester D-Lysine (**3.2a**) was obtained from Mariya Chigrinova in pure form and was synthesized from Boc-D-Lys-OH in an analogous fashion to **3.1c**.

Procedure:

Fmoc-Gly-OH (0.589 g, 1.98 mmol) and HATU (0.754 g, 1.98 mmol) were dissolved in DMF (10.0 mL) at room temperature and stirred for 5 minutes under a nitrogen atmosphere. **3.2a** (0.600 g, 1.98 mmol) was dissolved in DMF (10mL) and added dropwise to the reaction, followed by 4-Methylmorpholine (0.240 mL, 2.18 mmol). The reaction was stirred overnight at room temperature, concentrated, and purified by column chromatography (20-50% EtOAc in Hexanes). The collected fractions contained Tetramethylurea as an impurity; therefore, a small portion of the product/urea mixture was purified by prep HPLC to obtain **3.2b** as a colourless oil. (28.2% yield), Rf = 0.15 (1:1 EtOAc:Hexanes) ^{1}H NMR (400 MHz, $CDCl_3$): 7.75 (d, J=7.5 Hz, 2H), 7.58 (d, J=7.3 Hz, 2H), 7.39 (t, J=7.4 Hz, 2H), 7.29((t, J=7.4 Hz, 2H), 6.30 (br s, 1H), 5.73

(br s, 1H), 5.13 (d, J=8.0 Hz, 1H), 4.41 (d, J=7.0 Hz, 2H), 4.21 (t, J=6.9 Hz, 1H), 4.13 (br s, 1H), 3.84 (br d, J=3.6 Hz, 2H), 3.29-3.19 (m, 2H), 1.80-1.68 (m, 1H), 1.65-1.48 (m, 3H), 1.45 (s, 9H), 1.43 (s, 9H), 1.40-1.31 (m, 2H). ^{13}C (125MHz, $CDCl_3$): 171.9, 169.0, 156.7, 155.6, 143.7, 141.3, 127.8, 127.1, 125.1, 120.0, 81.9, 79.7, 67.2, 53.7, 47.1, 44.5, 39.3, 32.7, 28.9, 28.4, 28.0, 22.5.

6-(2-Amino-acetylamino)-(2R)-2-tert-butoxycarbonylamino-hexanoic acid *tert*-butyl ester (3.2c):

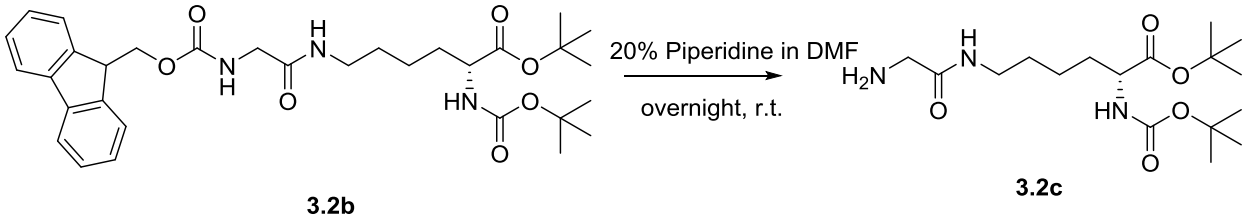

3.2b **3.2c**

Procedure:

3.2b (0.300 g, 0.520 mmol) was dissolved in 20% Piperidine in DMF (20.0 mL) and stirred at room temperature under nitrogen atmosphere overnight. The reaction was concentrated *in vacuo*, pre-absorbed on silica and purified by column chromatography (1:1 EtOAc:Hexanes; 20% EtOH in $CHCl_3$ + 1% Et_3N). 0.156 g (84.4% yield) of clear oil was obtained. Rf = 0.05. ^{1}H NMR (400 MHz, $CDCl_3$): 7.31 (s, 1H), 5.12 (d, J=8.2 Hz, 1H), 4.07-4.02 (m, 1H), 3.25 (br s, 2H), 3.18 (q, J=6.7 Hz, 2H), 1.83 (br s, 2H), 1.74-1.65 (m, 1H), 1.58-1.42 (m, 3H), 1.37 (s, 9H), 1.35 (s, 9H), 1.33-1.25 (m, 2H). ^{13}C NMR (100 MHz, $CDCl_3$): 172.6, 171.9, 155.4, 81.9, 80.1, 53.8, 44.6, 38.6, 32.5, 29.1, 28.3, 22.6.

(2R)-2-*tert*-Butoxycarbonylamino-6-(2,2-dimethyl-5-oxo-imidazolidin-1-yl)-hexanoic acid *tert*-butyl ester (3.2d):

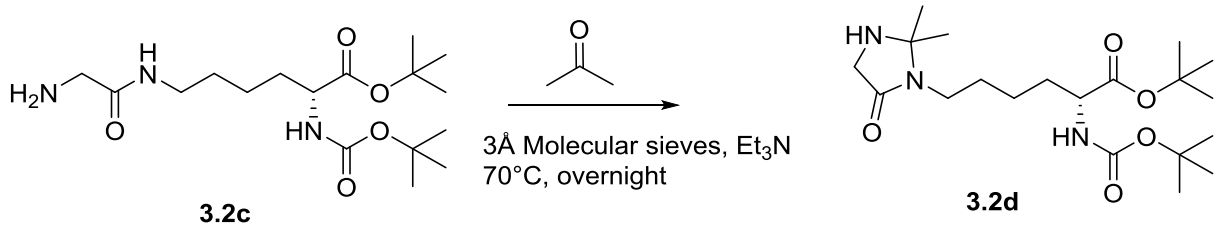

3.2c **3.2d**

Procedure:

3.2c (0.156 g, 0.430 mmol) was transferred to a flame-dried round bottom flask with acetone, followed by removal of the solvent. 3 Å molecular sieves (0.200 g) were added, followed by acetone (0.500 mL, 6.78 mmol) and Triethylamine (0.307 mL, 2.20 mmol). The flask was fitted with a reflux condenser and heated to 70°C overnight. The residue was taken up in Methanol, filtered through Celite, concentrated and purified by column chromatography (5% MeOH in DCM). 0.056 g obtained as a brown oil, 32.6% yield. Rf = 0.28. ^{1}H NMR (400 MHz, $CDCl_3$): 5.05 (d, J=8.2 Hz, 1H), 4.15-4.10 (m, 1H), 3.41 (s, 2H), 3.10 (t, J=7.8 Hz, 2H), 1.81-1.70 (m, 1H), 1.63-1.54 (m, 3H), 1.43 (s, 9H), 1.41 (s, 9H), 1.34 (s, 6H), 1.22 (s, 2H), 0.87-0.76 (m, 1H). ^{13}C NMR (100 MHz, $CDCl_3$): 173.5, 171.9, 155.4, 81.8, 79.6, 78.1, 53.7, 48.2, 40.1, 32.6, 29.7, 29.0, 28.3, 28.0, 26.5, 22.9.

(2R)-2-*tert*-Butoxycarbonylamino-6-(2,2-dimethyl-5-oxo-3-oxy-2,5-dihydro-imidazol-1-yl)-hexanoic acid *tert*-butyl ester (3.2e):

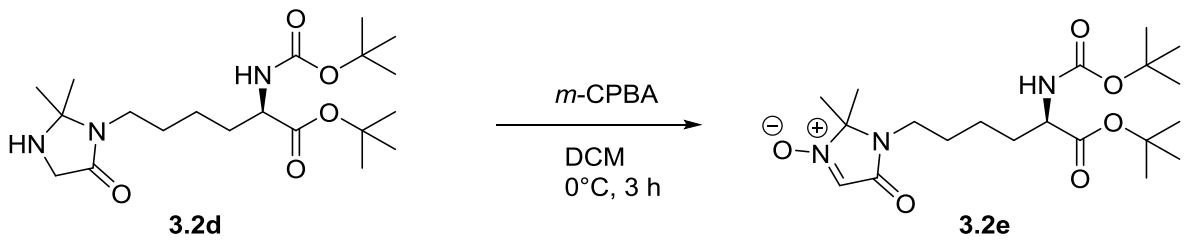

3.2d **3.2e**

Procedure:

3.2d (0.010 g, 0.025 mmol) was dissolved in DCM (1.00 mL, dried over 3 Å molecular sieves) and cooled to 0°C. *meta*-Chloroperoxybenzoic acid (0.014 g, 0.063 mmol) was added in one portion and stirred at 0°C for 3 hours. Upon completion, excess *m*-CPBA was quenched with 1 M Sodium thiosulfate followed by saturated sodium bicarbonate. The reaction was extracted with DCM (3x10 mL). The combined organic phases were washed with saturated Sodium bicarbonate (10.0 mL) and brine (10.0 mL), dried over anhydrous Sodium sulfate, filtered, and concentrated *in vacuo*. Purified by column chromatography (0-5% MeOH in DCM). 0.010 g of **3.2e** was obtained as a brown oil (96.7% yield). Rf = 0.22. ^{1}H NMR (400 MHz, $CDCl_3$): 7.00 (s, 1H), 5.06 (d, J=8.0 Hz, 1H), 4.15 (dd, J=13.2, 8.1 Hz, 1H), 3.42-3.29 (m, 2H), 1.84-1.75 (m, 1H), 1.74-1.66 (m, 2H), 1.62 (s, 3H), 1.44 (s, 9H), 1.42 (s, 9H), 1.40-1.33 (m, 2H), 1.23 (s, 1H). ^{13}C NMR (100 MHz, $CDCl_3$): 171.8, 162.0, 155.4, 123.9, 90.2, 79.7, 53.5, 40.5, 32.6, 28.7, 28.3, 28.0, 24.8, 24.7, 22.7.

(2R)-2-Amino-6-(2,2-dimethyl-5-oxo-3-oxy-2,5-dihydro-imidazol-1-yl)-hexanoic acid (3.2):

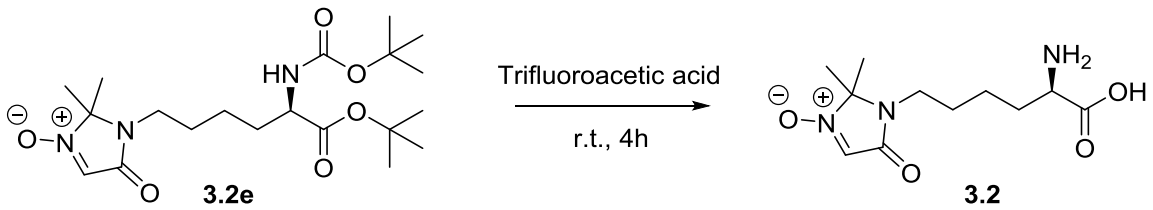

Procedure:

Trifluoracetic acid (0.300 mL, 3.91 mmol) was added to **3.2e** (0.010 g, 0.024 mmol) and stirred at room temperature for 4 hours. Reaction progress was monitored by LCMS. Upon completion, the reaction was concentrated and distilled as an azeotrope from Methanol to remove excess TFA, affording 0.026 g of **3.2** as a dark brown oil (quantitative yield). Rf = 0.09 (20% MeOH in DCM). ^{1}H NMR (400 MHz, MeOD): 7.29 (s, 1H), 3.98 (t, J=6.4 Hz, 1H), 3.49 (t, J=7.4 Hz, 2H), 2.08-1.88 (m, 2H), 1.79-1.69 (m, 2H), 1.65 (s, 6H), 1.60-1.45 (m, 4H). ^{13}C NMR (100 MHz, MeOD): 170.4, 162.8, 124.5, 90.6, 52.3, 39.6, 29.6, 28.3, 23.3, 23.3, 21.9.

Unnatural Amino Acid Synthesis: Nitrones **3.3** and **3.4**

(2R)-2-*tert*-Butoxycarbonylamino-3-[(2-methyl-1-oxy-3,4-dihydro-2H-pyrrole-2-carbonyl)-amino]-propionic acid *tert*-butyl ester (3.3a):

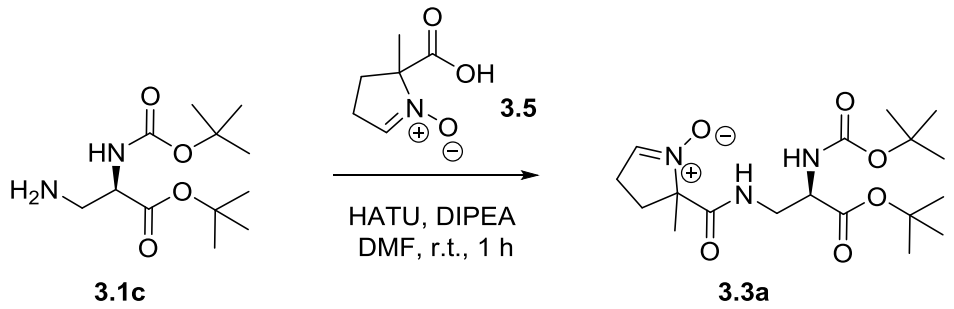

3.1c **3.3a**

3.3a was obtained in pure form from Mariya Chigrinova in the Pezacki group and was prepared in an analogous fashion to **3.2b**. ^{1}H NMR (400 MHz, CD_3OD): 7.31-7.25 (m, 1H), 4.24-4.18 (m, 1H), 3.70-3.62 (m, 1H), 3.53-3.44 (m, 1H), 2.81-2.70 (m, 3H), 2.25-2.18 (m, 1H), 1.68 (s, 3H), 1.49 (s, 9H), 1.47 (s, 9H). ^{13}C NMR (100 MHz, CD_3OD): 171.3, 169.8, 163.0, 141.9, 81.9, 79.3, 78.9, 54.0, 40.3, 30.8, 27.4, 26.9, 25.0, 21.8.

(2R)-2-Amino-3-[(2-methyl-1-oxy-3,4-dihydro-2H-pyrrole-2-carbonyl)-amino]-propionic acid (3.3):

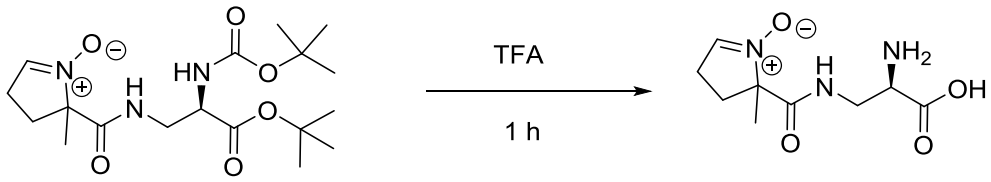

3.3a **3.3**

3.3 was obtained in pure form from Mariya Chigrinova in the Pezacki group and was prepared in an analogous fashion to **3.1**. ^{1}H NMR (400 MHz, CD_3OD): 7.29 (s, 1H), 4.19-4.15 (m, 1H),

3.90-3.68 (m, 2H), 2.76-2.66 (m, 3H), 2.27-2.18 (m, 1H), 1.69 (s, 3H). ^{13}C NMR (100 MHz, CD_3OD): 172.2, 168.5, 142.5, 79.3, 52.9, 39.3, 31.1, 25.4, 20.9.

(2R)-2-*tert*-Butoxycarbonylamino-6-[(2-methyl-1-oxy-3,4-dihydro-2H-pyrrole-2-carbonyl)-amino]-hexanoic acid *tert*-butyl ester (3.4a):

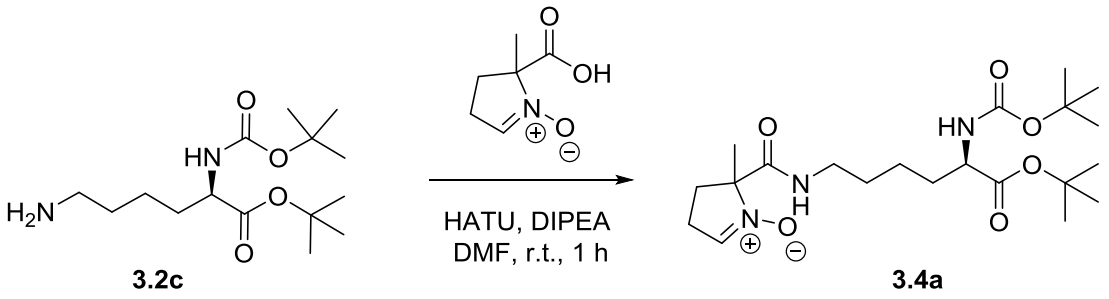

3.2c 3.4a

3.4a was obtained in pure form from Mariya Chigrinova in the Pezacki group and was prepared in an analogous fashion to **3.3a**. ^{1}H NMR (400 MHz, CD_3OD): 7.23 (s, 1H), 3.96-3.92 (m, 1H), 3.29-3.22 (m, 2H), 2.78-2.68 (m, 3H), 2.25-2.20 (m, 1H), 1.69 (s, 3H), 1.66-1.52 (m, 4H), 1.48 (s, 9H), 1.46 (s, 9H), 1.45-1.36 (m, 3H). ^{13}C NMR (100 MHz, CD_3OD): 172.4, 156.8, 141.4, 81.0, 79.0, 54.4, 38.9, 31.0, 30.8, 28.4, 27.3, 26.9, 26.7, 25.0, 22.8, 21.6.

(2R)-2-Amino-6-[(2-methyl-1-oxy-3,4-dihydro-2H-pyrrole-2-carbonyl)-amino]-hexanoic acid (3.4):

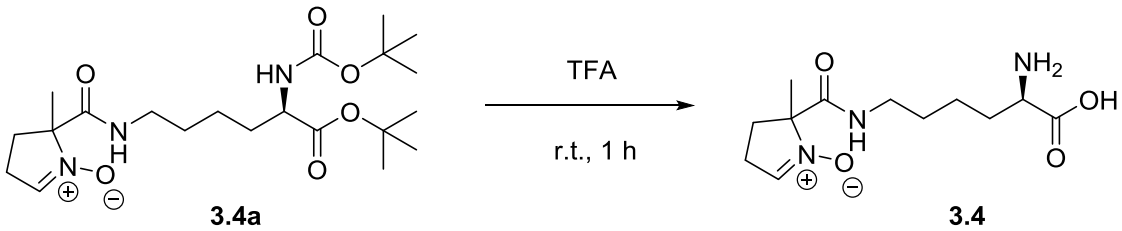

3.4a 3.4

3.4 was obtained in pure form from Mariya Chigrinova in the Pezacki group and was prepared in an analogous fashion to **3.3**. ^{1}H NMR (400 MHz, CD_3OD): 7.23 (s, 1H), 3.29-3.22 (m, 2H),

2.74-2.66 (m, 3H), 2.25-2.16 (m, 1H), 2.00-1.83 (m, 2H), 1.67 (s, 3H), 1.63-1.56 (m, 2H), 1.50-1.38 (m, 3H). ^{13}C NMR (100 MHz, CD_3OD): 170.4, 141.5, 79.2, 52.4, 38.5, 31.0, 29.6, 28.3, 25.1, 21.7, 21.7, 21.3.

Vancomycin probe synthesis

of 3,4-Dihydro-2-methyl- 2H-pyrrole-2-carboxylic acid ethyl ester 1-oxide (3.5b):

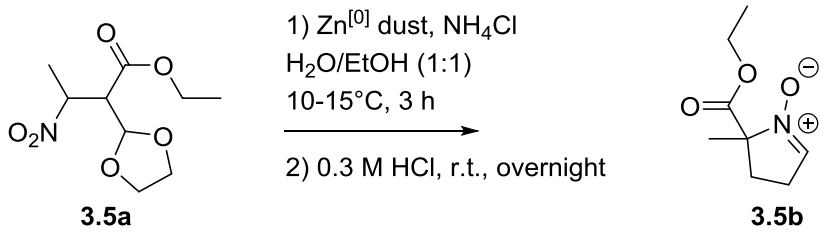

3.5a **3.5b**

α-methyl-α-nitro-1,3-Dioxolane-2-butanoic acid ethyl ester (**3.5a**) was obtained from Dr. Louis-Philippe Bonhomme-Beaulieu in the Pezacki group and used without further purification.

Procedure:

α-Methyl-α-nitro-1,3-Dioxolane-2-butanoic acid ethyl ester (3.00 g, 12.2 mmol) was dissolved in H_2O/EtOH (1:1) to which ammonium chloride (0.653 g, 12.2 mmol) was added and cooled to 10°C. Zinc dust (4.37 g, 66.8 mmol) was added portion-wise over 10 minutes. The reaction was stirred at 10-15°C for 3 hours, filtered through cotton, washed with Ethanol, concentrated *in vacuo,* taken up in 0.3 M HCl and stirred at room temperature overnight. Excess acid was quenched with aqueous Ammonium hydroxide 0.400 g of 3,4-Dihydro-2-methyl- 2H-pyrrole-2-carboxylic acid ethyl ester 1-oxide (**3.5b**) was obtained as a mixture with Ethylene glycol (^{1}H NMR signals are reported in square brackets) as a yellow oil (19.3% yield). ^{1}H NMR (400 MHz, $CDCl_3$): 4.88-4.86 (m, 1H), 4.20 (q, J=7.1 Hz, 2H), [3.97-3.92 (m, 2H), 3.86-3.82 (m, 2H)],

1.83-1.63 (m, 4H), 1.29 (s, 3H), 1.27 (t, J=7.2 Hz, 3H). ^{13}C NMR (100 MHz, $CDCl_3$): Matches spectrum reported in reference 21.

3,4-Dihydro-2-methyl- 2H-pyrrole-2-carboxylic acid 1-oxide (3.5):

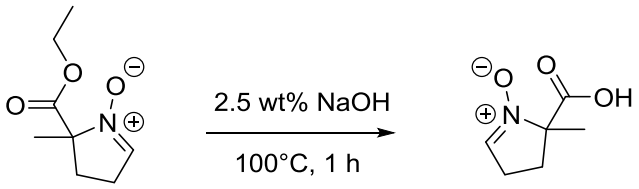

3.5b **3.5**

3,4-Dihydro-2-methyl- 2H-pyrrole-2-carboxylic acid ethyl ester 1-oxide (**3.5b**, 0.400 g, 2.34 mmol) was dissolved in aqueous Sodium hydroxide (2.5% by weight, 8.20 mL, 2.46 mmol) in a round bottom flask. The flask was equipped with a reflux condenser and the reaction was heated to 100°C for 1 hour. The reaction was cooled to room temperature and passed through a column containing Biorad AG 50W-X8 resin, 100-200 mesh, hydrogen form and eluted with water. The fractions collected were freeze dried to afford 0.063 g of 3,4-Dihydro-2-methyl- 2H-Pyrrole-2-carboxylic acid 1-oxide (**3.5**, 19.2% yield) as an orange solid. ^{1}H NMR (400 MHz, CD_3OD): 7.23 (s, 1H), 3.55 (s, 1H), 2.74 (s, 2H), 2.56 (s, 1H), 2.24-2.19 (m, 1H), 1.61 (s, 3H). ^{13}C NMR (100 MHz, CD_3OD): Matches spectrum reported in reference 22.

2-Methyl-1-oxy-3,4-dihydro-2H-pyrrole-2-carboxylic acid (3-{2-[2-(3-amino-propoxy)-ethoxy]-ethoxy}-propyl)-amide (3.6a):

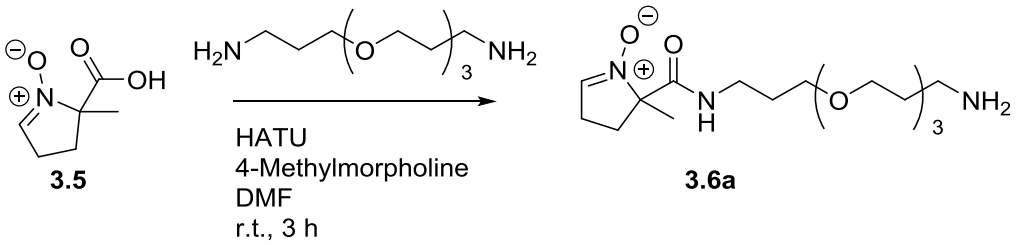

Procedure:

3.5 (0.063 g, 0.450 mmol) was dissolved in DMF to which HATU (0.171 g, 0.450 mmol) was added, followed by 4,7,10-Trioxa-1,13-tridecane diamine (0.599 g, 2.72 mmol) and 4-Methylmorpholine (0.138 g, 1.36 mmol) were added. The reaction was stirred at room temperature for 3 hours, concentrated *in vacuo*, and purified by column chromatography (gradient of 20% EtOH in $CHCl_3$ +1% Et_3N to 60% EtOH in $CHCl_3$ +1% Et_3N, followed by pure MeOH + 1% Et_3N). 0.062 g of **3.6a** was obtained as a yellow oil (39.6% yield).

2-Methyl-1-oxy-3,4-dihydro-2H-pyrrole-2-carboxylic acid (3-{2-[2-(3-amino-propoxy)-ethoxy]-ethoxy}-propyl)-amide vancomycin (3.6):

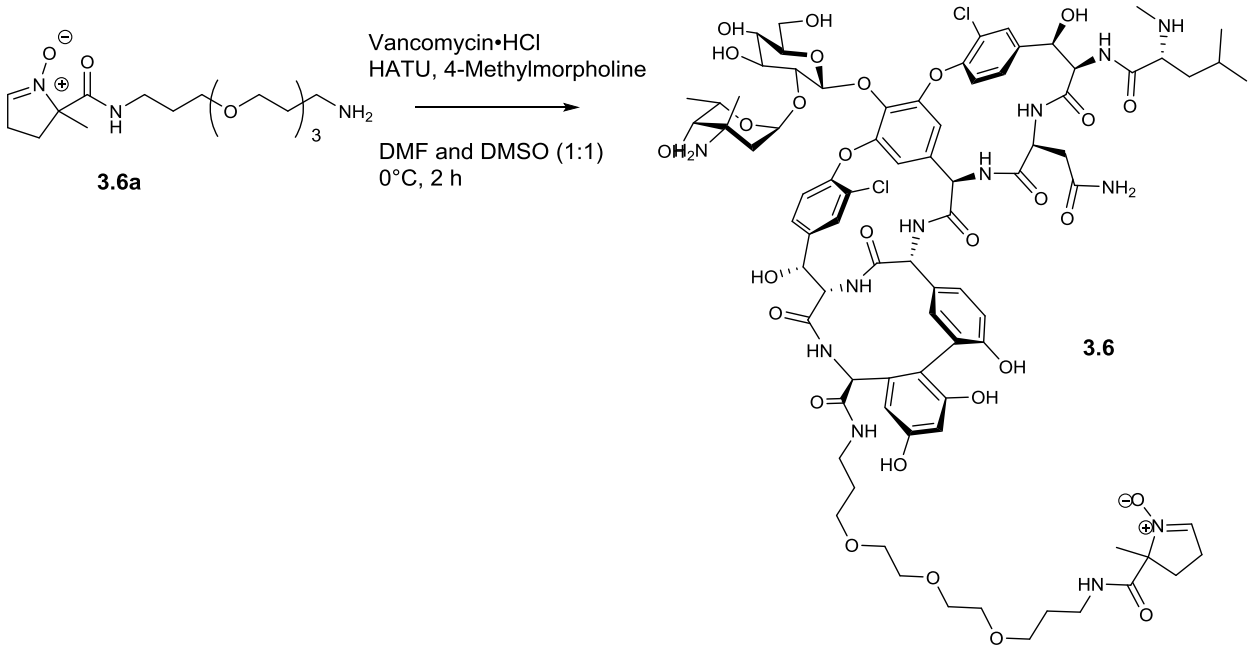

Procedure:

3.6a (0.060 g, 0.170 mmol) was dissolved in DMF and DMSO (1:1) to which Vancomycin hydrocholoride (0.089 g, 0.060 mmol) was added, followed by HATU (0.023 g, 0.060 mmol) and 4-Methylmorpholine (0.017 g, 0.170 mmol). The reaction was stirred at room temperature for 3 hours. Purified by HPLC (gradient 10-25% MeCN + 0.1% formic acid over 10 minutes, retention time ~1.5 minutes). The collected fractions were concentrated *in vacuo* to remove acetonitrile, then freeze dried to afford 0.022 g of a white fluffy solid (20.8% yield). Due to the complexity of the molecule, the compound identity was confirmed by mass spectrometry. Calculated mass ($C_{82}H_{104}N_{12}O_{28}Cl_2$) = 1774.5228 Found: LRMS (ESI, Positive ionization) = 598.6 (M+3/3), HRMS = 1813.6211 (M+K)

BCN Alexafluor-488 conjugate synthesis

Carbonic acid (1R,8S,9s)-bicyclo[6.1.0]non-4-yn-9-ylmethyl ester 4-nitro-phenyl ester (3.7a):

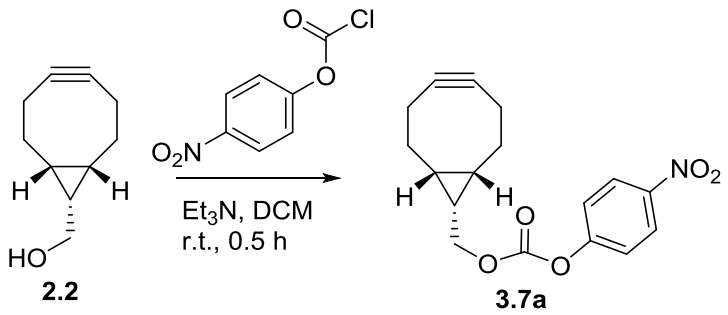

2.2 **3.7a**

Procedure:

Bicyclo[6.1.0]nonyne (**2.2**, 0.044 g, 0.290 mmol) was dissolved in dry DCM (purchased from Sigma-Aldrich) to which Triethylamine (0.074 g, 0.730 mmol) was added. The mixture was stirred for 5 minutes before 4-Nitrophenyl chloroformate (0.119 g, 0.590 mmol) was added. The reaction was stirred for 15 minutes until **2.2** had been consumed as judged by TLC. Excess Triethylamine was quenched with saturated Ammonium chloride (5.00 mL). The reaction was then extracted with DCM (3x15 mL). Combined organic phases were dried over anhydrous Sodium sulfate, filtered, and concentrated *in vacuo*. Purified by column chromatography (15% EtOAc in Hexanes) to afford 0.053 g of a white powder (57.7% yield). Rf = 0.59. ^{1}H NMR (400 MHz, CD_3OD): 8.31 (d, J=9.2 Hz, 2H), 7.47 (d, J=9.2 Hz, 2H), 4.43 (d, J=8.3 Hz, 2H), 2.32-2.17 (m, 6H), 1.71-1.60 (m, 2H), 1.51 (quintet, J=8.6 Hz, 1H), 1.09-1.00 (m, 2H). ^{13}C NMR (100 MHz, $CDCl_3$): Matches spectrum reported in reference 23.

(3-{2-[2-(3-Amino-propoxy)-ethoxy]-ethoxy}-propyl)-carbamic acid *tert*-butyl ester (3.8a):

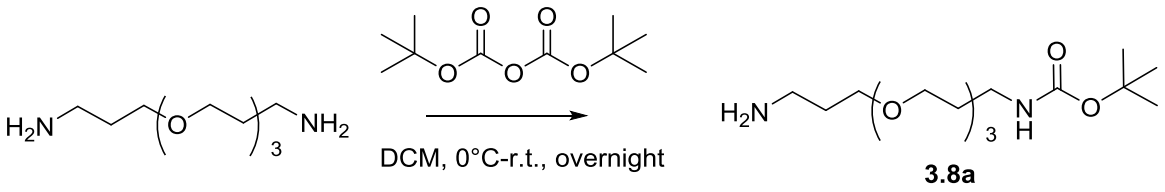

3.8a

Procedure:

4,7,10-Trioxa-1,13-tridecanediamine (3.40 g, 15.4 mmol) was dissolved in DCM (60.0 mL) and cooled to 0°C. Di-*tert*-butyl-dicarbonate was dissolved in DCM (20.0 mL) and added drop-wise over 15 minutes. The reaction was allowed to warm to room temperature and stirred overnight. Upon completion, the reaction was washed with 0.1 M HCl (2x10mL) and separated. The combined aqueous phases were extracted with DCM (5x15 mL). The combined organic phases were dried over anhydrous Sodium sulfate, filtered, and concentrated to afford 1.78 g of **3.8a** as a pale yellow oil (71.4% yield). ^{1}H NMR (400 MHz, $CDCl_3$): 3.65-3.51 (m, 12H), 3.21 (q, J=6.0 Hz, 2H), 2.79 (t, J=6.7 Hz, 2H), 1.78-1.69 (m, 4H), 1.42 (s, 9H) ^{13}C NMR (100 MHz, $CDCl_3$): 156.1, 78.9, 70.6, 70.3, 70.2, 69.6, 69.5, 39.7, 38.5, 33.2, 29.7, 28.5.

5-(3-{2-[2-(3-*tert*-Butoxycarbonylamino-propoxy)-ethoxy]-ethoxy}-propylcarbamoyl)-pentanoic acid (3.8b):

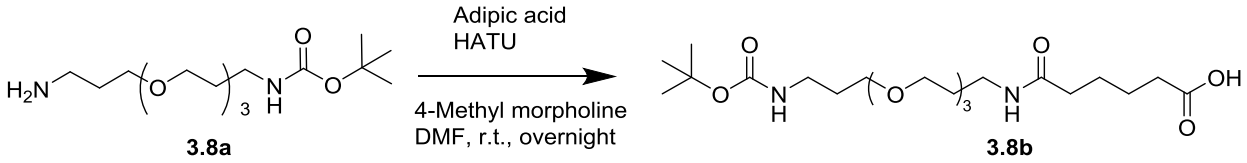

3.8a **3.8b**

Procedure:

Adipic acid (1.14 g, 7.80 mmol) was dissolved in DMF (5.00 mL) to which HATU (0.593 g, 1.56 mmol) was added. The reaction was stirred for 30 minutes before adding a solution of **3.8a**

(0.500 g, 1.56 mmol in 5.00 mL DMF) drop-wise at room temperature, followed by 4-Methylmorpholine (0.158 g, 1.56 mmol). The reaction was stirred at room temperature overnight. The mixture was concentrated *in vacuo* and purified by column chromatography (75% EtOAc in hexanes → 100% EtOAc → 20% EtOH in $CHCl_3$) to afford 0.312 g of **3.8b** as a pale yellow oil (44.6% yield). ^{1}H NMR (400 MHz, $CDCl_3$): 3.59-3.45 (m, 12H), 3.28 (q, J=6.0 Hz, 2H), 3.13 (br, 2H), 2.27 (t, J=6.7 Hz, 2H), 2.17 (t, J=6.7 Hz, 2H), 1.73-1.65 (m, 4H), 1.63-1.53 (m, 4H), 1.36 (s, 9H) ^{13}C NMR (100 MHz, $CDCl_3$): 176.5, 173.4, 156.2, 150.5, 128.8, 120.3, 79.0, 70.4, 70.1, 69.4, 38.4, 38.0, 36.1, 33.6, 29.6, 28.7, 28.4, 25.1, 24.4. (Calculated $C_{21}H_{40}N_2O_8$: 448.56; found 447.3 (M-, ESI negative).

5-(3-{2-[2-(3-Carboxyamino-propoxy)-ethoxy]-ethoxy}-propylcarbamoyl)-pentanoic acid (3.8):

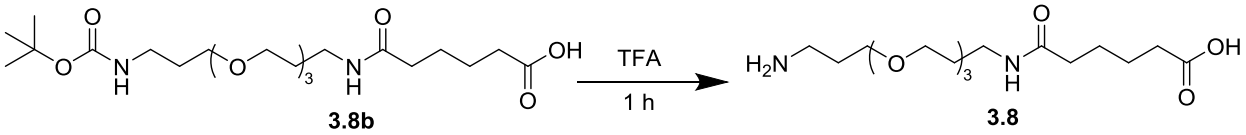

Procedure:

3.8b (0.146 g, 0.330 mmol) was dissolved in Trifluoroacetic acid (3.16 g, 18.9 mmol) and stirred at room temperature for 3 hours. Upon completion, excess Trifluoroacetic acid was removed *in vacuo* by distillation as an azeotrope from Methanol. Identity confirmed by mass spectrometry (Calculated $C_{16}H_{32}N_2O_6$: 348.4; found: 349.3 (M+, ESI positive)

5-[3-(2-{2-[3-(1R,8S,9s)-(Bicyclo[6.1.0]non-4-yn-9-ylmethoxycarbonylamino)-propoxy]-ethoxy}-ethoxy)-propylcarbamoyl]-pentanoic acid (3.7b):

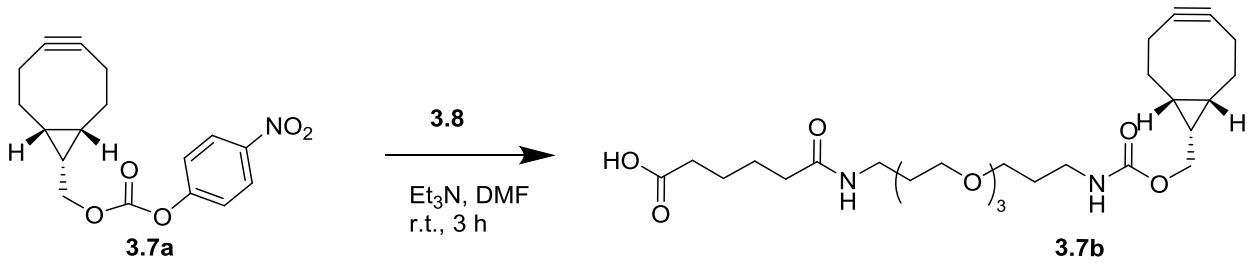

Procedure:

3.8 (0.010 g, 0.280 mmol) was dissolved in DMF (1.50 mL) and added drop-wise to a solution of **3.7a** (0.015 g, 0.475 mmol) in DMF (1.00 mL) at room temperature followed by Triethylamine (0.003 g, 0.028 mmol) under nitrogen atmosphere. Upon completion, the reaction was concentrated *in vacuo* and purified by HPLC (5-95% MeCN in H_2O + 0.1% Formic acid over 10 minutes) Identity was confirmed by mass spectrometry (Calculated $C_{27}H_{44}N_2O_8$: 524.6; found: 523.4(M-, ESI negative), 525.4 (M+, ESI positive).

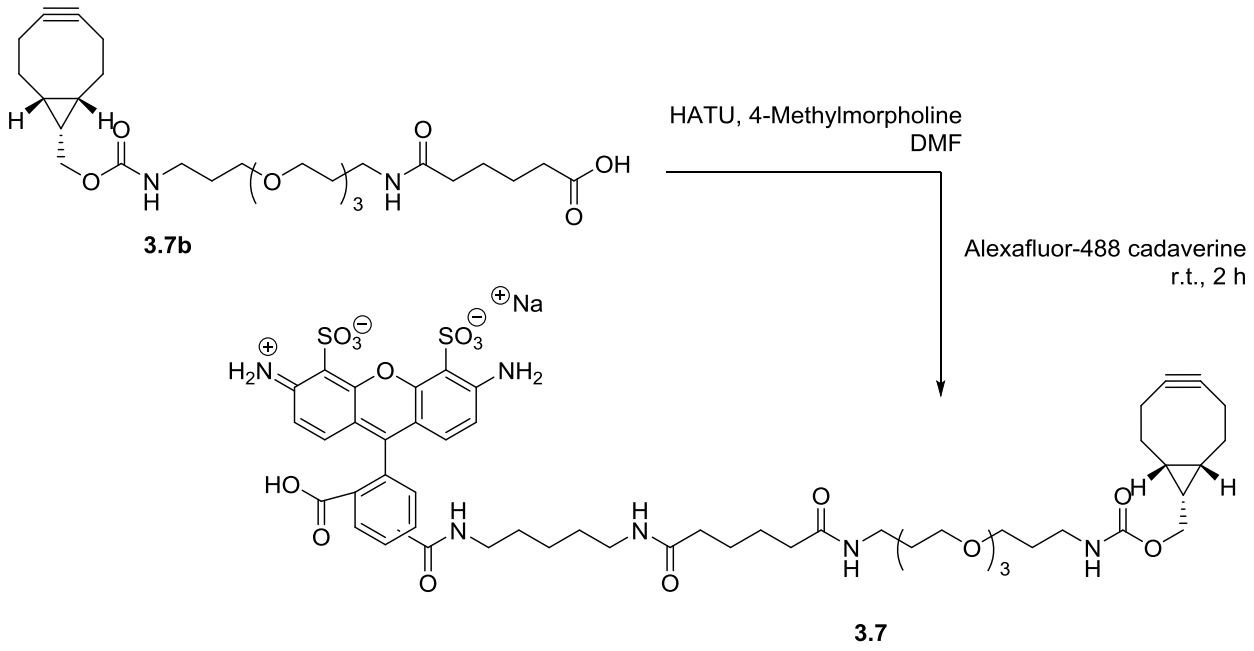

Procedure:

HATU (0.001 g, 0.002 mmol) was added to a solution of **3.7b** (0.001 g, 0.002 mmol) in DMF (1.20 mL) and placed in a flame-dried flask under nitrogen atmosphere and stirred for 15 minutes. Alexafluor-488 cadaverine (0.001 g, 0.002 mmol) was dissolved in DMF (5x0.2 mL) and added to the reaction, followed by 4-Methylmorpholine (2.00×10^{-4} g, 0.002 mmol) at room temperature. The flask was covered in aluminum foil and stirred in the dark for 2 hours. Purified by HPLC and used directly in metabolic labelling experiments.

References

(1) Saxon, E.; Luchansky, S. J.; Hang, H. C.; Yu, C.; Lee, S. C.; Bertozzi, C. R. *Journal of the American Chemical Society* **2002**, *124*, 14893.

(2) Wu, Y.; Yang, H.; Jeon, Y.-J.; Lee, M.-Y.; Li, J.; Shin, H.-J. *Biotechnol Bioproc E* **2014**, *19*, 747.

(3) Kovacic, S.; Samii, L.; Lamour, G.; Li, H.; Linke, H.; Bromley, E. H. C.; Woolfson, D. N.; Curmi, P. M. G.; Forde, N. R. *Biomacromolecules* **2014**, *15*, 4065.

(4) Peyrot, S. M.; Nachtergaele, S.; Luchetti, G.; Mydock-McGrane, L. K.; Fujiwara, H.; Scherrer, D.; Jallouk, A.; Schlesinger, P. H.; Ory, D. S.; Covey, D. F.; Rohatgi, R. *Journal of Biological Chemistry* **2014**, *289*, 11095.

(5) Kim, Y.; Kim, S. H.; Ferracane, D.; Katzenellenbogen, J. A.; Schroeder, C. M. *Bioconjugate Chemistry* **2012**, *23*, 1891.

(6) Kuru, E.; Hughes, H. V.; Brown, P. J.; Hall, E.; Tekkam, S.; Cava, F.; de Pedro, M. A.; Brun, Y. V.; VanNieuwen Hze, M. S. *Angewandte Chemie International Edition* **2012**, *51*, 12519.

(7) Siegrist, M. S.; Whiteside, S.; Jewett, J. C.; Aditham, A.; Cava, F.; Bertozzi, C. R. *ACS Chemical Biology* **2012**, *8*, 500.

(8) Shieh, P.; Siegrist, M. S.; Cullen, A. J.; Bertozzi, C. R. *Proceedings of the National Academy of Sciences* **2014**, *111*, 5456.

(9) Ning, X.; Temming, R. P.; Dommerholt, J.; Guo, J.; Ania, D. B.; Debets, M. F.; Wolfert, M. A.; Boons, G.-J.; van Delft, F. L. *Angewandte Chemie International Edition* **2010**, *49*, 3065.

(10) Temming, R. P.; Eggermont, L.; van Eldijk, M. B.; van Hest, J. C. M.; van Delft, F. L. *Organic & Biomolecular Chemistry* **2013**, *11*, 2772.

(11) McKay, C. S.; Blake, J. A.; Cheng, J.; Danielson, D. C.; Pezacki, J. P. *Chemical Communications* **2011**, *47*, 10040.

(12) Sherratt, A. R.; Chigrinova, M.; McKay, C. S.; Beaulieu, L.-P. B.; Rouleau, Y.; Pezacki, J. P. *RSC Advances* **2014**, *4*, 46966.

(13) Typas, A.; Banzhaf, M.; Gross, C. A.; Vollmer, W. *Nat Rev Micro* **2012**, *10*, 123.

(14) MacKenzie, D. A.; Pezacki, J. P. *Canadian Journal of Chemistry* **2014**, *92*, 337.

(15) Dai, X.; Miller, M. W.; Stamford, A. W. *Organic Letters* **2010**, *12*, 2718.

(16) Hodges, J. C.; Wang, W.; Riley, F. *The Journal of Organic Chemistry* **2004**, *69*, 2504.

(17) Gandhi, M.; Chikindas, M. L. *International Journal of Food Microbiology* **2007**, *113*, 1.

(18) Wright, E.; Neethirajan, S.; Warriner, K.; Retterer, S.; Srijanto, B. *Lab on a Chip* **2014**, *14*, 938.

(19) Kell, A. J.; Simard, B. *Chemical Communications* **2007**, 1227.

(20) Kell, A. J.; Stewart, G.; Ryan, S.; Peytavi, R.; Boissinot, M.; Huletsky, A.; Bergeron, M. G.; Simard, B. *ACS Nano* **2008**, *2*, 1777.

Appendix

A. Kinetic Data for cycloadditions with BCN and acyclic nitrones

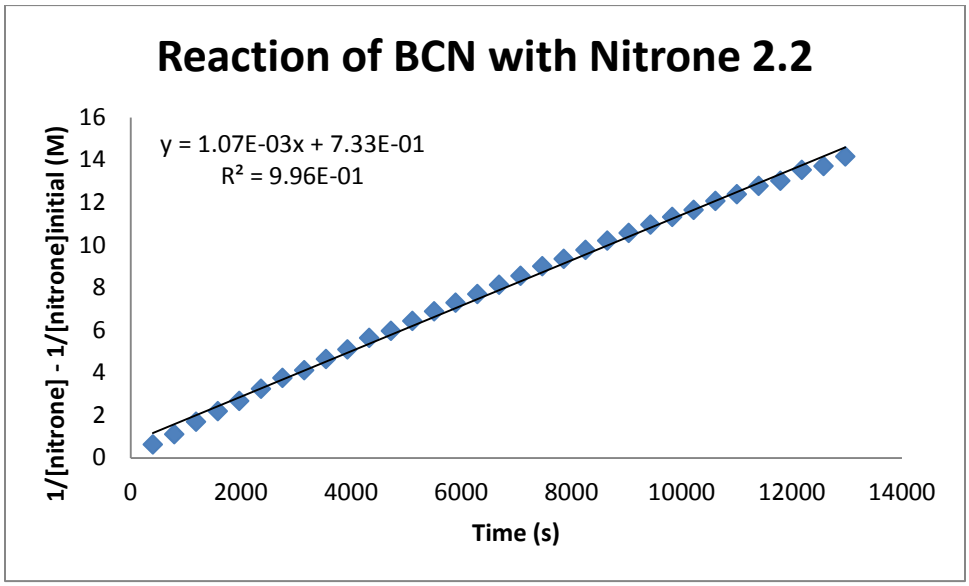

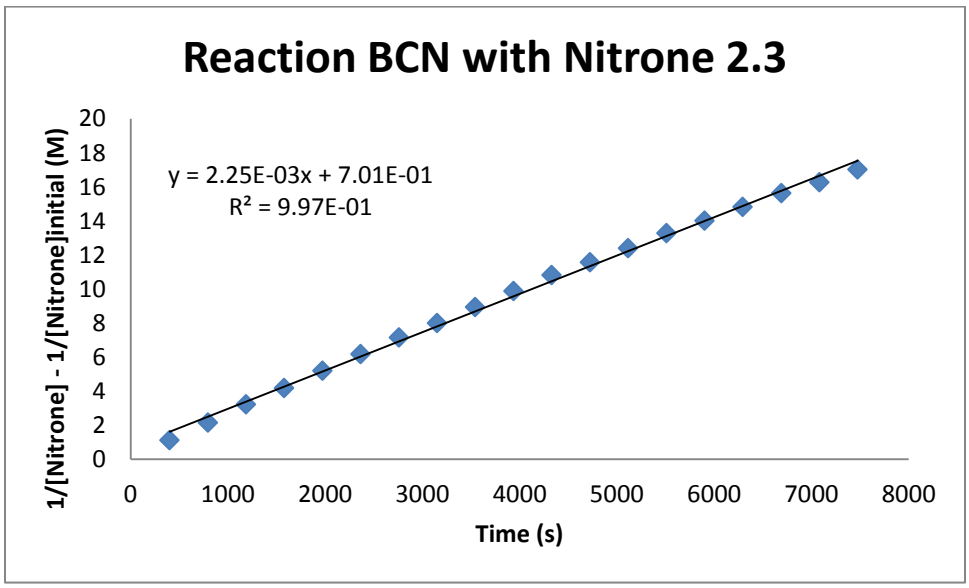

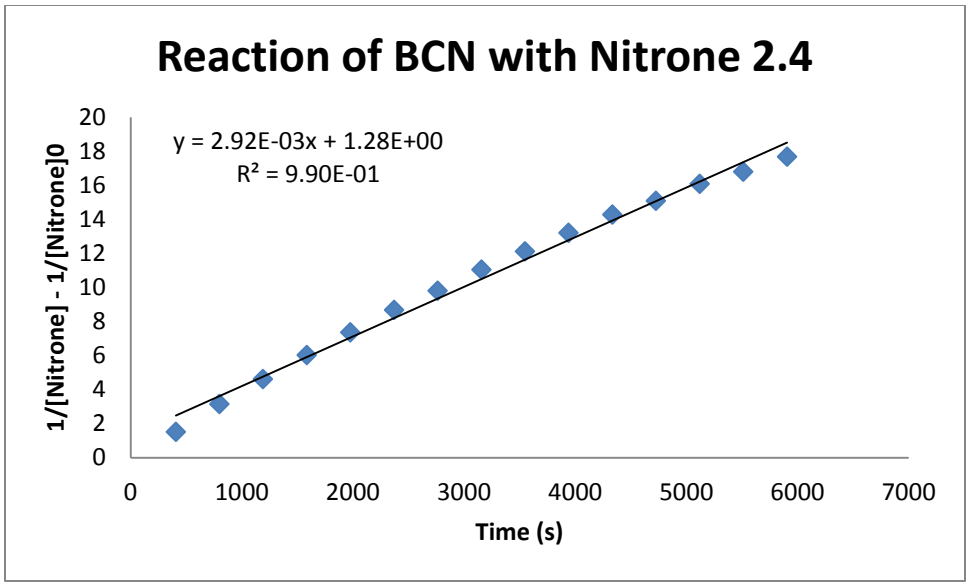
Reaction of BCN with Nitrone 2.4
y = 2.92E-03x + 1.28E+00
R² = 9.90E-01
1/[Nitrone] - 1/[Nitrone]0
Time (s)
0
2
4
6
8
10
12
14
16
18
20
0
1000
2000
3000
4000
5000
6000
7000

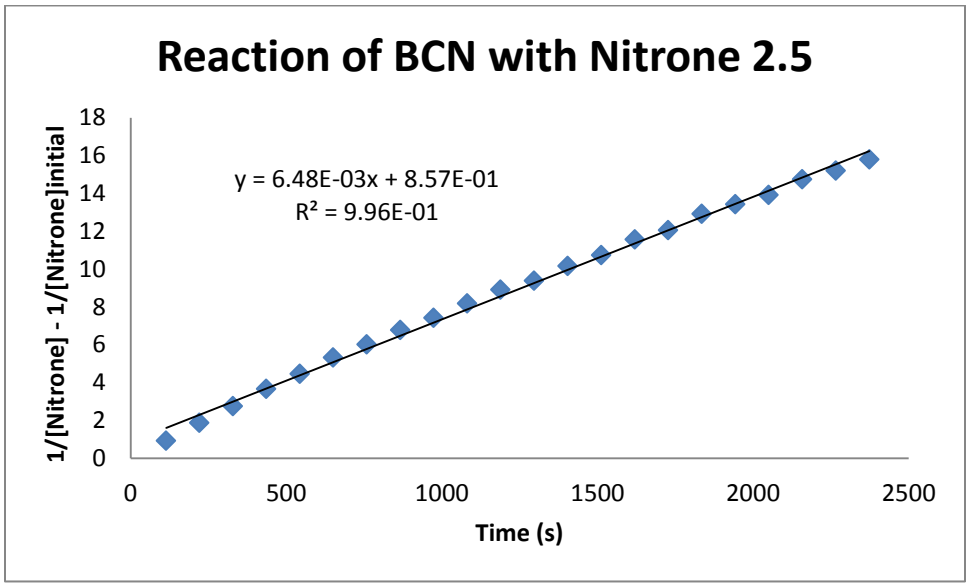
Reaction of BCN with Nitrone 2.5
y = 6.48E-03x + 8.57E-01
R² = 9.96E-01
1/[Nitrone] - 1/[Nitrone]initial
Time (s)
0
2
4
6
8
10
12
14
16
18
0
500
1000
1500
2000
2500

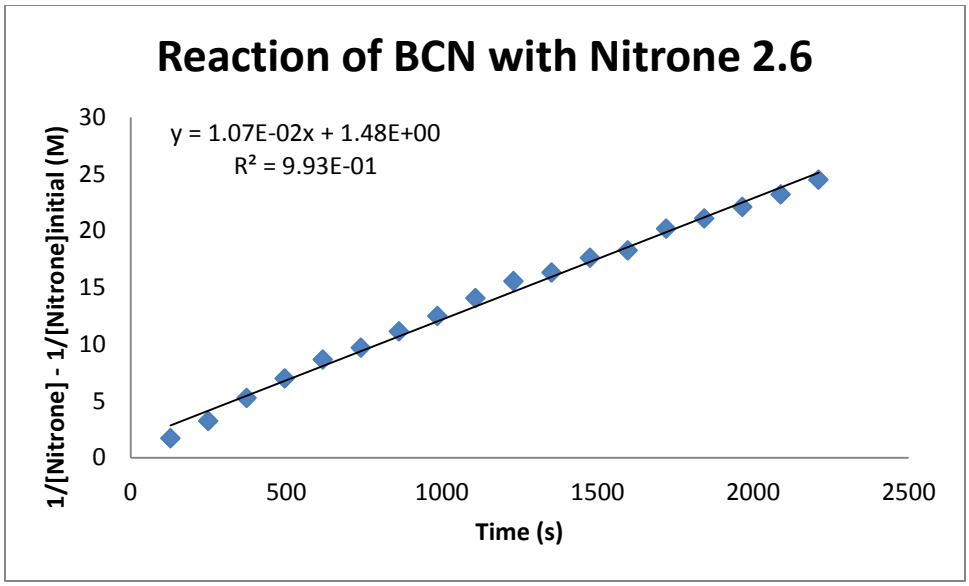
Reaction of BCN with Nitrone 2.6
y = 1.07E-02x + 1.48E+00
R² = 9.93E-01
1/[Nitrone] - 1/[Nitrone]initial (M)
Time (s)
0
5
10
15
20
25
30
0
500
1000
1500
2000
2500

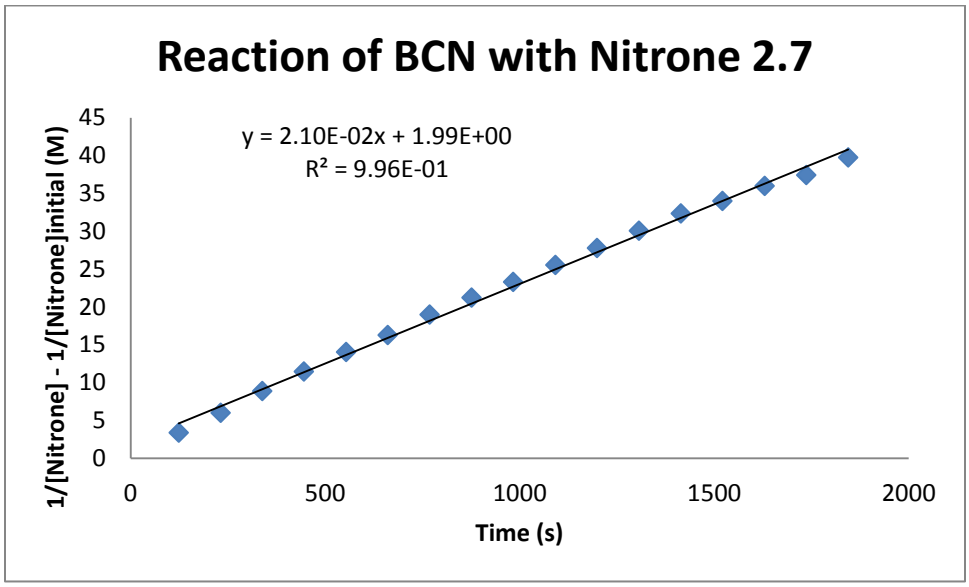
Reaction of BCN with Nitrone 2.7
y = 2.10E-02x + 1.99E+00
R² = 9.96E-01
1/[Nitrone] - 1/[Nitrone]initial (M)
Time (s)
0
5
10
15
20
25
30
35
40
45
0
500
1000
1500
2000

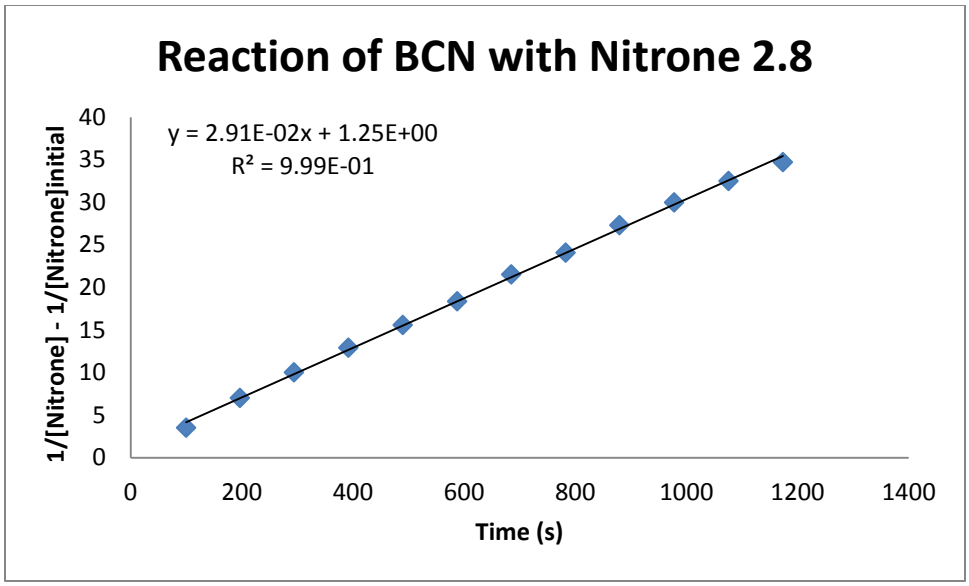
Reaction of BCN with Nitrone 2.8
y = 2.91E-02x + 1.25E+00
R² = 9.99E-01
1/[Nitrone] - 1/[Nitrone]initial
Time (s)
0
5
10
15
20
25
30
35
40
0
200
400
600
800
1000
1200
1400

B. Kinetic Data for cycloadditions with BCN and cyclic nitrones

Nitrone	Structure	Concentration of BCN (M)	k_{obs} (s^{-1})
2.9	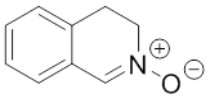	0.0050	3.20E-03
		0.0045	2.92E-03
		0.0040	2.68E-03
		0.0035	2.21E-03
		0.0030	1.91E-03

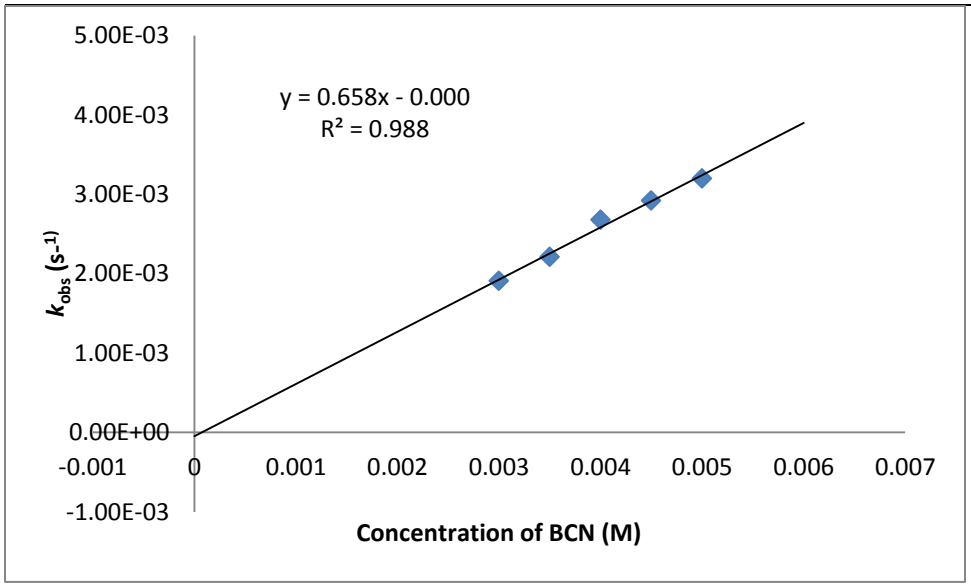

Nitrone	Structure	Concentration of BCN (M)	k_{obs} (s^{-1})
2.10	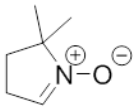	0.00250	1.28E-04
		0.00225	1.14E-04
		0.00200	1.04E-04
		0.00175	9.01E-05
		0.00150	8.05E-05

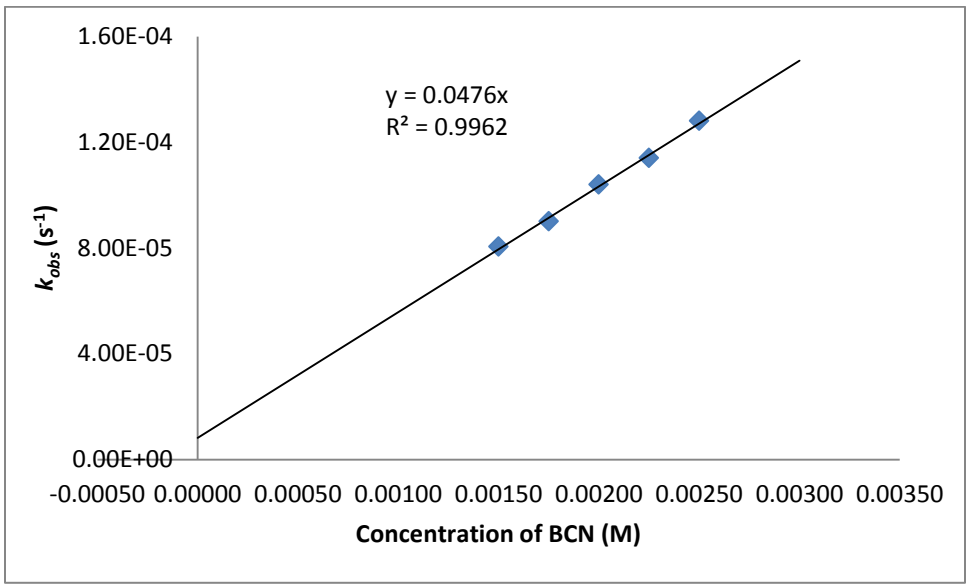

Nitrone	Structure	Concentration of BCN (M)	k_{obs} (s^{-1})
2.11	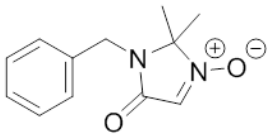	0.0050	7.30E-03
		0.0045	6.87E-03
		0.0040	6.15E-03
		0.0035	5.40E-03
		0.0030	4.63E-03

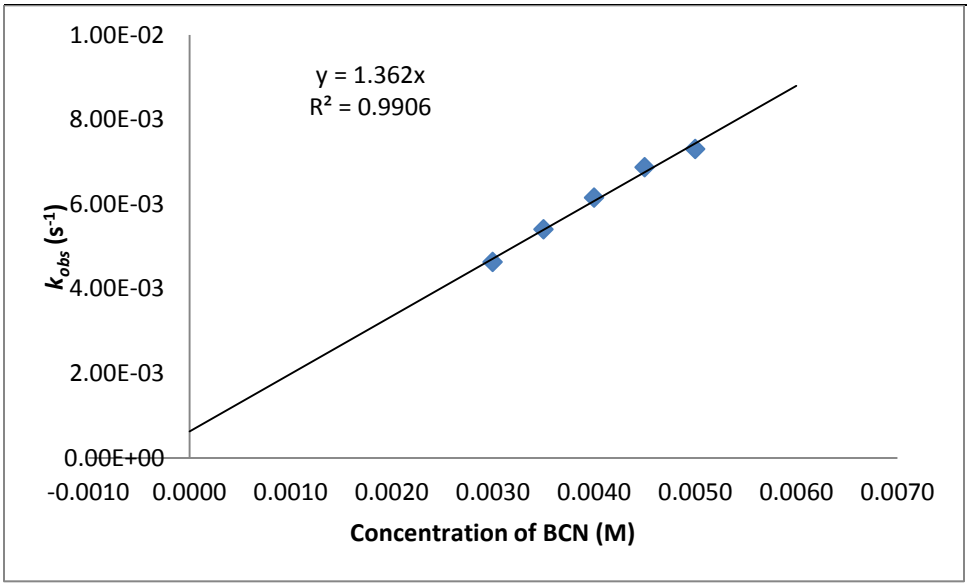

Competition Experiment

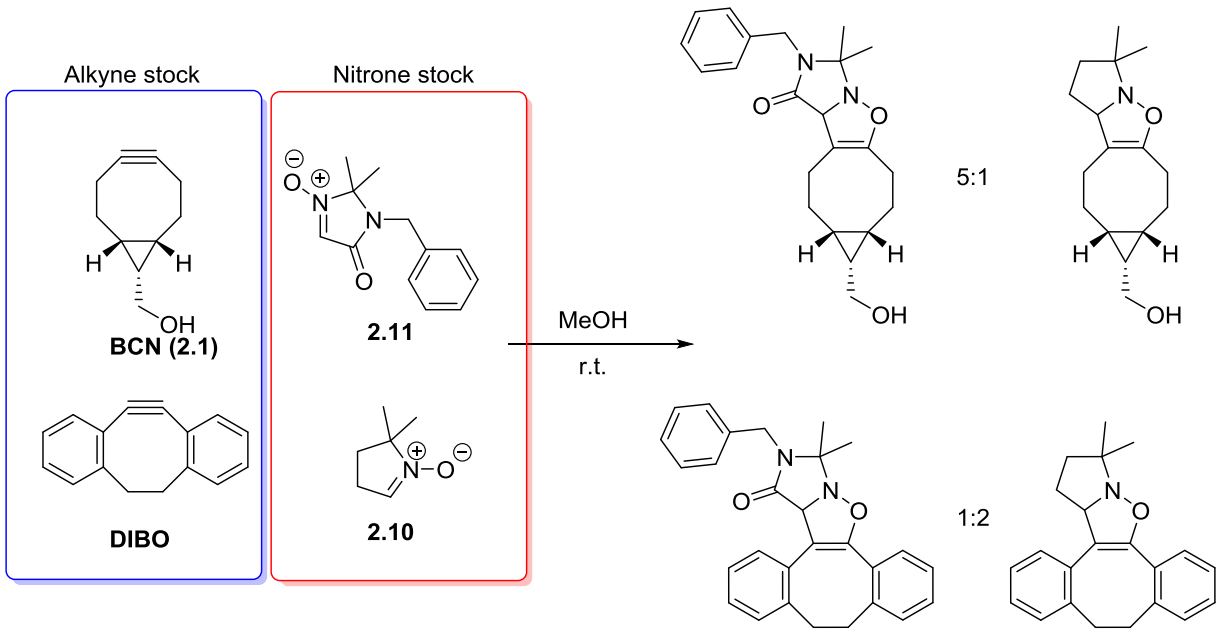

Alkyne stock:

0.012 g of DIBO was dissolved in 3 mL of MeOH (18.0 mM).

0.012 g of BCN was dissolved in 1 mL of MeOH (76.6 mM).

1.00 mL of DIBO stock (0.018 mmol) was mixed with 0.235 mL of BCN stock (0.018 mmol) to make 1.24 mL of alkyne stock at a final concentration of 14.6 mM.

Nitrone stock:

0.012 g of nitrone **2.11** was dissolved in 2.00 mL MeOH (27.7 mM).

0.009 g of nitrone **2.10** was dissolved in 1.00 mL MeOH (82.2 mM)

0.650 mL of nitrone **2.11** stock (0.018 mmol) was combined with 0.219 mL of nitrone **2.10** stock (0.018 mmol) and 0.366 mL of MeOH to make 1.24 mL of nitrone stock at a final concentration of 14.6 mM.

0.500 mL of nitrone stock was combined with 0.500 mL of alkyne stock at room temperature with stirring. The reaction was monitored by LCMS and the distribution of products was determined by integrating the LCMS trace in positive ESI ionization mode.

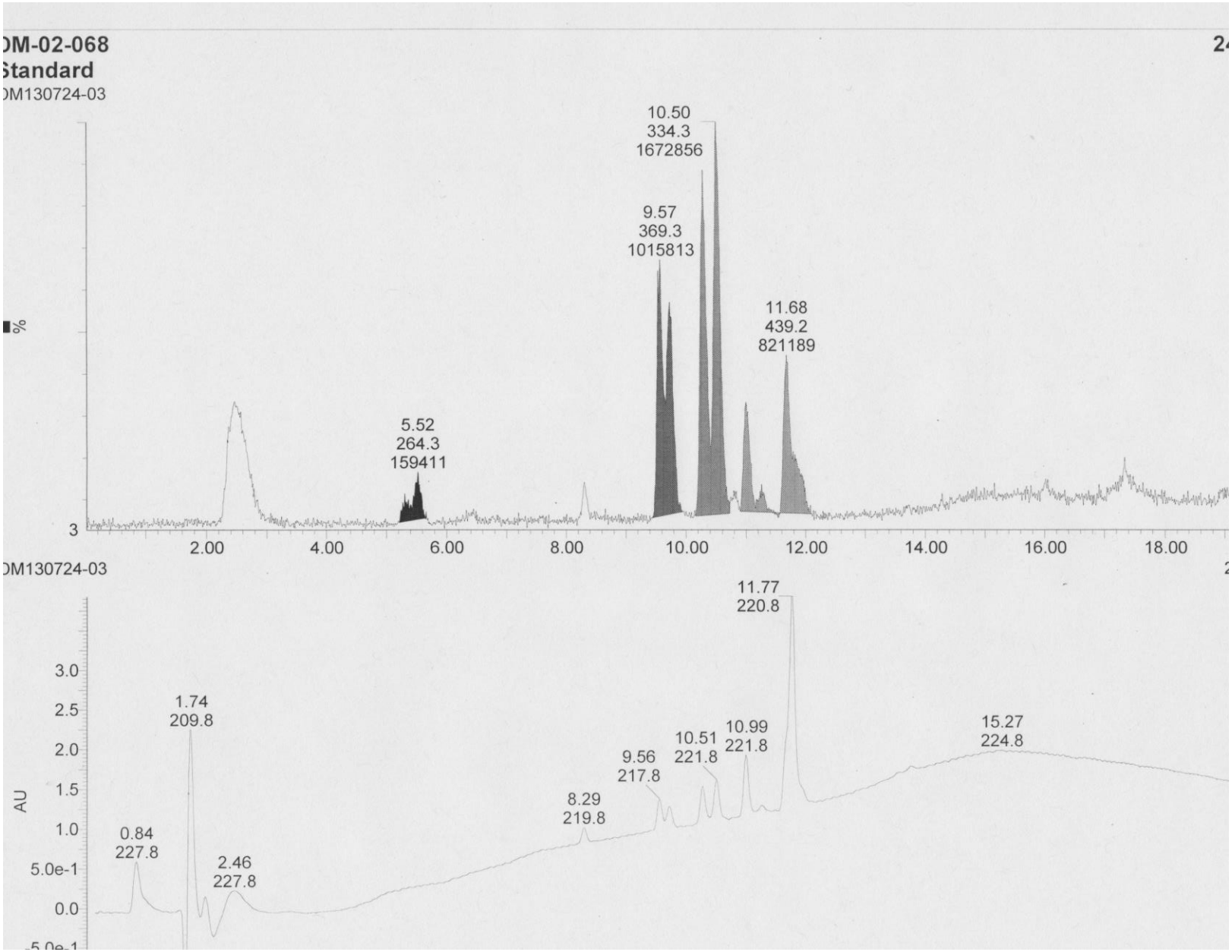
DM-02-068
Standard
DM130724-03
10.50
334.3
1672856
9.57
369.3
1015813
11.68
439.2
821189
5.52
264.3
159411
%
3
2.00
4.00
6.00
8.00
10.00
12.00
14.00
16.00
18.00
DM130724-03
11.77
220.8
1.74
209.8
15.27
224.8
10.99
221.8
10.51
221.8
9.56
217.8
8.29
219.8
0.84
227.8
2.46
227.8
AU
3.0
2.5
2.0
1.5
1.0
5.0e-1
0.0

Metabolic labelling

Listeria innocua:

L. innocua for each experiment was inoculated from a frozen glycerol stock (-80˚C) into 1.00 mL of BHI media and incubated over-night at room temperature without shaking. Cultures with an OD_{600} of 0.05 were started in BHI media and incubated at 30˚C for 2 hours. 100 µL aliquots were placed in 1.50 mL Eppendorf tubes and treated with 1µL of either DMSO (negative control), 500 mM **3.1**-**3.4** in DMSO, or 500 mM azido D-Alanine in DMSO. Cultures were incubated at 30˚C for 30 minutes then washed with 200 µL of PBS buffer (3X). Pellets were formed by centrifugation at 12 000 g, supernatant was removed and the pellets were resuspended in 100 µL of 2.50 µM or 25.0 µM DIBO Alexafluor-488, DIBO Alexafluor-555, or BCN Alexafluor-488 (**3.7**) and incubated at 37˚C for 10 minutes. Cultures were washed with 200 µL of PBS buffer (3X), pelleted by centrifugation at 12 000 g, and resuspended in PBS buffer to prepare microscope slides.

Lactococcus lactis:

L. lactis was treated in the same manner as *L. innocua* with the exception of being shaken during growth.

Imaging:

Once the slides were prepared, imaging was carried out using an Olympus 1X81 spinning-disk confocal microscope equipped with a FITC filter (Semrock, Excitation: 465-499 nm, Emission: 516-556 nm), Cy3 filter (Semrock, Excitation: 510-560 nm, Emission: 570-620 nm) and a Photometrics (Coolsnap ES) camera using 100x magnification. Images were taken of samples

and controls using bright-field, FITC channel (2-4 second exposure), and Cy3 channel (2-4 second exposure). Image processing was done using ImageJ software, applying pseudocolour to FITC channel images. The same pixel intensity ranges were applied and displayed for all images in each set of experiments.